ISTANBUL TECHNICAL UNIVERSITY ★ GRADUATE SCHOOL

EXPERIMENTAL AND NUMERICAL STUDY ON THERMAL BEHAVIOR OF SPACE EQUIPMENT BY USING TWO RESISTOR MODEL

M.Sc. THESIS

Sima Aslım YAKUT

Department of Aeronautics and Astronautics Engineering

Aeronautics and Astronautics Engineering Programme

JANUARY 2023

ISTANBUL TECHNICAL UNIVERSITY ★ GRADUATE SCHOOL

EXPERIMENTAL AND NUMERICAL STUDY ON THERMAL BEHAVIOR OF SPACE EQUIPMENT BY USING TWO RESISTOR MODEL

M.Sc. THESIS

Sima Aslım YAKUT
(511191137)

Department of Aeronautics and Astronautics Engineering

Aeronautics and Astronautics Engineering Programme

Thesis Advisor: Assis. Prof. Dr. Özge ÖZDEMİR

JANUARY 2023

ISTANBUL TEKNİK ÜNİVERSİTESİ ★ LİSANSÜSTÜ EĞİTİM ENSTİTÜSÜ

UZAYDA KULLANILAN EKİPMANLARIN ISIL DAVRANIŞLARININ İKİ DİRENÇLİ MODEL İLE DENEYSEL VE SAYISAL İNCELENMESİ

YÜKSEK LİSANS TEZİ

Sima Aslım YAKUT
(511191137)

Uçak ve Uzay Mühendisliği Anabilim Dalı

Uçak ve Uzay Mühendisliği Programı

Tez Danışmanı: Dr. Öğr. Üyesi Özge ÖZDEMİR

OCAK 2023

Sima Aslım Yakut, a M.Sc. student of ITU Graduate School student ID 511191137 successfully defended the thesis entitled “Experimental And Numerical Study On Thermal Behavior Of Space Equipment By Using Two Resistor Model”, which she prepared after fulfilling the requirements specified in the associated legislations, before the jury whose signatures are below.

Thesis Advisor : **Assis. Prof. Dr. Özge Özdemir** ....
İstanbul Technical University

Jury Members : **Prof. Dr. Alim Rüstem Aslan** ....
Istanbul Technical University

Assis. Prof. Dr. Serhat Yılmaz ....
National Defence University

Date of Submission : 30 December 2022
Date of Defense : 17 January 2023

To my family,

FOREWORD

In this thesis, the thermal behavior of space equipment is investigated by experimental and numerical methods. The correlation of the experimental results was made using two resistor models.

First of all, I would like to thank my mentor Assist. Prof. Dr. Özge Özdemir who did not withhold her support from me during my master's degree education process, and devoted her time to me during the thesis process. I would like to thank a few more people here. Specially Mehmet Emin Albayrak who has been guiding me every step of the way, always there for me and answered my questions faithfully and did not spare his support during the analysis process I made. Dear Saruhan Yangın, who sharing my stress during this process, supporting me in every way, and answering sincerely every question I asked. My manager Atayıl Koyuncu and my chef Duygu Ceylan for supporting and helping me to use this work done at Turkish Aerospace in my thesis. My twin and Res. Assist. Sena Ecem Yakut, and my friend Semih Türkoğlu for supporting and helping me throughout my thesis process.
Finally, I would like to thank my dear father İmdat Yakut, mother Sevgi Yakut, and grandmother Nevriye Aydın, who have always supported me, who have been by my side under all circumstances, very much.

December 2022

Sima Aslım YAKUT
(Astronautical Engineer)

TABLE OF CONTENTS

Page

ABBREVIATIONS

2R-CTM	: Two Resistor Compact Thermal Model
AOCS	: Attitude Determination & Control
BGA	: Ball Grid Array
CAD	: Computer Aided Design
CAM	: Computer Aided Engineering
CTM	: Compact Thermal Model
DC	: Direct Current
DGK	: Dahili Güç Kaynağı
DTM	: Detailed Thermal Model
ECAD	: Electronic Computer-Aided Design
ECSS	: European Cooperation for Space Standardization
EMC	: Electromagnetic Compatibility
EMI	: Electro Magnetic Interference
ESC	: Electronic System Cooling
EQM	: Engineering Qualification Model
FEM	: Finite Element Method
FFT	: Full Functional Test
FDIR	: Failure Detection Isolation and Recovery
FEA	: Finite Element Analysis
GaN	: Gallium Nitride
GEO	: Geostationary Orbit
GTO	: Geostationary Transfer Orbit
IC	: Integrated Circuit
IPS	: Internal Power Supply
ISS	: International Space Station
JWST	:James Webb Solar Telescope
JPL	: Jet Propulsion Laboratory
LEO	: Low Earth Orbit
LSI	: Large Scale Integration
MEO	: Medium Earth Orbit

MLI : Multilayer Insulation Blanket
MLP : Micro Leadframe Package
MOS : Margin of Safety
MOSFET : Metal Oxide Semi-Conductor Field Effect Transistor
MRAM : Magnetoresistive Random Access Memory
MTSA : Modified Top Surface Area
NTC : Negative Temperature Coefficient
OBC : On-Board Computer
PCB : Printed Circuit Board
PM : Processor Module
PTH : PCB-Through-Hole Mounting
PCDU : Power Control and Distribution Unit
PERIMA Algorithm : Package's Evaluated thermal Resistances by Inverse-Method
PTASP : Package Thermal Automation Simulation Platform
RFT : Reduced Functional Test
PTC : Positive Temperature Coefficient
RF : Radio Frequency
RTMM : Reduced Thermal Mathematical Model
SAR : Synthetic Aperture Radar Satellite
SiC : Silicon Carbide
SMT : Surface Mounting Technology
SOHO : Solar Telescope
SSO : Polar Orbit And Sun-Synchronous Orbit
SST : Space System Thermal
STM : Structural-Thermal Model
TBT : Thermal Balance Test
TC : Telecommand
TCT : Thermal Cycling Test
TM : Telemetry
TRP : Thermal Reference Point
TTC : Telemetry and Telecommand Subsystem
TVAC : Thermal Vacuum Chamber
TVCT : Thermal Vacuum Cycling Test
TVTS : Thermal Vacuum Test System

QFP **:** Quad Flat Package
QM **:** Qualification Model

SYMBOLS

A	: Area
$\boldsymbol{c}$	: Heat capacity
C	: Thermal capacitance
$\boldsymbol{F_{ij}}$	: View Factor
G	: Thermal conductance
$\mathbf{h_c}$	: Thermal contact conductance
I	: Current
k	: Conductivity
$\mathbf{k_{underfill}}$	: Thermal conductivity of underfill material
L	: Length
$\mathbf{N_i}$	: Shape function
R	: Resistance
$\mathbf{R_c}$	: Thermal contact resistance
T	: Temperature
t	: Time
TM/TC	: Telemetry and Telecommand Subsystem
$\mathbf{t_{underfill}}$	: Underfill material thickness
Q	: Heat
q	: Heat flow / Charge
q’’	: Heat flux
V	: Voltage
$\boldsymbol{\theta_{underfill}}$	: Underfill material resistance
$\boldsymbol{\theta_{ja}}$	: Junction to ambient thermal resistance
$\boldsymbol{\theta_{jb}}$	: Junction to board thermal resistance
$\boldsymbol{\theta_{jc}}$	: Junction to case thermal resistance
$\boldsymbol{\theta_{jt}}$	: Junction to top thermal resistance
$\boldsymbol{\Delta T}$	: Temperature Difference
$\boldsymbol{\alpha}$	: Absorptivity
$\boldsymbol{\eta}$	: Efficiency

$\boldsymbol{\varepsilon}$	**:** Emissivity
$\boldsymbol{\rho}$	**:** Density
$\boldsymbol{\varphi}$	**:** Reflectivity
$\boldsymbol{\tau}$	**:** Transmissivity

LIST OF TABLES

Page

LIST OF FIGURES

Page

EXPERIMENTAL AND NUMERICAL STUDY ON THERMAL BEHAVIOR OF SPACE EQUIPMENT BY USING TWO RESISTOR MODEL

SUMMARY

In this study, the qualification level Thermal Balance Test (TBT) performed on the On-Board Computer (OBC) developed within the framework of the satellite programs of the Turkish Aerospace is explained. The numerical solution developed using Simcenter 3D is explained. Test and analysis correlations were made, results and recommendations were explained.

The IPS module, the power module of the OBC, has been tested in a vacuum environment. The main reason for choosing the IPS module is to evaluate heat generation and heat dissipation and thermal design. A IPS module (carrier and PCB), cover and baseplate are included in this work. It takes a lot of time to include every component on the PCB in the thermal analysis. For this reason, only components that emit heat above 50 mW are included in the analysis. The aim of this study is to validate the thermal analysis. This study does not contain electrical information. IPS module connections were chosen as AISI 310 stainless steel. According to the data sheets, thermal pads are placed under the components that require thermal pad application. In addition, thermal pad was applied between the carrier and the baseplate. Aluminum bulk structures had to be placed under 2 components due to supply problems. The DC-DC converters, which dissipate a lot of heat, are located in the lower part of the PCB. In order to conduct heat, the upper surface of the PCB under these components is left as copper. The layout of the other components is placed in such a way that they do not heat each other thermally according to the electrical constraints. The carrier design has been meticulously made with ECSS requirements in mind, to ensure mechanical strength and transfer heat to the baseplate by conduction. The baseplate is designed to hold the backplane and supporting all boards, dissipating the equipment heat to the satellite panel. It is also used to support the baseplate cover and carriers, hold them together and provide thermal conduction. There are 8 mounting holes in total for OBC equipment. The equipment is designed with these interfaces to be mounted on the satellite panel and the thermal plate in the thermal vacuum chamber.

For this equipment to be used in the satellite system, the space environment is reflected in the thermal vacuum chamber. The qualification temperature range of the equipment is [-30°C, +60°C]. Hot case of qualification level was tested within the scope of this thesis. The thermal balance test was performed for the hot case, because in previous thermal camera measurements and analysis showed that the components were overheated. The thermal balance test was carried out at the Assembly, Integration and Test Center (AIT) of the Turkish Aerospace company. The HVT400 thermal vacuum chamber inside the clean room at AIT is used for equipment testing. Thermocouple placement was done before the equipment was put into the TVAC. Thermocouples are placed on components that emit heat above 50mW, on the PCB 1 mm away from the components, near the bolt connections, on the cover and on the baseplate. A total of 33 thermocouples are placed on the equipment. The IPS module is mounted on the

plate in the thermal vacuum chamber using appropriate interfaces. After the necessary checks and connections are made, the door is closed. First, the pressurization process was carried out. The pressure in the chamber was reduced to 10^{-5} mbar. Tests were performed for 60°C with certain power configurations. Thermal stabilization criteria was determined as 0,5°C/hour for 60°C. The thermocouples data were read, the room temperature and pressure were normalized, and the door was opened.

Analysis was performed using Simcenter 3D software. The Thermal/Flow solver was chosen for the solution of the thermal analysis. The Space Systems Thermal Solver ignores convection and creates a suitable solution environment for the space environment. One of the advantages of Simcenter 3D software for electronic equipment is that PCB material properties can be calculated. PCB layers, percentage of dielectric and copper material and layout can be seen, therefore the thermal conductivity is calculated by the software. Thanks to its automatic meshing feature, PCB and components are created automatically in 2D.

As the analysis method, two resistor thermal modeling method was chosen among the compact modeling methods. The purpose of choosing this method is that it is simple and the data can be easily accessed. Simcenter 3D offers 2 different methods for modeling with two resistors. First; resistors from junction to case and from junction to board; the second: the resistors from junction to case and from case to board. These resistance values are calculated according to JEDEC standards. These resistors are supplied from component data sheets or manufacturers. In this study, an analysis model was created by using the resistors from junction to case and case to board. These resistance values were obtained from datasheets and manufacturers. Various assumptions were made for the values that could not be found. Other parameters required for modeling are maximum junction temperature, maximum case temperature, and heat dissipation of the components. The maximum junction temperature value and the maximum case temperature value are usually obtained from the datasheet. The heat dissipation values were obtained from the hardware design team working in the Turkish Aerospace company. The heat dissipation value calculation is not included in this thesis. Afterwards, boundary conditions were entered into the analysis. Ambient temperature, thermal plate temperature and radiation are given as boundary conditions. In order to calculate the radiation, the emissivity values of the components, aluminum parts and PCB were included in the analysis. View factors were calculated with the help of enclosure radiation property of Simcenter 3D. Three separate view factor values were assigned for the open sides and the closed side of the equipment. The conductivity value between materials depends on the material to fill the gap, surface roughness, material, surface finishing method and pressure. These values are usually obtained experimentally. As a result of the researches, many conductivity values were found for steel, aluminum and copper. Optimized results were obtained by performing several iterations.

Finally, the analysis was reached to an acceptable level as a result of various iterations. The difference between test and analysis results is determined as 10% for acceptable level. This is well accepted value among the companies which conduct equipment thermal analysis. As a result, the correlation of analysis and test results has been completed.

UZAYDA KULLANILAN EKİPMANLARIN ISIL DAVRANIŞLARININ İKİ DİRENÇLİ MODEL İLE DENEYSEL VE SAYISAL İNCELENMESİ

ÖZET

Bu çalışmada, Türk Havacılık ve Uzay Sanayii'nin uydu programları çerçevesinde geliştirilen Merkezi Uydu Bilgisayarı (MUB) üzerinde gerçekleştirilen kalifikasyon seviyesi Termal Denge Testi (TBT) ve Simcenter 3D kullanılarak geliştirilen sayısal yöntem anlatılmıştır. Test ve analiz korelasyonu yapılmış, sonuçlar ve öneriler açıklanmıştır.

MUB'nın güç modülü olan DGK modülü vakum ortamında test edilmiştir. DGK modülünün seçilmesinin ana nedeni, ısı üretimi, ısı yayılımını ve termal tasarımını değerlendirmektir. Bir DGK modülü (taşıyıcı ve PCB), kapak ve taban plakası bu çalışmaya dahil edilmiştir. PCB üzerinde bulunan her komponentin analize dahil edilmesi çok zaman gerektirir. Bu nedenle sadece 50 mW üzeri ısı yayan komponentler analize dahil edilmiştir. Bu çalışmanın amacı geliştirilen termal analizi doğrulamaktır. Elektriksel anlamdaki bilgileri içermemektedir. DGK modülü bağlantıları AISI 310 paslanmaz çeliği ile gerçekleştirilmiştir. Data sheetlere göre termal pad uygulaması gerekli görülen komponentlerin altına termal pad yerleştirilmiştir. 2 adet komponentin altına tedarik sorunları nedeniyle alüminyum plaka konulması gerekmiştir. Çok ısı yayan DC-DC dönüştürücüleri PCB'nin alt bölgesine yerleştirilmiştir. Isıyı iletmek için bu komponentlerin altında kalan PCB'nin üst yüzeyi bakır olarak bırakılmıştır. Diğer komponentlerin yerleşimi elektriksel kısıtlara göre termal açıdan da birbirlerini ısıtmayacak şekilde yerleştirilmiştir. Taşıyıcı tasarımı ECSS gereksinimleri göz önünde bulundurularak, mekanik dayanımı sağlamak ve ısıyı iletim yoluyla taban plakasına iletmek için özenle yapılmıştır. Taban plakası, tüm kartları destekleyen arka arayüz kartını tutmak, ekipman ısısını uydu paneline atmak için tasarlanmıştır. Aynı zamanda taban plakası kapağı ve taşıyıcıları desteklemek, bir arada turmak ve ısıl iletimi sağlamak için kullanılır. MUB ekipmanı için toplamda 8 adet montaj deliği bulunmaktadır. Uydu paneline ve TVAC'e bu arayüzlerle montaj yapılmaktadır.

Uydu sisteminde kullanılacak olan bu ekipman için uzay ortamı termal vakum odasında yansıtılmıştır. Ekipmanın kalifikasyon sıcaklık aralığı [-30°C, +60°C]'dir. Termal denge testi sıcak durumu test etmek için yapılmıştır, çünkü daha önce yapılan termal kamera ölçümlerinde ve analizlerde komponentlerin çok fazla ısındığı gözlemlenmiştir. Termal denge testi Türk Havacılık ve Uzay Sanayii şirketi Uydu Sistem ve Entegrasyon Merkezi'nde (USET) gerçekleştirilmiştir. USET'te bulunan temiz oda içerisindeki HVT400 termal vakum odası ekipman testleri için kullanılmaktadır. Ekipman TVAC içerisine konmadan önce ısıl çift yerleşimi yapılmıştır. Isıl çiftler, 50mW üzeri ısı yayan komponentler üzerine, komponentlerden 1 mm uzağa PCB üzerine, civata bağlantılarına yakın yerlere, kapağa ve taban plakası üzerine yerleştirilmiştir. Toplamda 33 adet ısıl çift ekipman üzerine yerleştirilmiştir. DGK modülü termal vakum odası içerisinde bulunan plaka üzerine uygun arayüzler kullanılarak monte edilmiştir. Gerekli kontroller ve bağlantılar yapıldıktan sonra kapı kapatılmıştır. İlk olarak basınçlandırma işlemi yapılmıştır. Oda içerisindeki basınç 10^-5 mbar'a kadar düşürülmüştür. Belirli güç konfigürasyonlarında 60°C için test

gerçekleştirilmiştir. Termal denge kriteri, 60°C için 0,5°C/saat olarak belirlenmiştir. Isıl çiftlerden veriler okunmuş, oda sıcaklığı ve bacınç normal duruma getirilmiş ve kapı açılmıştır.

Analiz, Simcenter 3D yazılımı kullanılarak gerçekleştirilmiştir. Termal/Akış çözücüsü termal analizin çözümü için seçilmiştir. Uzay Sistemleri Termal çözücüsü (space system thermal) konveksiyonu yok sayarak, uzay ortamı için uygun çözüm ortamı oluşturmaktadır. Simcenter 3D yazılımının elektronik ekipmanlar için avantajlarından biri PCB malzeme özelliklerinin hesaplanabilmesidir. PCB katmanları, yalıtkan ve bakır malzeme oranları ve yerleşimleri görülebilirken, termal iletkenlik katsayısı yazılım tarafından hesaplanır. Otomatik ağ yapısı oluşturma özelliği sayesinde PCB ve komponentler 2 boyutlu olarak otomatik oluşturulur.

Analiz yöntemi olarak kompakt modelleme yöntemleri arasından iki dirençli modelleme yöntemi seçilmiştir. Bu yöntemin seçilmesindeki amaç basit ve datalara ulaşmanın nispeten kolay olmasıdır. İki dirençli modelleme için Simcenter 3D 2 farklı yöntem sunmaktadır. İlki; bağlantı yerinden kasaya ve bağlantı yerinden karta olan dirençler, ikincisi: bağlantı yerinden kasaya ve kasadan karta olan dirençlerdir. Bu direnç değerleri JEDEC standartlarına göre hesaplanmaktadır. Bu dirençler komponent veri sayfalarından veya üretici firmalardan tedarik edilmektedir. Bu çalışmada bağlantı yerinden kasaya ve kasadan karta olan dirençler kullanılarak analiz modeli oluşturulmuştur. Bu direnç değerleri veri sayfalardan ve üreticilerden elde edilmiştir. Bulunamayan değerler için çeşitli varsayımlar yapılmıştır. Modelleme için gerekli diğer parametreler bağlantı noktası maksimum sıcaklık değeri, kasa maksimum sıcaklık değeri ve ısı yayınım değeridir. Bağlantı noktası maksimum sıcaklık değeri ve kasa maksimum sıcaklık değeri genellikle veri sayfasından elde edilir. Isı yayınım değerleri Türk Havacılık ve Uzay Sanayi şirketinde çalışan kart tasarım ekibinden elde edilmiştir. Isı yayınım değeri hesaplaması bu tez çalışmasına dahil edilmemiştir. Sonrasında, analize sınır koşulları girilmiştir. Ortam sıcaklığı, termal plaka sıcaklığı ve radyasyon sınır koşulu olarak verilmiştir.

Radyasyon hesaplanabilmesi için muhafaza radyasyonu özelliği kullanılarak görünüm faktörleri hesaplanmıştır. Komponentlerin, alüminyum parçaların ve PCB'nin yayınım değerleri analize dahil edilmiştir. Komponent ve PCBlerin yayınım değerleri için literatür araştırması yapılmış ve 0,8 olarak analize dahil edilmiştir. Alüminyum parçaların yayınım değeri 0,05 olarak bulunmuş ve analize dahil edilmiştir. Ekipmanın açık olan tarafı ve kapalı olan tarafı için 3 ayrı görünüm faktörü değeri hesaplanmış ve analize eklenmiştir. Malzemeler arasındaki iletkenlik değeri arada kalan boşluğun malzemesine, yüzey pürüzlülüğüne, malzemeye, yüzey sonlandırma yöntemine ve iki yüzeyin birbirine uyguladığı basınca bağlıdır. Bu değerler genellikle deneysel olarak elde edilmektedir. Araştırmalar sonucu çelik, alüminyum ve bakır için birçok iletkenlik değeri bulunmuştur. Türk Havacılık ve Uzay Sanayi'de daha önce gerçekleştirilen deneysel çalışmaların sonucu bir öngörü oluşturması amacıyla analize girdi olmuştur. Isı transfer katsayısı ve termal pad kullanılan alanlar için termal dirençler tanımlanmıştır. Çeşitli iterasyonlar yaparak optimize sonuçlar elde edilmiştir.

Son olarak çeşitli iterasyonlar sonucunda analiz kabul edilebilir bir düzeye ulaşmıştır. Elektronik ekipman üreten farklı firmalardan ve yurtdışında alınan eğitimlere göre test ve analiz sonuçları arasındaki fark %10 olarak belirlenmiştir. %10 fark elektronik ekipman termal analizleri için kabul edilebilir bir farktır.

Bu, ekipman termal analizi yapan şirketler arasında kabul görmüş bir değerdir. Sonuç olarak, analiz ve test sonuçlarının korelasyonu tamamlanmıştır.

1. INTRODUCTION

Electronic equipment design for space is one of the most critical processes for operating any spacecraft in a vacuum environment for a certain lifetime. It is very important to consider protective precautions for spaceborne equipment to improve the reliability. One of the most critical issue is the thermal behavior in the design of spaceborne electronic equipment. Verifying the thermal design of electronic equipment is critical as system-level operations must be conducted throughout the life of a spacecraft.

Electronic packaging has become a rapid developing area because of higher functionality and operating, miniaturization, further reliability, low cost and competing customer requires. Electronic components are points which heat as they are exposed to an electrical current flowing through a resistor. Further downsizing of electronic components has led to a significant increase in heat generation per unit volume. Therefore, thermal design and control for electronic equipment has become more critical.

Thermal control has become a critical factor during the design process of the electronic equipment because of the recent trends in the electronic industry towards increased miniaturization of components and device heat dissipation. A great demand on the system performance and reliability also intensified the needs for a better thermal management. The further evidence of importance of thermal consideration to an electronic system is due to the survey by the U.S. Air Force indicating that more than fifty percent of all electronics failures are caused by the undesirable temperature control.

Two resistor model is a numerical analysis method used to demonstrate the thermal behaviour of electronic equipment. The method is easy to carry out and gives quite good results. Correlation the analysis model with test is considerable issue to specify unknown parameters. Parameters found are used in the following analyses.

1.1 Purpose of Thesis

The purpose of the thesis is the development of a thermal mathematical model of spaceborne electronic equipment and correlation with the results of the test made in a thermal vacuum chamber.

Thermal balance test is performed in order to demonstrate maximum heat dissipation at steady state condition. Information about thermal balance test and thermal vacuum chamber will be given in the following sections.

Two resistor model will be introduced and numerical solution will be carried out by using Simcenter 3D thermal analysis software package.

Comparison and verification of analysis results will be accomplished with experimental results.

1.2 Literature Review

The continuous reduction of microelectronic device size has led to a remarkable improvement in the performance of electronic products, but will result in higher operating temperature. All electronic packages are affected by temperature directly and impact the overall electronic system, as well.

According to Wang Z. & et al. [1], thermal design and analysis are necessary part of electronic packaging. In their study, thermal performance of Quad Flat Package (QFP) packages is analyzed by an equivalent thermal resistance network, which is composed of resistances and nodes. Firstly, thermal resistances are estimated and they are used to calculate equivalent thermal resistance using thermal network method. Secondly, QFP is simulated in ANSYS Software. Estimated equivalent thermal resistance is compared with the calculated value in ANSYS Software. Three methods are proposed to decrease the total thermal resistance.

Similarly, Zhang Y. W., Liang L., and Xia Y. [2] thermal simulation and analysis has important role in development of new generation of integrated circuit (IC) package design. One way of overcoming this simulation easily, Package Thermal Automation Simulation Platform (PTASP) is developed with ANSYS Workbench. Application of the PTASP to Micro Leadframe Package (MLP) package family (with general methodology and interface of the simulation program) is presented in their study. It is aimed that engineers who do not know finite element analysis (FEA) and heat transfer can run the simulation easily and accurately. Results are compared with classis ANSYS, and it can be shown that results are almost the same.

Compact thermal model (CTM) can be defined as the calculation of temperature and heat flux only at the desired points. It predicts die temperatures and provides fast and short process when compared to detailed thermal model (DTM). It is indicated that two-resistor model is the simplest and popular CTM among the end-users. Tal Y. [3] proposes an expanded approach for the application of a two-resistor model. This approach is called as Modified Top-Surface-Area (MTSA). MTSA offers modified top surface area for dissipating heat to the environment instead of the total area. Better prediction of junction temperature and heat dissipation on the top surface is aimed. MTSA approach was compared with a traditional 2R-CTM and detailed thermal model (DTM). Junction temperature, case temperature and heat dissipation through either top or board of the package values are evaluated. The study finalized as, errors were found within ±10% which is applicable for many common engineering approaches. Moreover, this investigation offers that MTSA can be bridge between typical 2R-CTM and complex CTMs.

Tal Y. & Nabi A. [4] presents a method, named PERIMA (Package's Evaluated thermal Resistances by Inverse-Method Algorithm) which converts standardized θ_{ja} and θ_{jc}, into a two-resistors model represented by junction-to-board thermal resistance (θ_{jb}) and junction-to-top thermal resistance (θ_{jt}). Thanks to PERIMA, there is no requirement for any further information besides the information given in a conventional data-sheet. In the absence of relevant and appropriate thermal data, PERIMA facilitates the creation of much more accurate models for IC packages in electronic systems.

In a study by Kim J. H. and Koo J. C. [5], it is stated that power dissipation is the most important parameter in the thermal analysis. A thermal model by using semi-empirical power dissipation method and surface heat model is developed for fast and efficient thermal design of a spaceborne electronic equipment. Developed thermal model is verified with the thermal cycling test.

Thermal failure of a transponder unit in the Korea LEO Earth Observation satellite under harsh space thermal environments is investigated by Seo, H. S., Rhee, J., Han

E. S., Kim I. S. [6]. The thermal failure occurred in an LM117 regulator which is microcircuit of the transponder unit. The thermal design, analysis and test was carried out considering LM117 regulator. To clarify the thermal failure of the LM117 regulator, the thermal vacuum cycling tests were performed. Two-resistor model (junction-to-case and case-to-board) was used to generate thermal network model of the LM117 regulator. Thermal network model and thermal vacuum test provided to obtain junction temperature of the LM117 regulator. The thermal resistance between the case and the junction is provided by the LM117 military-based specification, and the thermal resistance between the case and the board was obtained by a thermal vacuum cycling test. Thermal pad was used to control the thermal contact resistance. It can be said that reworking of thermal pad is very effective for junction, case and board temperatures. After rework process, the temperature of the junction and the case both decreased while the temperature of the board increased, therefore electrical shutdown was prevented.

As mentioned before, thermal contact resistance has an crucial effect on junction temperature. In one of these studies, Yovanovich M. M. *et al.* [7] developed the relationships for determining contact, gap and joint conductance for conforming rough surfaces. It is remarked that conductance is related to the contact pressure, surface parameters, conductivity ratio and a fluid parameter which depends upon several gas and surface characteristics. The proposed conductance is validated by some experimental results. It is suggested that much more empirical data are acquired for all contact conditions.

Peterson G. P. and Fletcher L. S. [8] also offers the experimental investigation of thermal contact conductance and effective thermal conductivity of anodized coatings. Using the experimental data, a dimensionless expression was developed that related the overall joint conductance to the coating thickness, the surface roughness, the interfacial pressure, and the properties of the aluminum substrate. Seven expressions were developed to relate thermal joint conductance with the coating thickness and interfacial pressure. The effective thermal conductivity was found to be 0.02 W/m.K. Therefore, all tests were evaluated for Al6061-T6. Investigations should be continued to determine whether the information obtained can be extended to oxides form of another alloys.

In a study carried out by Toh, K. C. and Ng K. K [9], prediction of thermal contact conductance at the different interfaces commonly encountered between materials used internally in electronic packages is presented. In addition, the experimental study explores interfaces at the external package surface, such as between mold compounds and heat sinks. Tests are generated for a mold compound FP4450 held in contact with Al6061-T6 having various surface finishes, under lightly loaded conditions, in a vacuum environment. It is stated that one of the major determinants of the thermal contact conductance is the pressure at which the two contacting surfaces are held together. This study also suggests that typical pressure range is not more than 3500 kPa for press fit and adhesive joints in electronic components, unlike earlier studies. The results show that experimantal studies for thermal contact conductance of uncoated Al6061-T6 surfaces, mold compound FP4450 to uncoated A16061 -T6 surfaces, and uncoated Al and mold compound FP4450 to anodized Al6061-T6 surfaces are substantially correlated with Yovanovich model and, Peterson and Fletcher model.

2. SATELLITE SYSTEM

Satellite systems consist of two different systems: satellite and ground station. While satellite is the component of the system that functions in orbit, ground station is the command control part of the space segment. Satellite is the only system that will be examined in this thesis [10].

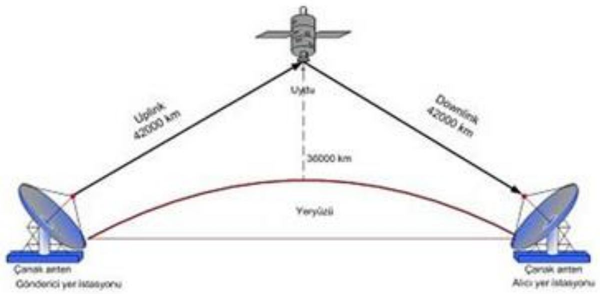

Figure 2.1 : Satellite system.

2.1 Satellite

Satellite is the component of the system that functions in orbit. An orbit can be described as a curved path in which an object in space (such as a star, planet, moon, asteroid, or spacecraft) revolves around another object due to gravity. As a result, gravity leads to an attraction of object in space that have mass to other nearby objects. Objects that have similar masses orbit each other with no center, small objects orbit around larger objects. For example, in our Solar System, the Moon orbits around Earth, Earth orbits and the Sun.

Satellites are launched with the rockets and put them into specific orbits. There, with the help of gravity, the satellite maintains its orbit. In space, there is no air and air friction especially higher orbits, only gravity keeps the satellite orbit around Earth. Satellites around Earth may have different missions and these missions are determined with needs. These enable the Earth to use technologies such as communication, observation and navigation in better and easily accessible ways [11].

2.1.1 Types of orbit

There are several specific types of orbits in which satellites are placed. These orbits are selected depending on what the satellite mission is going to be. First of all, missions of satellite will be explained [12].

- Geostationary orbit (GEO)
- Low Earth orbit (LEO)
- Medium Earth orbit (MEO)
- Polar orbit and Sun-synchronous orbit (SSO)
- Transfer orbits and geostationary transfer orbit (GTO)
- Lagrange points (L-points)

2.1.1.1 Geostationary Orbit (GEO)

A geostationary orbit is defined as a geosynchronous orbit at zero inclination. Satellites in geostationary orbit (GEO) travel around the Earth from west to east above the equator - 23 hours 56 minutes 4 seconds - moving at exactly the same speed as Earth. Speed of satellites in this orbit should be 3 km per second at an altitude of 35.786 km. GEO is preferred for the communication satellites. The benefit is that antennas on Earth can be fixed to stay pointed towards that satellite. GEO can also be used by weather monitoring satellites, as these satellites constantly observe certain areas to see how weather trends are unfolding there. Satellites in GEO cover a wide range of Earth, so three equally spaced satellites can provide almost global coverage.

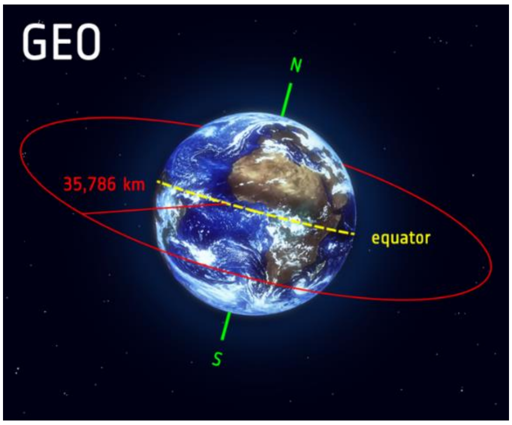

Figure 2.2 : Geostationary orbit (GEO).

2.1.1.2 Low Earth Orbit (LEO)

Low Earth orbit is an orbit that is relatively close to Earth's surface. Its altitude normally between 160 km and 1000 km above Earth. Satellites in this orbit travel at a speed of around 7.8 km per second. LEO's proximity to Earth is useful due to several reasons. It is the most commonly used orbit for earth observing satellites because its proximity to Earth provides higher resolution. It is also the orbit used for the International Space Station (ISS), as it is easier for astronauts to travel to and from it at a shorter distance.

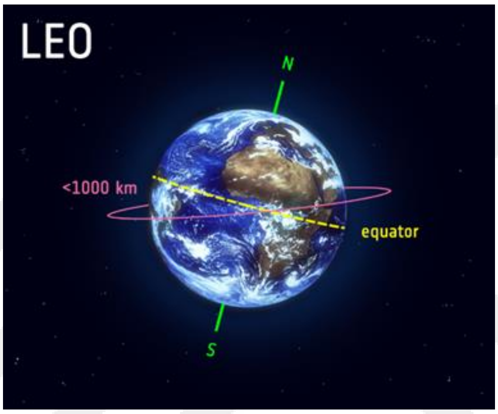

Figure 2.3 : Low earth orbit (LEO).

2.1.1.3 Medium Earth Orbit (MEO)

Medium Earth Orbit consists of a wide range of orbits anywhere between LEO and GEO. Satellites in this orbit travel at a speed of around 3-8 km per second. It is used by a several of satellites with many different applications. The orbit is very commonly used by navigation satellites, like the European Galileo system.

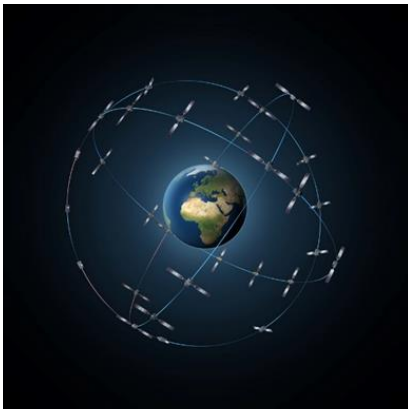

Figure 2.4 : Medium earth orbit (MEO).

2.1.1.4 Polar Orbit and Sun-Synchronous Orbit (SSO)

Polar orbit is defined for orbit of satellites which travel past Earth from north to south, passing over Earth's poles. Polar orbits are classified in low Earth orbit as they are at low altitudes between 200 and 1000 km.

Sun-synchronous orbit (SSO) is a specific type of polar orbit. As can be understood from its name, satellites in SSO are synchronous with the Sun. For clarifying the matter, to give an example, satellite always visits the same region at the same time.

A satellite in a Sun-synchronous orbit would usually be at an altitude of between 600 to 800 km. It will be travelling at a speed of approximately 7.5 km per second at 800 km. Generally, this orbit can be used for scientific researches.

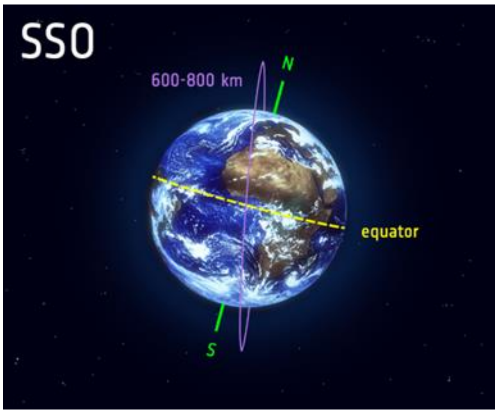

Figure 2.5 : Polar orbit and sun-synchronous orbit (SSO).

2.1.1.5 Transfer Orbits and Geostationary Transfer Orbit (GTO)

Transfer orbits are a special type of orbit used to move from one orbit to another. Generally, satellites are not put into their final orbit directly when they are launched from Earth. They are placed on a transfer orbit, so as to use little energy.

Geostationary transfer orbit (GTO) is one of the most common transfer orbit that is used to reach GEO. After takeoff, a launch vehicle travels into space, following the path indicated by the yellow line in the (Figure 2.6). The launcher leaves the payload at the final destination, following the blue line which sends the payload farther away from Earth. When the payload (satellite) reaches geostationary orbit (GEO) at the altitude of 35.786 km, engines start to fire and payload enters the GEO orbit and stays there, follows the redline in (Figure 2.6). Blue line in Figure 2.6 defines the geostationary orbit.

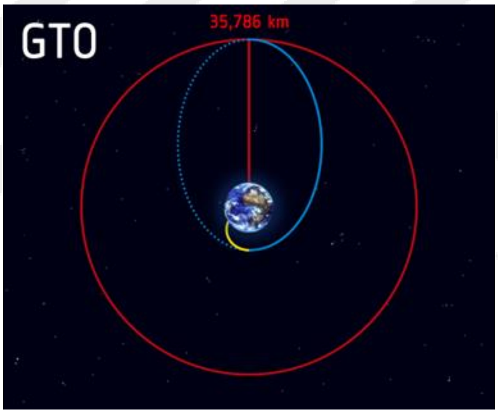

Figure 2.6 : Transfer orbits and geostationary transfer orbit (GTO).

2.1.1.6 Lagrange Points

Lagrange points are specific points in space very far away where the gravitational fields of the Earth and the Sun converge in such a way that the spacecraft orbiting them remain stationary and thus can be anchored relative to the Earth. If a spacecraft is launched to points in space too far from Earth, they will naturally enter an orbit around the Sun, and these spacecraft will soon move away from Earth, making communication difficult. Instead, spacecraft launched at these particular L-spots remain stationary and stay close to Earth with minimal effort, without entering a different orbit. L1 and L2 are the most used L-points. For example, solar telescope (SOHO) was placed in L1 point and Gaia and James Webb Solar Telescope (JWST) were placed in L2 points.

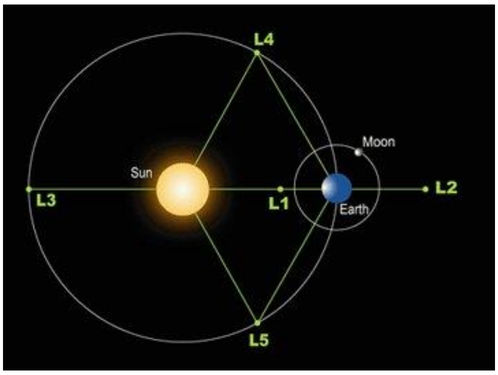

Figure 2.7 : Lagrange points.

2.1.2 Mission of satellite

Satellites generally divide into two modules as service and payload modules.

- Service module is a module in which units that can be used exactly or with minimal changes in satellites carrying different payloads are collected. In this way, it can be used in satellites with different payloads either exactly or with minimum changes.
- Payload module is the module in which units that can vary greatly depending on the mission. It is redeveloped for each satellite with a different payload [13].

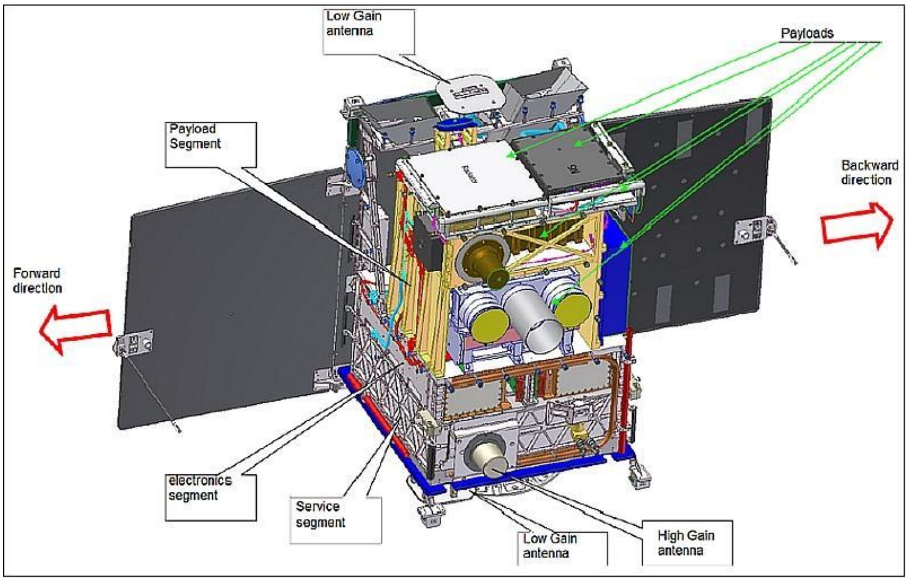

Figure 2.8 : Modular design.

Generally, payload module depends on the mission. Equipment in payload module differs from one mission to another, while service module equipment generallly stays the same. There are several types of satellite mission which operates around the Earth.

2.1.2.1 Earth Observation Satellite (Electro-Optical)

The task of the satellite is to provide electro-optical images of the desired region on the Earth via the electro-optic camera it carries. They are found in low altitude orbit, most are in Sun-synchronous orbits. The data from these satellites are used for several applications covering agriculture, water resources, urban planning, rural development, mineral prospecting, environment, forestry, ocean resources and disaster management.

As an example, Göktürk 2 is the earth observation satellite which is designed and developed by Turkey. It is launched from Jiuquan Launch Area 4/SLS-2 in China by a Long March 2D on December 18, 2012. The satellite, which weighs 409 kg, has a resolution of 2.5 meters in black and white and 5 meters in color. It was placed into Low Earth Orbit (LEO) of 686 km. It is the first satellite produced for taking high resolution images throughout the history of the Republic of Turkey [14].

Figure 2.9 : Göktürk-2 (Earth-Observation Satellite) [15].

2.1.2.2 Communication Satellite

Communication satellites ensure that the communication signals (TV broadcast, internet, etc.) are broadcast to the desired regions through the transmitters they carry. Ku, Ka and C-bands are primarily used for communication satellites. C-bands are transmitted with low power, and thus larger antennas are needed to receive these signals. Ku- and Ka-bands have more power and need less antenna diameter, so they are ideal for direct-to-home broadcasting, data communications, and telecommunications [16].

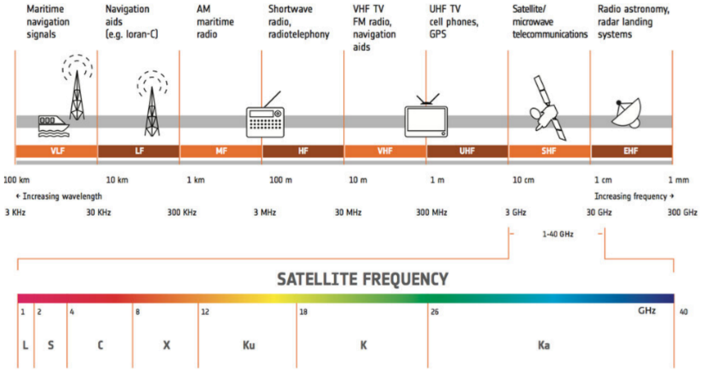

Figure 2.10 : Frequency bands.

Communication satellites are often placed in a geostationary orbit so that Earth-based satellite antennas (located on Earth) do not have to rotate to track them but can be pointed permanently at the position in the sky where the satellites are located. TURKSAT 6A is given as an example for communication satellites in (Figure 2.11) [17].

Figure 2.11 : Türksat-6A.

2.1.2.3 Synthetic Aperture Radar Satellite (SAR)

The mission of the satellite is to provide radar images of the desired regions in the world via the synthetic aperture radar. Satellites with Synthetic Aperture Radar (SAR) orbit the Earth in a sun-synchronous LEO. Synthetic Aperture Radar (SAR) payload meets the satellite image needs day and night in all weather conditions.

2.1.2.4 Navigation Satellite System (GPS)

Navigation satellite systems provide the navigation signals necessary for users to calculate location, speed and time information. Navigation satellite systems orbit the Earth in MEO.

2.1.2.5 Meteorology Satellite

Meteorology satellites provide weather related data such as cloudiness, temperature, humidity, wind speed and direction. They can circle around Earth in LEO (polar orbit-sun synchronous) which provides higher resolution. They can observe any location on Earth and see each location twice a day under the same general lighting conditions due to nearly constant local solar time. Also, they can orbit the Earth in GEO because they remain stationary with respect to the rotating Earth and thus can record or transmit images of the entire hemisphere below continuously with their visible-light and infrared sensors [18].

2.1.3 Satellite subsystems

Satellites are structures in which many subsystems work together. Each subsystem must work in conjunction with each other. The equipment are placed in the panels that make up the outer structure of the satellite in an optimized way and works to fulfill the mission of the satellite. Each subsystem will be described in detail below. Satellite consists of many subsystems such as,

- Structural,
- Thermal Control,
- Propulsion,
- Attitude Determination & Control (AOCS),
- Power Control,
- Telemetry and Telecommand Subsystem,
- Command and Data Handling.

2.1.3.1 Structural subsystem

It is to keep other subsystems together throughout the life of the satellite. It protects the satellite against mechanical loads in ground operations, launching and orbit, and environmental impacts in orbit.

Structural components can be classified as primary structures (structural panels, central cylinder or cone) [19], secondary structures (equipment support brackets + cable brackets) [20] , and separation ring [21].

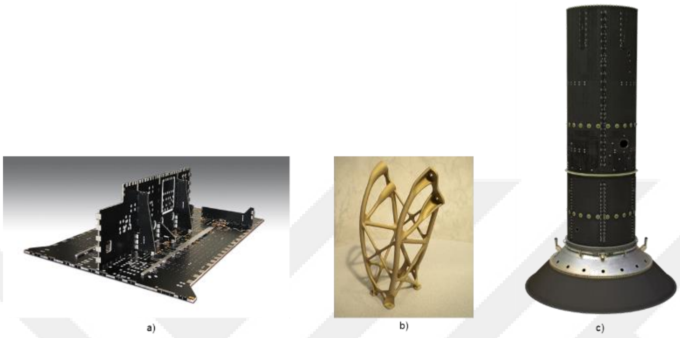

Figure 2.12 : a) Primary structures. b) Equipment support bracket. c) Central cylinder + separation ring.

2.1.3.2 Thermal control subsystem

The purpose of thermal control subsystem is keeping satellite equipment within the required temperature ranges. Basically, it provides thermal insulation, detects temperatures, ensures temperature limits, distributes of excess heat generated by equipment, and removes of excess heat generated by the equipment.

Thermal control subsystem components can be separated as multilayer insulation blanket, radiator, heat pipe, thermistor, thermostat, and heater [22].

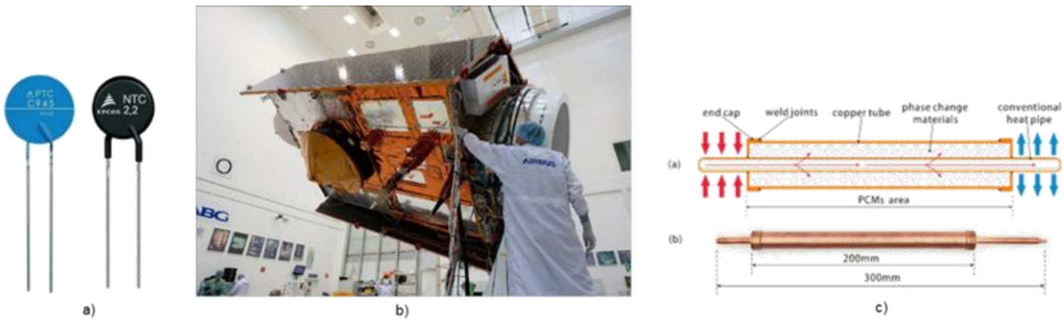

Figure 2.13 : a) Thermistor. b) Multilayer insulation blanket. c) Heat pipe.

2.1.3.3 Propulsion subsystem

Propulsion subsystem can be divided into two major categories such as chemical and electrical systems. The main purposes of these systems is orbital station-keeping and attitude control of satellites. The comparison of these two systems is explained below.

Chemical Propulsion Engines: Combustion engines have been used more widely throughout the history of space travel. Chemical engines have a much higher weight to thrust ratio than electric propulsion systems.

Electric Propulsion Engines: Electric thrusters typically use much less propellant than chemical rockets. Allow for more sustained flight. Electric propulsion can provide a small thrust for a long time [23].

Filling drain valve, pressure gauge, pyro valve, fuel filter, tank and thrusters are given as an example for the components of propulsion subsystem.

a) b)

Figure 2.14 : a) Electrical propulsion system. b) Chemical propulsion system.

2.1.3.4 Attitude determination and control subsystem

Functions of attitude determination and control subsystem (AOCS) are determining the satellite's position in orbit, determining attitude of satellite and controlling attitude of satellite. Star tracker, sun sensor, gyroscope, magnetometer and reaction wheel can be given as an example for AOCS equipment [24].

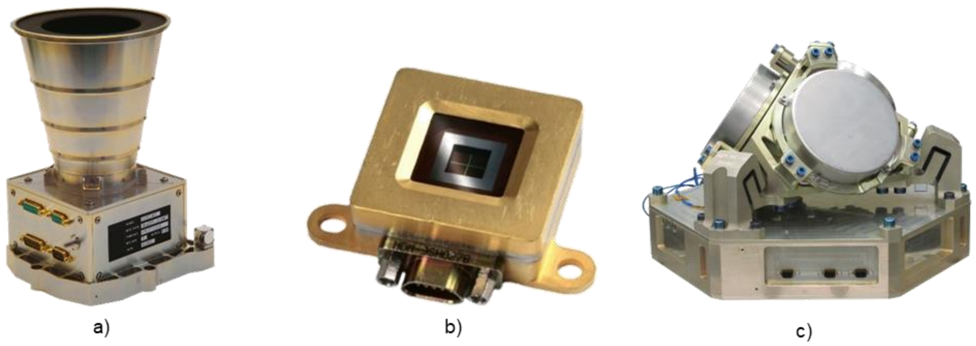

Figure 2.15 : a) Star tracker. b) Sun sensor. c) Gyroscope.

2.1.3.5 Power control subsystem

Power control subsystem is essential for a spacecraft. The sun provides about 1.4 kilowatts of power per square meter in Earth orbit, which is an amazing resource that the designer wanted to make the most of. Solar arrays and batteries are the fundamental equipment of this subsystem. Batteries are used when solar arrays are not deployed yet, just after launch, and also when satellite goes into the Earth shadow. After deployment of solar arrays, as long as solar arrays are Sun pointed, solar arrays take on the generation of power in Earth orbit. Today, efficiency of solar cell is around %30 and Li-Ion batteries are preferred for the satellite batteries. The power equipment are generally the heaviest ones in the equipment of a satellite and also heat rejection is quiet high. New trend is reducing the size of equipment and simultaneously decreasing the heat dissipation with the shrinking area while increasing the efficiency in the power electronics. Gallium Nitride (GaN) and silicon carbide (SiC) are the advanced components which can be used for achieving these goals. Main purposes of the power control system is power generation, power control, power distribution and energy storage. Besides solar arrays and batteries, power control and distribution unit (PCDU) is a very important equipment. Electrical loads of a satellite may change depending on which equipment of subsystem is active at that time. Power distribution and control unit controls the exchanges of power between solar cells and batteries, ensures that while the equipment are charged, battery can be replenished, and avoid the battery discharge. Consequently, power subsystem is the only resource of the satellite, its protection is substantially crucial [25].

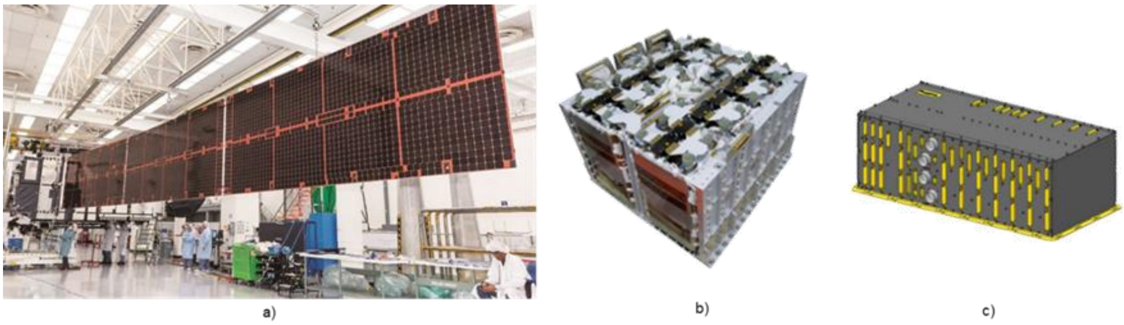

Figure 2.16 : a) Solar array. b) Battery. c) PCDU.

2.1.3.6 Telemetry and telecommand subsystem

A satellite's telemetry and telecommand (TM/TC) subsystem provides a link between the satellite itself and facilities on the ground. The purpose of the TM/TC function is to check how satellite executes. Regardless of the mission, telemetry, tracking and control subsystem is necessary for all satellites. The main tasks of this subsystem are tracing the status of the satellites via collection, processing and transmission of data from the subsystems, specifying the satellite's position, and controlling of the spacecraft via reception, processing, and implementation of commands transmitted from the ground [26].

2.1.3.7 Command and data handling subsystem

Command and data handling subsystem is the brain of the entire satellite. It controls the all operations of satellite and internal communication between the satellite subsystems. The main tasks of this subsystem are; managing all forms of data on the satellite, performing command which are sent from Earth, preparing data for transferring to Earth, collecting and processing information about all subsystems and payloads [27].

2.1.3.7.1 Onboard Computer (OBC)

Onboard computer (OBC) is the heart of the command and data handling subsystem. OBC can be referred to as the computer of satellite's avionic subsystem. It runs the spacecraft's on-board software which controls the critical functions needs to be performed effectively. The onboard computer is the equipment which acts as a bridge that connects the other subsystems with each other. OBC is the microprocessor board, consisting of microprocessor, non-volatile memories, volatile memories and the companion chip that connects the microprocessor to different peripherals and also it consists flight software. OBC is responsible for telecommand decoding and processing, telemetry gathering, formatting and transmission, handling of data storage, time management, system telemetry (analog and digital) acquisition, system supervision and failure detection isolation and recovery (FDIR) execution, AOCS sensors data gathering, AOCS loops execution and actuators commanding, temperature acquisition, thermal control loop execution and actuators commanding, system data formatting and transmission etc.

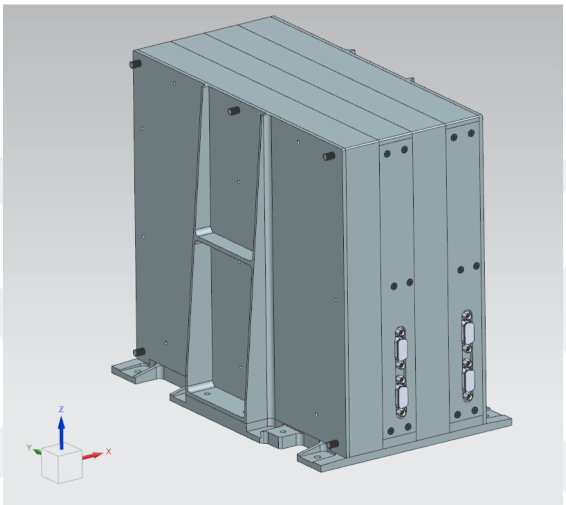

Figure 2.17 : On-board computer.

Processor provides processing and control capability. Flight Software runs and stores on this module. It provides time management function, housekeeping telemetry storage, interfaces of typical avionics busses (CAN, SpW, 1553, UARTs, etc.).

The TC decoder performs the command sent from the ground segment to the satellite and the decoding of these telecommands. It has a transfer frame structure and includes header, data and error control parts. In order to reach the raw data in these commands, incoming TCs must be decoded. TM encoder is the opposite of TC decoder. When OBC read housekeeping and monitoring TMs to ensure the health and status of all equipment, TM encoder create TM frame and we add some parts like header, trailer etc. And these TMs send to ground segment.

High Priority Commands defined for critical situation/equipments. These commands are proceed without SW. Ground segment access and managed this functions independently from SW. Command Pulse Distribution performs this function.

Reconfiguration unit, incase of harware or software error, this function has ability to reconfigure autonomously. Safe guard memory is store critical parameters to be shared between PMs. Safe Guard Memory is going to be utilized mainly for modules configuration information. On/Off statuses, isolated equipments etc. Are also goiing to be included into the information in order to make them available for Processor module in case of switch over event.

2.1.4 Spaceborne electronic equipment

Each satellite subsystem consists of electronic equipment. Electronic components are comprised from electronic box, printed circuit board (PCB), component, and cable. Electronic packaging is the design and manufacture of enclosures for electronic equipment ranging from individual semiconductor devices to complete systems. Protection from mechanical damage, cooling, radio frequency noise emission and electrostatic discharge must be aimed for electronic systems. Electronic packaging is an important discipline in mechanical engineering. It is based on mechanical engineering principles such as dynamics, stress analysis, heat transfer and fluid mechanics.

Electronic packaging can be sorted by levels as follows:

- Level 0 – Chip. Protecting a bare semiconductor die from contamination and damage.
- Level 1 – Component. For example, semiconductor package design and the packaging of other discrete components.
- Level 2 - Printed circuit board (PCB).
- Level 3 – Assembly. One or more PCB and associated components.
- Level 4 – Module. Assemblies integrated in an overall enclosure.
- Level 5 – System. A set of modules combined for some purpose.

An electronics assembly consists of component devices, circuit card assemblies (CCAs), connectors, cables and components such as diodes, transistor, inductor, switches, etc. that may not mount on the circuit card. Electronic components can be found either in discrete or integrated form. Discrete form is a term used only for individual components such as a transistor, diode, resistor, capacitor, and inductor. When it comes to integrated circuits, an IC is a collection of other discrete components. Integrated circuits (ICs) are the cornerstone of modern electronics, which are the heart and brain of most circuits. They are present nearly any circuit board. In terms of thermal analysis of electronic equipment, it is quite important to understand them, inside and out [28].

2.1.4.1 Components of electronic equipment

Many types and numbers of components are found in electronic equipment mounted on the PCB. Their package type, mounting properties, heat dissipation and surface area properties, and installation on PCB is critical for heat distribution and rejection. Printed circuit board (PCB), components and their features are listed below.

Printed Circuit Board: Printed Circuit Boards (PCB) can be defined as robust non-conductive boards built on substrate-based structure. The PCBs are mainly utilized to provide electrical connection and mechanical support to the electrical components of a circuit. They are common in electronic devices and in most cases, they are easily identifiable as green colored board. Based on the design specifications and requirements, many active (such as batteries) and passive components (such as inductors, resistors, and capacitors) are mounted on the PCBs. The connection between the components on a PCB are managed with copper interconnects, called traces, which act as the pathway for the electrical signals [29]. In Figure 2.18, traces and PCB can be shown.

Figure 2.18 : (a) Traces of PCB. (b) PCB.

PCBs have complex design which starting from single layer to 20 to 30 layers with hidden vias and embedded components. PCB vias can be specified as vertical interconnect accesses for establishing the electrical and thermal connection through one or more adjacent layers of the circuit board. PCB and layout of PCB which demonstrates traces are shown in (Figure 2.19).

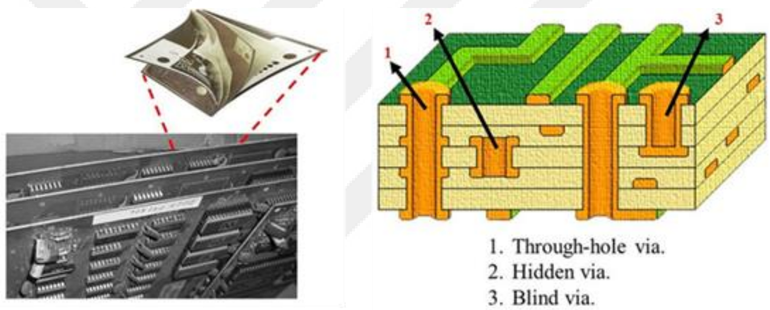

Figure 2.19 : (a) Layers of PCB. (b) Vias of PCB.

Each PCB consists of various electronic components on it. These components are typically industrial products manufactured individually. Their type, functionality and application determine the package type. The common classification of electronic components is made by energy source. Components which act as energy sources are called active components, while components that require external energy sources to work are called passive components.

Battery: Batteries supply needed voltage to the circuit. Generally, these are used in DC circuits. It is an active component that converts chemical energy into electrical energy and provides power. Batteries include one or more cells and each cell has an anode, cathode, and electrolyte. Batteries varies in sizes and voltages. Moreover, these can be grouped as primary and secondary. Primary ones are utilized until they discharge the power, whereas secondary ones can be used after drained out by recharging them. In electronic circuits, it is often used 1.5V AA Batteries or 9V PP3 Batteries [30].

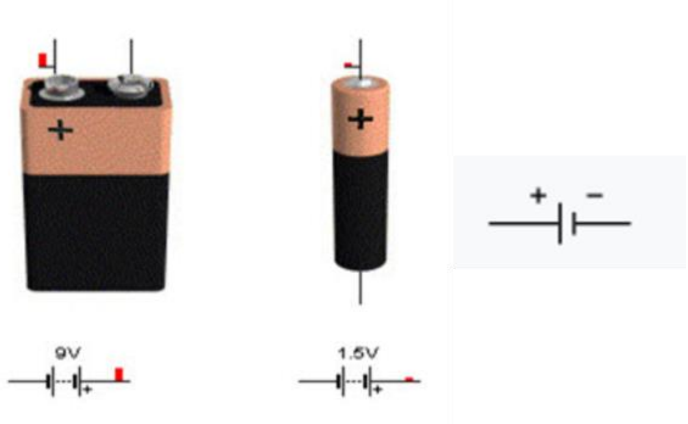

Figure 2.20 : (a) Battery. (b) Battery symbol.

Capacitor: A capacitor is the basic electrical and electronic circuit element formed by placing an insulating material between two metal layers, taking advantage of the ability of electrons to be polarized and store electrical charge in the electric field. It is a two-terminal passive electronic component. It is used for electric charge storage, reactive power control, information loss prevention, conversion between AC/DC and is an indispensable element of all integrated electronic circuits. A capacitor interferes the DC signals and allows the AC signals. The characteristics of capacitors can be counted as;

- The type of insulator used between the plates,
- Working and withstand voltages,
- The amount of cargo they can store.

countable. After considering these criteria, the capacitor suitable for the requirement is preferred. The physical size of capacitors depends on their operating voltage and the amount of charge they can store. Voltage value is considered for thermal analysis. The effect of a capacitor is known as capacitance. Capacitors and their symbols are shown in (Figure 2.21) [30].

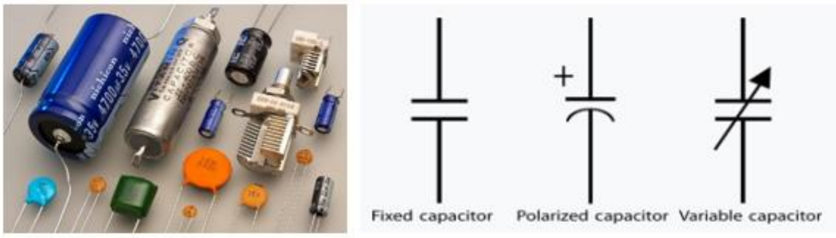

Figure 2.21 : (a) Capacitor. (b) Capacitor symbols.

Resistor: A resistor is a passive two-terminal electrical component which applies electrical resistance. According to Ohm's law, it is a circuit element that causes a voltage drop between its terminals. Resistors are common elements of electronic circuits and are omnipresent in electronic equipment. In electronic circuits, resistors are used to decrease current flow, arrange signal levels, dividing voltages, deflecting active elements, and terminating transmission lines. The resistors are separated into two groups as to electrical power, which are high-power resistor and low-power resistor. High-power resistor is above 2W whereas low-power resistors are under 2W. Besides, according to usage requirement, resistors can be grouped as fixed, adjustable, thermistor and photoresistor. Fixed resistors are used for applications required fixed resistance value. Precision is critical for this kind of resistors. Adjustable resistors can be applied in cases where variable resistor value is required. Sensitivity is not that important. Thermistors are resistors that change under the influence of heat. It can be divided into 2 classes as PTC (Positive Temperature Coefficient), which is a resistance whose value increases with the effect of heat, and NTC (Negative Temperature Coefficient), which is a resistance whose value decreases with the effect of heat. The effect of a resistor is known as resistance. Resistor and resistor symbol are given in (Figure 2.22) [31].

Figure 2.22 : (a) Resistor. (b) Resistor symbol.

Inductor: A device that creates current (induction current) by changing the magnetic flux in alternating current circuits. An inductor is a circuit element, a kind of current source, that creates a potential difference between its two ends as the current flowing through it changes. The inductance of a circuit depends on the geometry of the circuit as well as the magnetic permeability of the surrounding materials. Unlike resistor, it depends on frequency. To avoid from resonance, selection of bobbin is a critic parameter. Inductor and inductor symbol are given in (Figure 2.23) [32].

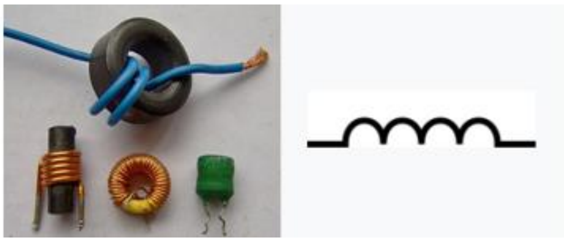

Figure 2.23 : (a) Inductor. (b) Inductor symbol.

Integrated Circuit (IC): An integrated circuit is a group of electronic circuits placed on a metal plate designed with semiconductor materials, usually silicon. Integrated circuits (microchip) are smaller in size than discrete circuits where each electronic circuit element is independent. DC-DC converters and MRAM are given as an example. DC-DC converters are circuits that convert one DC (direct current) voltage to another DC voltage of different amplitude and control the average value of this voltage. It is carried out using at least one active and one passive element. The working principle of DC-DC converters is based on switching a DC voltage onto the load [33]. MRAM (Magnetoresistive Random Access Memory) is non-volatile memory that stores data magnetically.

Switch: A switch is a circuit element that allows to interrupt the current in electrical circuits or change the direction of the current from one conductor to another conductor. In its simplest form, a switch has 2 contacts (electrical connection). The circuit is "closed circuit" when there is no current decoupling between these two contacts in the "open" position of the switch, and the circuit is "open circuit" when there is a current decoupling in the "closed" position of the switch [30].

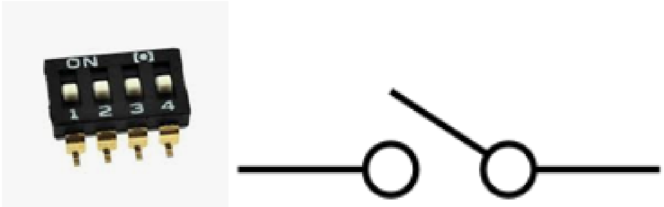

Figure 2.24 : (a) Switch. (b) Switch symbol.

Transistor: A transistor is a semiconductor circuit element used to control a large amount of current or voltage with a small voltage or current. Thanks to these properties, transistors are used in electronic devices to amplify or change the power of electrical signals. Transistors can be used to turn current in a circuit on or off as an electrically controlled switch, where the current is determined by other circuit elements. MOSFET (Metal Oxide Semi-Conductor Field Effect Transistor) is the most popular transistor and used for power balancing purposes in analog and digital circuits. There are two types of transistors, called PNP and NPN. Transistors with two blocks of n-type semiconductor material and one block of p-type semiconductor material are called NPN. Similarly, if it has one layer of n-type material and two layers of p-type material, the transistor is called PNP. Transistors have three terminals, emitter, collector, and base. Symbols of NPN and PNP type transistors are given in (Figure 2.25) [34].

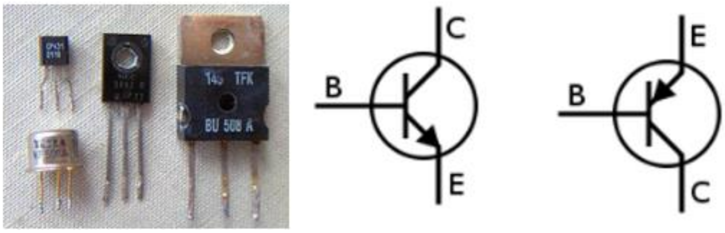

Figure 2.25 : (a) Transistor. (b) NPN bipolar transistor notation. (c) PNP bipolar transistor notation.

Diode: A diode is a circuit element that only passes current in one direction. Elements whose resistance in one direction is negligibly small, and whose resistance in the other direction is very large. Diode and diode symbol are shown in (Figure 2.26) [35].

Figure 2.26 : (a) Diode, (b) Diode symbol.

Rectifier: A rectifier is an electrical circuit used to convert an alternating current consisting of one or more semiconductor elements (for example, a diode) into a direct current. All rectifiers are made by connecting several diodes to each other in a certain way in order to make the process of converting AC to DC, which is possible with a single diode, more efficient.

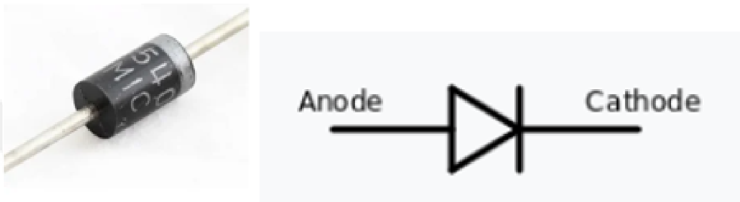

Figure 2.27 : (a) Rectifier diode, (b) Rectifier diode symbol.

Connector: Electrical connector is an electromechanical device used to join electrical conductors and form an electrical circuit. It is used for power, data, and audiovisual applications. For the electronic equipment, PCB mount connectors and chassis connectors are used. PCB mount connectors are soldered to a printed circuit board supplies a point for cable or wire attachment. Chassis or panel connectors are attached to a frame of equipment so users can connect a cable to a stationary device [36].

Figure 2.28 : (a) Connector. (b) Connector symbol.

The main heat source of the electronic equipment is power source. Another heat source can be counted as other electronic equipment in satellite. Equipment can warm up other equipment via conduction and radiation. The equipment on the satellite dissipates heat through the structural panel by conduction. Moreover, heat is rejected from the outer surface of equipment by radiation.

Power sources on the equipment are components. A certain part of component's power is wasted. Efficiency is used term which defines the ratio of energy output to energy input. Efficiency of components determines how much energy will transform to heat. Calculation of efficiency can be done with the following formula [37],

$$\eta = \frac{E_{out}}{E_{in}} x100\% \tag{2.1}$$

2.1.4.2 Electronic packaging

Electronic components are available in discrete or integrated form. The discrete form is saved only for individual components such as a transistor, diode, resistor, capacitor, or inductor. Semiconductor packaging is the enclosure of a semiconductor component. The structure of a semiconductor package consists of a semiconductor chip, a carrier on which the chip is placed (package PCB, lead frame, etc.) and a molding component surrounding them. Molding compounds has a crucial role to reject the heat from inside and protecting the chip from external damages.

The packaging is as important as the component itself. There are three main purposes which can be listed as,

- Protection of semiconductor from physical impacts,
- Protection from corrosion,
- Decision of how to place the electrical contacts from the semiconductor device via a PCB.

Packaging technology consists of internal structure technology, external structure technology, and surface mounting technology (SMT) [38].

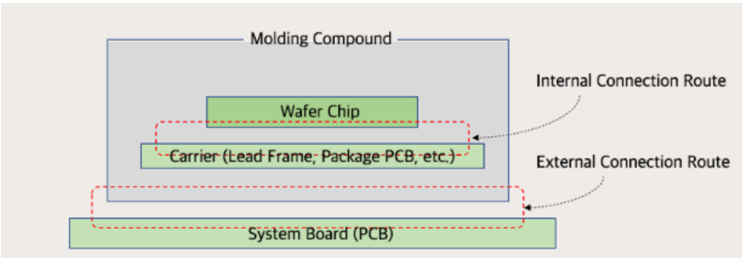

Figure 2.29 : Internal and external structure of semiconductor package.

The internal and external connections provide to connect signals from internal chips to the outside. As package size reduces in time, the volume of connection wires increased with it. This problem was solved with bumps instead of metal wires. Nowadays, bumpers or balls are the most popular connection types.

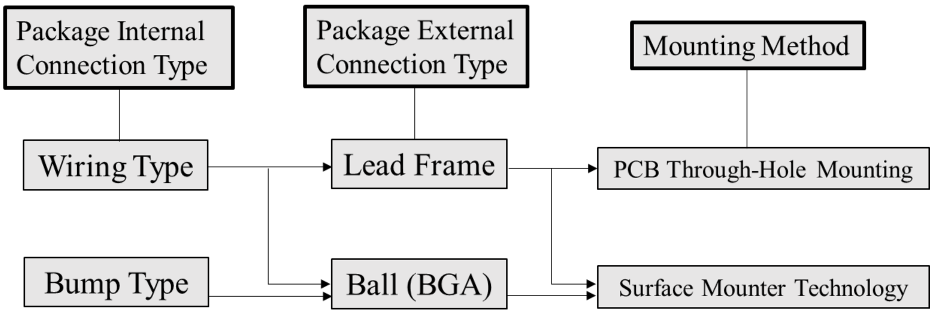

Figure 2.30 : Diagram of connection types and mounting method.

The usage of lead frame was shifted to balls (BGAs) for the same reasons. While the "wire – lead frame – PCB through-hole mounting" was used before, "bump – ball grid array (BGA) – surface mounter technology" is currently used method.

Semiconductor packages can be divided into two groups in terms of internal structure: wiring and flip chip. In the wiring method, the chip and the carrier are connected through wire bonding, while die is a face up. The flip chip method connects the carrier and the chip with small balls, named bumps, with a face down. The flip chip method is a groundbreaking method with a shorter signal travel distance and a more powerful adhesion strength. The most important advantages of the flip chip method are that reduction of the volume of the package and improvement of the power consumption and signal flow. In addition, epoxy material between bumps and carrier is another matter. The size of the chip can be decreased after molding. Internal package types can be shown in (Figure 2.31).

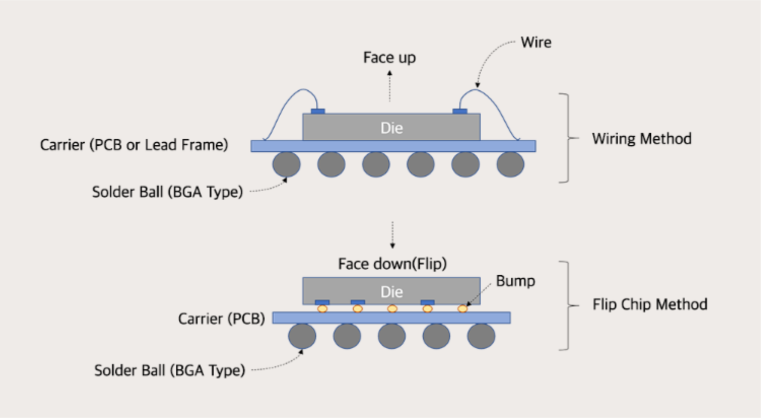

Figure 2.31 : Internal package types.

There are large number of packaging types. External package types are also called as integrated circuit packaging. The IC packages can be classified based on mounting type. As mentioned above, all IC packages fall into two main categories, such as PCB-through-hole mounting (PTH) and surface mounter technology. In through-hole packages, IC leads are designed to be passed through holes on the PCB before soldering. PTH was generated in order to work with printed circuit boards having tracks on both sides and inner layers. PTHs are bigger and easy to work with. Through-hole mounting is still available in commercial circuits where surface-mount cannot be used. Surface-mount packaging enables that component is mounted directly on the external side of the PCB. SMT fixes a chip to the system board surface by means of soldering. Surface-mount packaging lets more component place automatically in a smaller area.

The second way to classify IC packages is how the pins are laid out of the device. All ICs have linear, rectangular, or square shapes. The pinout can be linear, in two parallel directions, all four sides, or matrix form.

As the third, IC packages also can be classes according to their pin shape. Pin shapes have various types, such as linear, mutual folding, L-shape, J-shape, electrode bud, needle shape, solder bud, tape/film shape.

The terminal count is another way of classification for IC packages. Two-terminal, three-terminal, four-terminal, five-terminal, six-terminal, and more than six-terminal IC packages are feasible.

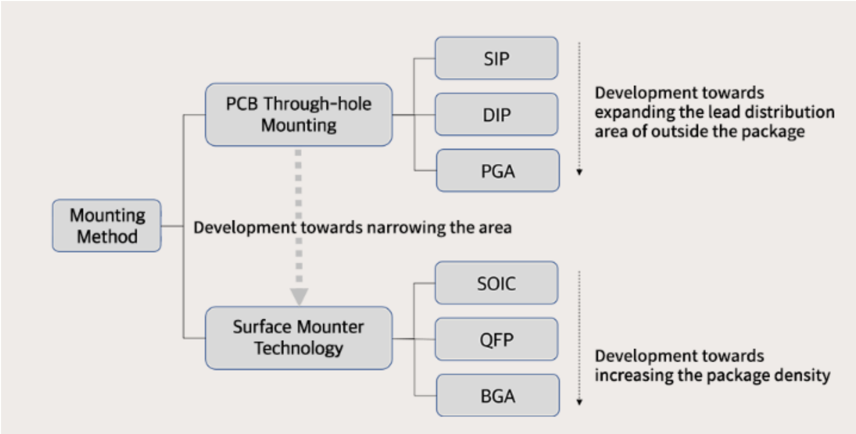

Figure 2.32 : Classification of mounting method.

As mentioned above, there are numerous numbers of IC packages classifications depends on different vendors, suppliers, and manufacturers [39]. The major IC packages types are listed in (Table 2.1).

Table 2.1 : IC package types.

IC Package Types	Figures
Single in-line	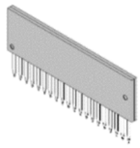
Zigzag in-line	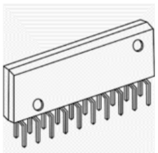
Dual in-line	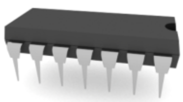
Quad in-line	
Ceramic flat pack	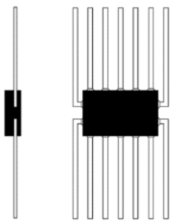

Table 2.1 (continued): IC package types.

IC Package Types	Figures
Surface-mount small-outline	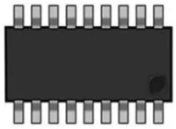
Surface-mount leadless (Flat Pack, Chip Carrier)	 
Grid Array/Matrix: (Pin Grid Array-PGA), (Ball Grid Array-BGA)	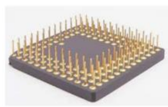 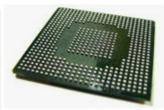

3. THERMAL BALANCE TEST

3.1 Test Objectives

Testing is the significant step for developing of space equipment. There is no doubt that test shows that equipment operates correctly both on ground and in space. It gives confidence to stand harsh environmental conditions and operate well in space [40]. During the equipment developing stage, various tests should be applied to an equipment such as environmental testing (thermal, random/sinus vibration, shock and acoustic), functional and performance (FFT/RFT), and electrical testing (EMI/EMC). Table 3.1 shows which tests are required or no-required for several types of equipment.

In space industry, there are strict rules to be obey. Several standards are determined to develop equipment. Generally, ECSS-E-ST-10-03C, which is one the standards of European Cooperation for Space Standardization (ECSS) established by European Space Agency (ESA), and MIL-STD-1540, one of the standards of the Department of Defense of USA, are mainly used standards. These standards are applicable to space systems and provide environmental and performance test requirements for a space systems, subsystems and equipment. A procurements contract is generally connected with successful test results. ESA states test requirements for space equipment [41]. These requirements must be fulfilled before a unit (or equipment) accepted. These tests can be separated into three groups:

- Qualification tests,
- Acceptance tests,
- Protoflight tests.

Qualification testing provides evidence that the space segment element or equipment is performing to its specifications in the intended environments with specified qualification margins. Qualification testing shall be performed on dedicated qualification models except when using protoflight approach. The qualification test level is applied to particular models such as structural-thermal model (STM), qualification model (QM), engineering qualification model (EQM) or others which have same dimensions, drawings, materials, tooling and methods as the flight equipment. It is a well-known fact that slight changes compared to the flight model can be applied to the QM as long as does not affect the qualification of the unit. It should be noted that environmental testing of a complete equipment may not be applicable, for this reason, qualification test may be applied on some assembly levels with the help of analysis and similarity assessment.

Acceptance testing provides evidence that the space segment element or equipment is performing to its specifications in the intended environments with specified acceptance margins. It shall be conducted on each flight model, except the one used as Protoflight. The acceptance test shall be performed after qualification test has been completed. The aim of acceptance testing is to determine whether equipment is conformed to fly. In contrast the qualification testing, acceptance testing should not exceed the margin of safety (MOS) and give rise to unrealistic modes of failure.

Protoflight testing is the combination of the qualification and acceptance testing objectives for the first flight model. The protoflight approach can be applied to each level of space system. Protoflight testing will be performed on the first flight model to confirm that the space segment element or equipment is performing to its specifications with specified margins of qualification in the envisaged environments and is ready for delivery and subsequent use, free from workmanship.

Table 3.1 : Electronic, electrical and RF equipment test requirements [41].

Test	Qualification Test	Acceptance Test	Protoflight Test
Functional and Performance (FFT/RFT)	R	R	R
Thermal Balance	R	R	R
Thermal Cycling	R	R	R
Sinusoidal Vibration	R	-	R
Random Vibration	R	R	R
Acoustic	-	-	-
EMC	R	R	R
Legend: R: Required -: Not Required			

The main focus on this thesis is thermal testing. Requirements of thermal testing are based on the three types of studies.

- ECSS standards (Europe),
- Equipment data which are brought together during qualification testing and operation in orbit,
- MIL and USAF standards, (United Stated).

The purpose of these studies was to systematize the test conditions for equipment thermal cycling and vacuum test. To accomplish these studies and to create a standard environment test specification, two important tasks were contemplated:

- Analysis of the effect of temperature limits on thermal design and philosophy of applying and determining temperature uncertainty.
- Test conditions were standardized by investigating test parameters such as temperature test duration (number of cycles and dwell time) and test environment conditions.

Based on these standards, temperature limits and margins of equipment thermal design are determined. There is a certain difference about temperature limits between US and Europe programme. European programmes present stricter temperature limits. In this thesis, thermal design limits and test levels are determined according to European standards.

There are three main objectives of thermal testing as described below:

- Environmental stress screening: It is the process which hardware is exposed to the physical stresses and forces failures that are not unobservable into observable failures. These hidden failures cause premature component failure. In thermal testing, test temperature, the number of test cycles, and the rate of temperature change are parameters which determine the performance of environmental stress screening. Temperature transition is slow compared to TCT, thus stress screening is the secondary concern in the thermal vacuum cycling test.

- Performance verification: It shows that an equipment can be operated in the extreme environment. Performance verification (or turn-on capability) can be demonstrated at hot and cold temperatures in the thermal testing.

- Survival demonstration: Survival demonstration objective demonstrates in what temperature range the equipment survives. The equipment shall be turned on at these temperature, on the other hand, it may not meet specifications at these severe temperatures. Moreover, the equipment or unit must not demonstrate performance degradation when the temperatures are bring to operational temperature range. The survival range has the most extreme temperatures for an equipment.

It is important to emphasize that the thermal cycle test is more applicable to achieve environmental stress screening while performance verification and survival demonstration are the second concern for thermal cycle test. The opposite case is true for thermal vacuum cycling test.

3.2 Thermal Testing

The main focus on this thesis is thermal testing. A standard equipment thermal testing falls into four different categories such as thermal cycling test (TCT), thermal vacuum cycling test (TVCT), thermal balance test (TBT) and burn-in. Functional tests should be performed during thermal cycling and thermal vacuum at temperature extremes.

3.2.1 Thermal cycling test

Thermal cycling test specifies that equipment are subjected to functional tests at ambient temperature. Functional tests are performed at the extreme temperature levels during the test. Equipment thermal cycling test is performed in a thermal cycling chamber with temperature controlled dry air. In order to perform at hot temperatures, the dry air is heated from the walls of the chamber. On the other hand, cooling is managed by pumping liquid nitrogen into the chamber baseplate. The environment is circulated by fans to prevent temperature gradients on the test object and accelerate temperature transitions. The capability of equipment resistance to extremely low and high temperatures and capability to resist cyclical exposures to these extreme temperatures are the main objectives of thermal cycling test. There are some important parameters for achieving thermal cycling test such as temperature range, number of cycles, dwell or soak duration, rate of temperature change during transitions, and operational conditions. Thermal dwell means that the time required to assure equipment have accomplished thermal equilibrium at hot and cold temperatures. Thermal soak duration is the time that equipment is operating and temperature of equipment's baseplate are kept within the allowable tolerance of the test temperature [42].

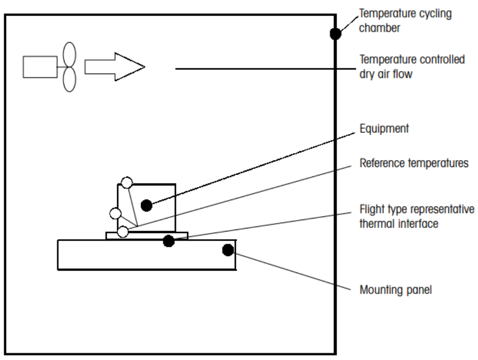

Figure 3.1 : Thermal cycling test.

The test starts with the equipment operating and the chamber environmental control is set to the hot temperature level. After the test temperature sensor reaches the test tolerance temperature, the thermal dwell period starts. Thermal soak is the duration with the unit operating between the start of the thermal dwell and the end of the functional test. At the end of the test, the equipment should met the performance requirements within acceptable tolerances.

Subsequently, chamber is set to cold temperature phase. This system is managed by turning off the chamber heating system and turning on liquid nitrogen cooling system. Equipment is set to be non-operating during the cold temperature phase to reach cold temperature as soon as possible.

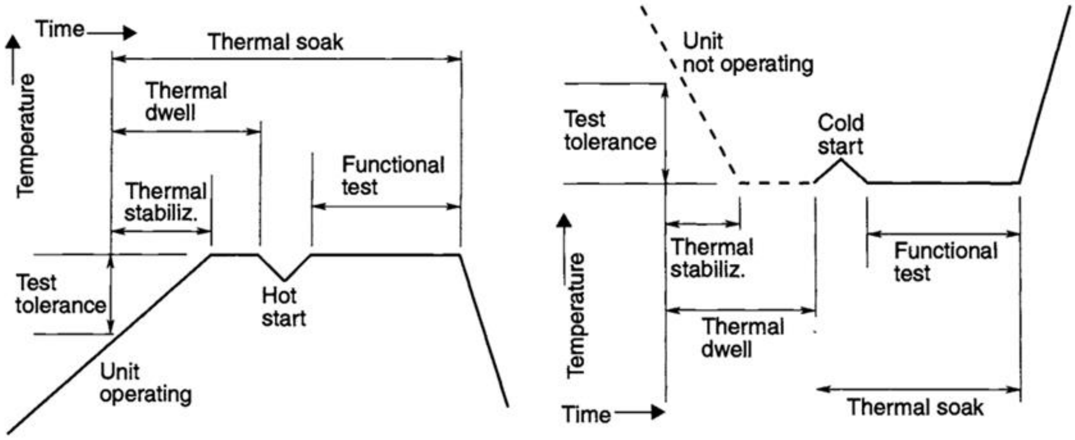

Figure 3.2 : Hot and cold temperature phases of TCT.

Thermal stabilization, thermal dwell, and thermal soak have generally similar meanings at cold and hot temperatures. Temperature stabilization is a criteria which determines the point of a test hardware to reach stable, almost steady, temperature. Temperature stabilization is accomplished when the unit with the determined thermal time constant is within 3°C of its steady-state value and the rate of change is less than 1°C per hour for steady-state thermal balance testing.

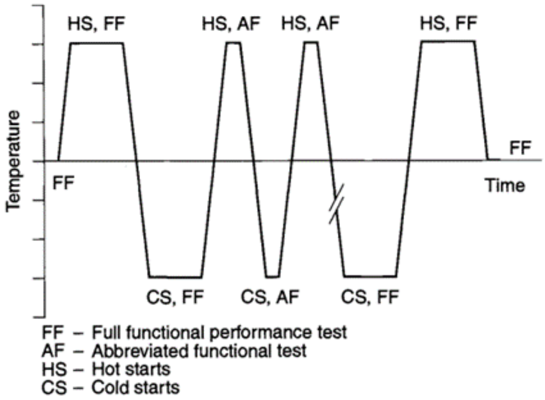

Figure 3.3 : Typical equipment thermal cycling test profile.

The thermal cycling test can be summarized with (Figure 3.3). After functional test, chamber environment is set to the hot temperature. When first cycle is completed, chamber environment is set to the cold temperature. The same procedure is applied to the each cycle (first and last). For intermediate cycles, abbreviated functional tests may be performed.

3.2.2 Thermal vacuum cycling test

Thermal vacuum cycling test defines that equipment are exposed to functional tests under vacuum environment. Test is performed to demonstrate the capability of the test equipment to operate according to requirements in vacuum at predefined temperature conditions. It simulates space environment in the absence of air and pressure. The equipment is subjected to a number of cycles under very hot and low temperatures [43]. Thanks to no convection environment, flight condition would be simulate better than thermal cycling test. At the qualification level, the test confirms the equipment design and shows that the equipment will stand the conditions of acceptance test. On the other hand, material and workmanship failures are detected because of the test at the qualification level.

A pressure of <10-5 hPa is recommended for TVAC [41]. This low pressure provides the elimination for the effects of convective heat transfer in simulation thermal conditions of space environment. An important characteristic of thermal vacuum testing is the monitoring of equipment that may display abnormal behavior in certain low pressure ranges.

The definitions which are given before for the thermal cycling test is identical to the thermal vacuum cycling test. Functional tests are performed at the extreme temperature levels during the test. After functional test, chamber environment is set to the hot temperature. When first cycle is completed, chamber environment is set to the cold temperature. The same procedure is applied to the each cycle (first and last). For intermediate cycles, abbreviated functional tests may be performed.

Equipment thermal vacuum cycling tests are separated into two categories for compatibility: the one where conduction is the dominant for cooling and the one where radiation to surrounding has considerable value or integrated in thermal analysis. The former is more possible for electronic boxes. Conduction from the baseplate of equipment is performed by mounting the equipment onto satellite panel. During the test, the mounting may not be represented as in reality, these differences can be explained with analysis or verified by testing at the system or the subsystem level. If components are cooled by radiation or both radiation and conduction, importance of heat paths increases. Radiative properties of components and equipment cases are added to the analysis and correlation with the test will be done. The temperature ranges and extremes in the thermal vacuum cycling test are similar with the thermal cycling test.

3.2.3 Thermal balance test

Thermal balance test is a part of system thermal vacuum test. It can be conducted on equipment and subsystems. Thermal balance test (TBT) is performed to confirm the sufficiency of the thermal model and the thermal design. The purpose of the test is to demonstrate the ability of electronic equiment to maintain temperatures within the specified operational limits and to verify that the equipment performs correctly under vacuum and thermal conditions. It can be performed under thermal vacuum environments at a pressure value corresponding to the type of mission, therefore it requires thermal vacuum chamber. The test is classified as a qualification development test, since it benefits to the thermal design and is only performed on the first hardware of a particular structure. Thermal balance tests are applicable for very dissipative equipment, equipment with important thermal gradients at vacuum conditions. Thermal data are taken during temperature transition (for transient correlation) or at equilibrium (for steady-state correlation). During the test, the equipment reaches steady-state temperatures in an energy balance with these environments. The thermal balance test includes dedicated thermal phases that simulate specific flight conditions. The test can include simulating various mission phases with one or more hardware configurations. The thermal balance test utilizes a defined environment and operational status for simulating the test phase. Hot-case and cold-case are simulated with thermal balance test. Hot case represents the state where the all the components dissipate maximum heat, whereas cold case on the other hand represents minimum power dissipation. It is allowed that equipment reach equilibrium temperature for that environment. Other simulations may involve transient cases that the equipment starts at an equilibrium condition and the environment and operational status are changed to reflect a flight condition, such as components drive for 0.5 ms. Almost all cases, flight hardware are exposed to thermal balance test. Qualification or engineering model of the equipment may be applied to this test. In Figure 3.4, thermal balance test profile is demonstrated. The test starts with closing the vacuum chamber door and assesment of chamber air. Pressure inside the chamber reduces below 10^{-6} mbar. Beginning of hot or cold operational phases is a choice which can be decided by contractors.

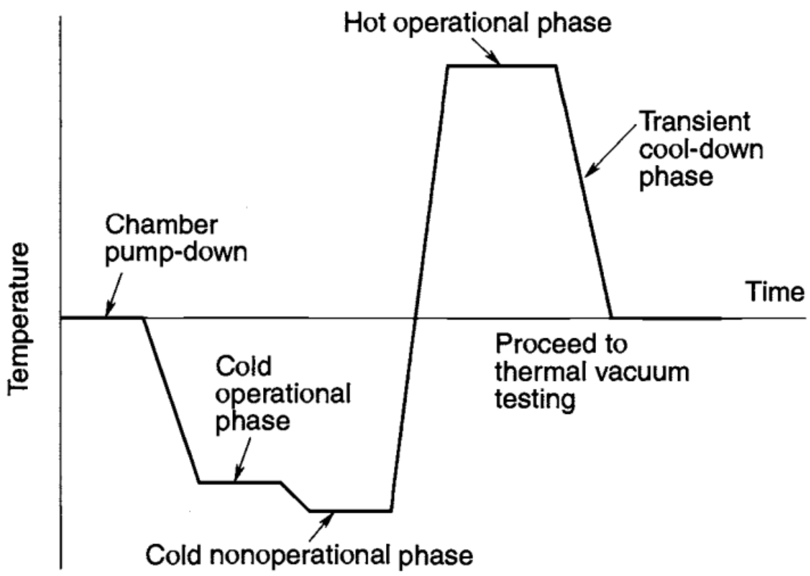

Figure 3.4 : Thermal balance test profile.

After the application of test, data from thermal balance tests are compared with the thermal model and adjustments required are made. The success criteria includes both demonstration of equipment operation and survival, and correlation of the test data with thermal mathematical model. The purpose is that correlation of test results to the thermal model predictions should be within ±3°C [44]. In practice, local locations or components of the thermal model may not correlate to within ±3°C. Insufficient knowledge of test conditions, a lack of understanding of how components interact are prevalent reasons as to why this may occur. Inability to fully correlate model and test may demonstrate the deficiency in the thermal model, test setup, or hardware. The best approach is to keep larger correlation errors and provide and explanation so as to why the difference between test and thermal model exceeds ±3°C. The correlated thermal mathematical model will be utilized to make temperature predictions for the various mission phases. Reliable steady-state data are obtained from stabilized temperatures during the test. The thermal stability requirement for thermal balance testing is more rigorous than it is for thermal cycle and thermal vacuum cycling testing. The requirement generally states that thermal stabilization should be achieved when the rate of temperature change is less than 1°C per hour, as measured over four hours. In this thesis, thermal balance test (TBT) shall be examined. Temperature ranges will be explained in the following section. The most severe operating configuration should be tested for power time domain, the power consumption and the thermal dissipation point of view.

3.2.4 Burn-in test

Burn-in testing defines that the equipment is run for an extended period of time to accelerate failures. During burn-in, beyond the thermal cycling and thermal vacuum test period, additional hours are accumulated until predetermined value is accomplished. This test provides the detection and correction of additional defects and also faultless performance is shown. Burn-in test is to monitor for workmanship errors, that’s why, it is only applicable for acceptance equipment.

3.3 Thermal Margins

Performance of electronic equipment should be confirmed on ground by measuring of input and output signals. Thermal behavior of the equipment, i.e. its capability to maintain its operation within the determined limits can only be predictable by applying thermal analytical methods. As a result, thermal design cannot provide limitless assurance that the anticipated temperatures cover all the operations of the equipment lifetime in space. These uncertainties are minimized by thermal analysis (simulation) verified by various ground tests of the equipment. The restrictions of this method are considered as uncertainties with the input parameters by the space industry.

At the beginning of the project, uncertainties are generally huge. Thermal designer should determine which uncertainties have significant effect on temperature and accordingly the designer should establish the test procedure over time. Test requirements are derived from design requirements which are strictly depend on design environment. Thermal design for space environment systems includes heat sources, heat distribution and heat sinks. In the space environment, heat sources are Sun, Earth and equipment internal heat generation while heat sink is the deep space. Heat distribution is accomplished via radiation, convection and conduction. In space environment, since there is no air or any gas, convection will be ignored from now on. These heat distribution modes will be described in detail in the following sections.

In the design phase of an equipment, thermal environment should be selected particularly to reflect the most severe temperature conditions, which can be called as worst-case environment. The worst-case environment is determined to be able to observe the operation of the equipment in the most severe conditions. The worst-case temperature environment should be determined to be considered the combination of some factors such as sun-orbit orientation, eclipse duration, operational mode and time of mission. These worst-case conditions are used to predict, via thermal analytic models, the hottest and coldest temperatures the unit or system may be exposed in its mission life. The hottest and coldest temperatures create a range called the nominal extreme temperature range which is the basis for all test temperatures.

The thermal uncertainty margin is a kind of margin of safety which are added to the nominal extreme temperatures. It shall be applied to worst-case analytic temperature forecasts. Complex view factors, surface finish and thermal insulating materials, joint conduction and surface roughness can be counted as uncertain parameters for thermal analysis. In the thermal analysis, there are lots of unpredictable values for the parameters. These margins cover the assumptions which are made for the development of thermal analysis. For example, equipment mounted internally on a satellite are modeled with the uncertainties relating to power dissipation, interface conduction, fasteners (number and torque value), whereas equipment mounted externally on a satellite are modeled with the uncertainties relating to view factors, environmental heating, power dissipation, interface conduction and so on. These uncertainties get reduced as the process advance. When the margin is added to worst-case temperature predictions, the resulting temperature generates the basis for the acceptance temperature range. The qualification thermal margin provides the increase in an environmental temperature which is expected during service life to show the durability in design and operation. It is added to acceptance temperatures for qualification testing. Moreover, protoqualification thermal margin is added to acceptance temperatures for protoqualification testing. This margin is considered to increase the severity of the acceptance test environment, whereas it does not create harsh environment as much as the qualification test environment.

Qualification test temperature range creates the envelope including acceptance temperature levels of spacecraft equipment. Taking full range of temperatures is reasonable choice to cover all temperatures under operating and non-operating conditions. There are different temperature ranges determined, such as Military Standards, NASA Jet Propulsion Laboratory (JPL), and European Cooperation for Space Standardization (ECSS, ESA-ESTEC).

According to MIL-STD-1540B, determination of test temperatures is given in (Figure 3.5). Thermal uncertainty margin can be large at the beginning of the project. The margin gets lower as the design and analysis are advanced. If the equipment needs heater, 25% excess heater control authorization is used instead of ±11°C margin. Equipment acceptance test levels are determined depending on the requirement that mounting surface or equipment baseplate would be -24°C for minimum temperature and +61°C for maximum temperature. For the equipment qualification tests, ±10°C margin is added to the acceptance test level [45].

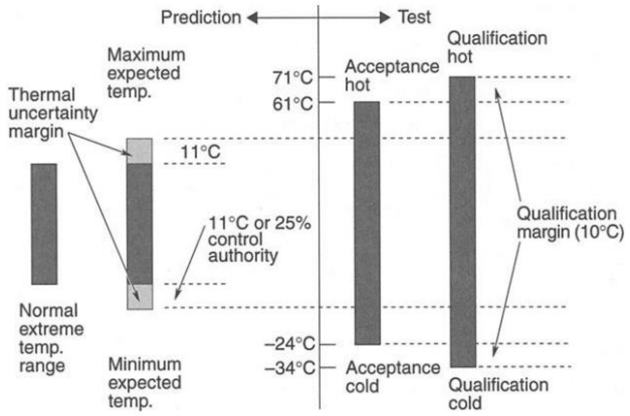

Figure 3.5 : Equipment level predicted and test temperature ranges (MIL-STD-1540B).

According to NASA JPL, thermal margin for equipment thermal test is given in (Figure 3.6). NASA JPL has used these margins to lead thermal analysis and provide positive thermal design margin, unlike military standard which depends on the thermal uncertainty and qualification margin to establish test temperatures. Many current NASA program use a qualification/protoflight temperature range of -35°C to +75°C [44].

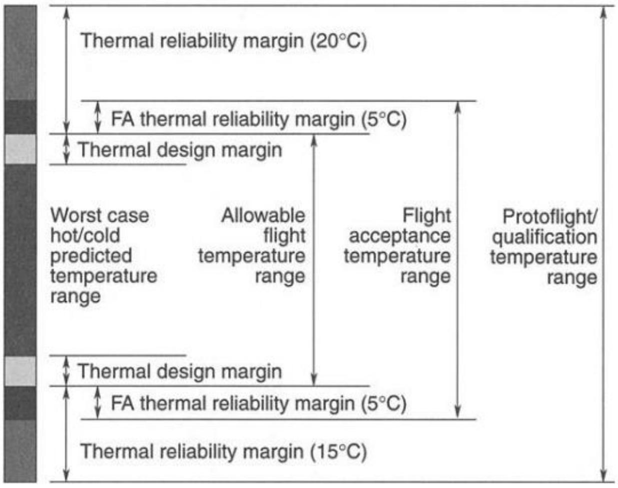

Figure 3.6 : Equipment level predicted and test temperature ranges (NASA JPL).

European and United States (US) programmes have different approach to define thermal limits. Generally, European programmes have more restrictive temperature limits than US programmes. According to European space industry, total uncertainty for unverified thermal mathematical model (TMM) predictions is at least ±15°C. This value can be decreased to ±8 to 10°C following the thermal verification process [46]. Besides unit qualification test temperature ranges, ECSS suggests unit internal design design temperature range for which components or parts selected.

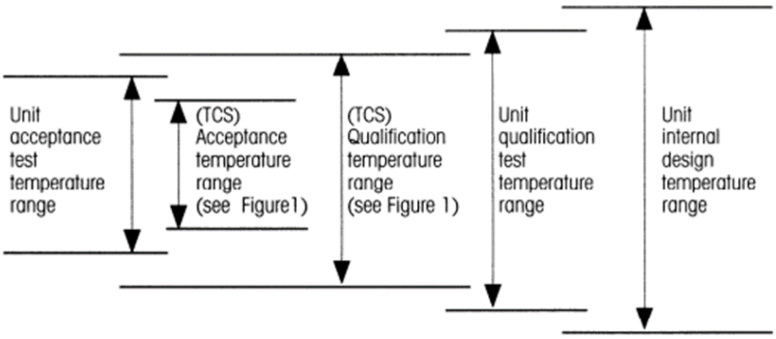

Figure 3.7 : Equipment level predicted and test temperature ranges (ESA).

Based on the type and function of the equipment, certain classifications have been made. Which subsystem the equipment is included in and the position of the equipment within the satellite are important parameters in determining this approach. The classification of equipment is separated into four groups,

- Servicing equipment (power, AOCS, TTC and data handling (OBC)),
- Payload units (TWT, OMUX and remote sensing instruments),
- Externally located equipment (antennas and solar arrays),
- Propulsion units.

3.4 Thermal Balance Test Evaluation

Thermal balance test was carried out at Turkish Aerospace, AIT (Assembly, Integration, and Test) Center on June 22-24, 2022. Test has been performed for 3 days constantly in HVT400 thermal vacuum chamber. In this context, within the framework of satellite programs carried out in Turkish Aerospace, a new On-Board Computer (OBC) is being developed. During the development of the OBC, it was decided that the IPS (Internal Power Supply), the module of the OBC, should first be tested for examination in terms of thermal targets. Temperature data were taken from the thermocouples on IPS module at specified TVAC temperatures and power configurations.

The present study focuses on qualification level TBT conducted on the IPS module and thermal mathematical model developed in order to assess the thermal behaviour of the equipment under vacuum environment. The following steps have been carried out:

1. Thermal balance testing of IPS module for the assessment the thermal behaviour of the equipment, and observation of heat dissipation.
2. Development of thermal mathematical model of the IPS module under vacuum environment.
3. Verification of thermal model using the test data.

3.4.1 Thermal vacuum test system

In this section, the characteristics of the desired vacuum environment and thermal wall conditioning for the thermal vacuum tests in the ECSS-E-ST-10-03C standard will be explained. Thermal test for OBC equipment has been performed in Angelantoni brand HVT400 thermal vacuum test system (TVTS) in Turkish Aerospace AIT Center [47,48].

Figure 3.8 : Thermal vacuum test chamber.

Two types of pumps are used in HVT400 TVTS to reach the desired vacuum level. These are the pre-vacuum pump (PVP) used for low vacuum levels and the turbo-molecular pump (TMP) used for high vacuum levels. PVP is a two-stage rotary pump that allows the pressure value in the test chamber to reach $5x10^{-2}$ mbar. TMP is used to reduce the pressure level in the test chamber to high vacuum levels (10^{-6} mbar). The working pressure of TMP is in the range of $10^{-3} – 10^{-7}$ mbar.

In the heating system, electric heaters are used to raise the temperature of the heat-carrying oil (baysilone oil) sent to the thermal walls (T_{max}=125ºC). These electric heaters, which are located on the line where baysilone oil circulates and are located in the heat exchanger, are automatically activated by the system in order to increase the temperature of baysilone oil. The heated baysilone oil is sent to the thermal walls by means of a circulation pump.

Cascade cooling system is used to reduce the temperature of the baysilone oil sent to the thermal walls. This system consists of 3 main elements. These elements can be listed as a chiller group, a high-stage compressor and a low-stage compressor. In order for the test system to reach low temperatures (T_{min}=-60°C), 4 different fluids (water, R452A, R23, Baysilone Oil) serve gradually. Thermal vacuum test system properties are given in (Table 3.1).

Figure 3.9 : Turkish Aerospace thermal vacuum chamber.

Table 3.2 : HVT400 Thermal vacuum test system properties [47,48].

Properties		Unit
Available Volume	400	L
Available Internal Dimensions (Diameter x Length)	800x800	mm
External Dimensions (Length x Width x Height)	3750x1600x2270	mm
Minimum/Maximum Temperatures	-60/+125	°C
Temperature Rate ΔT/dt	1,5	°C/min
Temperature Sensitivity in Steady-State	±1	°C
Temperature Difference in Steady-State	±2	°C
First Degree Vacuum Level	5 x 10^{-2}	torr
	(6,7 x 10-2 mbar)	
High Vacuum Level	1 x 10-6	
	(1,3 x 10-6 mbar)	torr
Maximum Power	18	kW
Internal Wall Emissivity Coefficient	ε>0,9	-
External Wall Emissivity Coefficient	ε≤0,1	-

Thermal balance testing requires the test model to achieve steady-state thermal conditions so that the equilibrium temperatures can be compared with temperature estimates from the thermal model. Actual equilibrium conditions require time, so that thermal stabilization criteria must be determined. Thermal stabilization must be defined to minimize the uncertainity without imposing unreasonable cost and schedule constraint on the test program. Thermal stabilization criteria was determined as 0,5°C per hour for the test. All thermocouples have been waited to reach 0,5°C temperature rate of change in an hour.

3.4.2 Tested device

The investigated OBC is an electronic device which is composed of a printed circuit board (PCB), components on PCB, and a chassis covering this PCB.

OBC has several interfaces with another subsystems like payload, power, attitude determination and control, and communication. The OBC will perform the following management functions:

- Telecommand decoding and processing
- Telemetry, gathering, formattin and transmission,
- Time management,
- System telemetry (analog and digital),
- Data storage,
- System data formatting and transmission,
- System supervision and FDIR execution,
- Run and store flight software.

The OBC is composed from 2 different modules, backplane, baseplate and 2 covers. Modules of OBC are Internal Power Supply (IPS) and Processor Module (PM). The processor module is a brain which contains software and processor. The internal power supply module transfers power to the processor module by reducing the voltage to appropriate levels. Backplane provides support to these boards, and transmission of data between 2 modules.

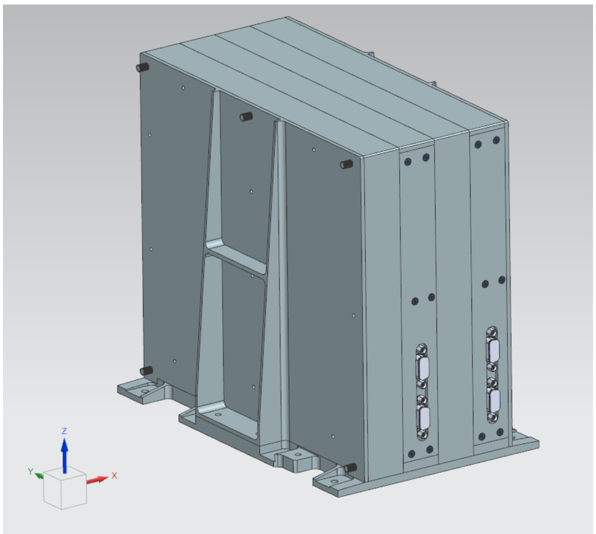

Figure 3.10 : On-board computer.

The OBC consists of an Aluminum 7075 rectangular box having a dimensions of 262x240x165 mm inside of which there are printed circuit boards (PCB) having the dimensions of 210x250x2,5 mm.

When the OBC is operational, components on the PCB act as localized heat sources. IPS module was tested, therefore numerical analysis is generated only for IPS module will be explained. DC-DC converters, transistors, rectifiers, switch, EMI input filter, controller and resistors are the components in IPS module which will be used in thermal analysis. Thermal properties of these components will be defined in the following sections.

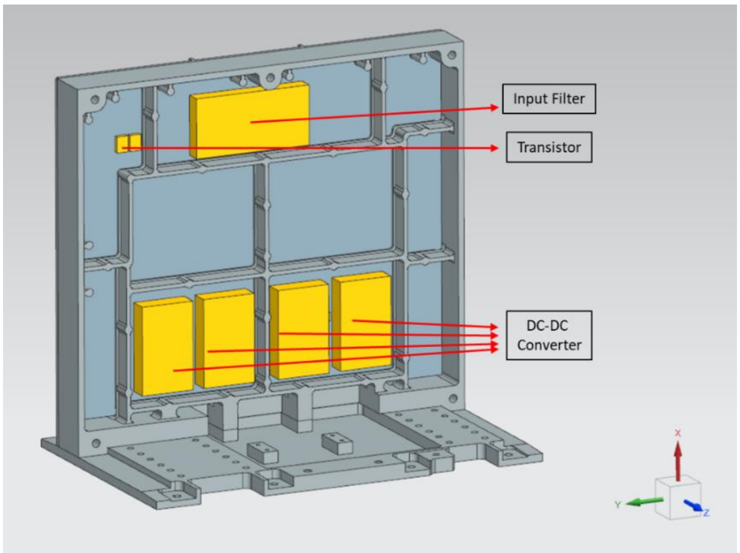

Figure 3.11 : Components on front side of IPS module.

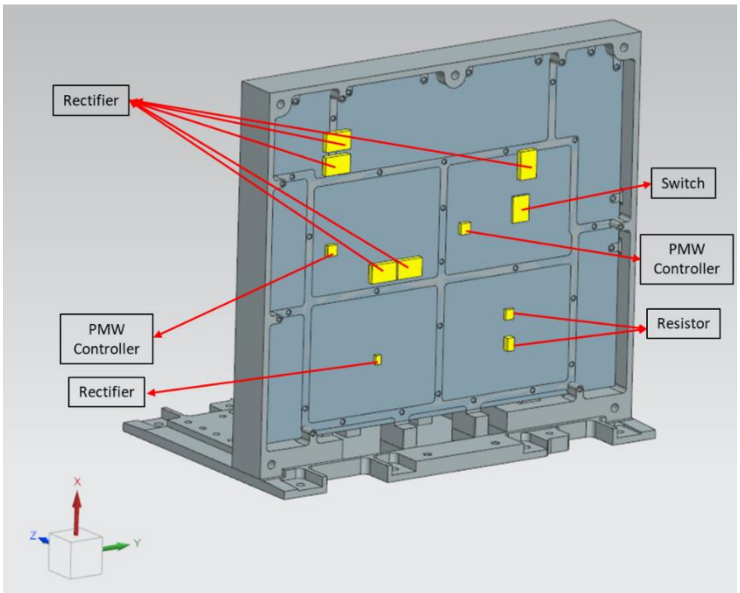

Figure 3.12 : Components on rear side of IPS module.

3.4.3 Determination of test levels

It is very critical to determine how hot the component will reach. The design of IPS module has been updated to dissipate and reject heat for avoiding from over-heating of the components. According to determined requirements for the OBC, acceptance temperature range is defined as [-25°C, +55°C] unit qualification test temperature range is defined as [-30°C, +60°C].

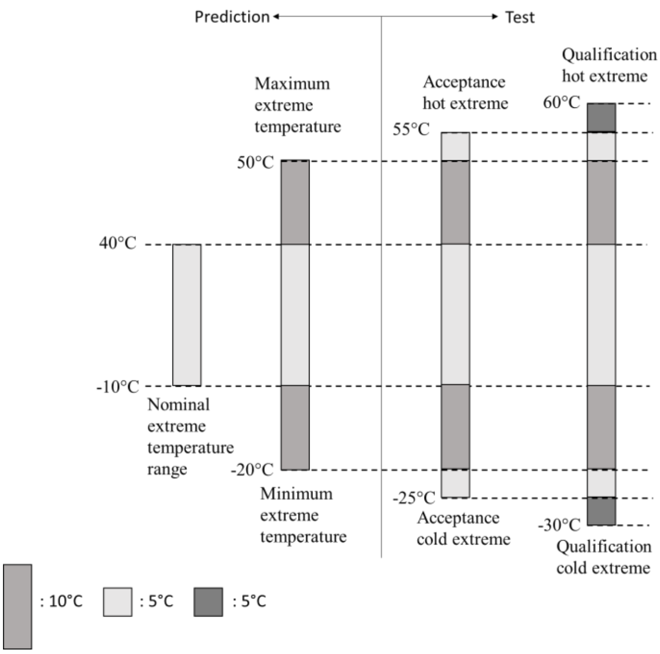

Figure 3.13 : Schematic representation of test temperature levels.

3.4.4 Location of the temperature sensors

In order to measure the temperatures during TBT, 33 temperature sensors were installed to different locations along the IPS module and 6 temperature sensors in TVAC, via aluminum kapton tapes. 7 of them were installed on aluminum parts, 19 of them were installed on components and 7 of them were installed on PCB, and the rest of them were installed inside the thermal vacuum chamber. Thermocouple layout is shown in (Figure 3.14, Figure 3.15, Figure 3.16, Figure 3.17).

Thermocouple layouts were determined as;

1. On components that are expected to get very hot,
2. Distance 1 mm from certain components to get an idea of the resistance between the component and the PCB,
3. To understand the effect of the bolted connection on the heat dissipation, 1 mm away from the bolted connection on the PCB,
4. Mechanical parts (cover, carrier, baseplate).

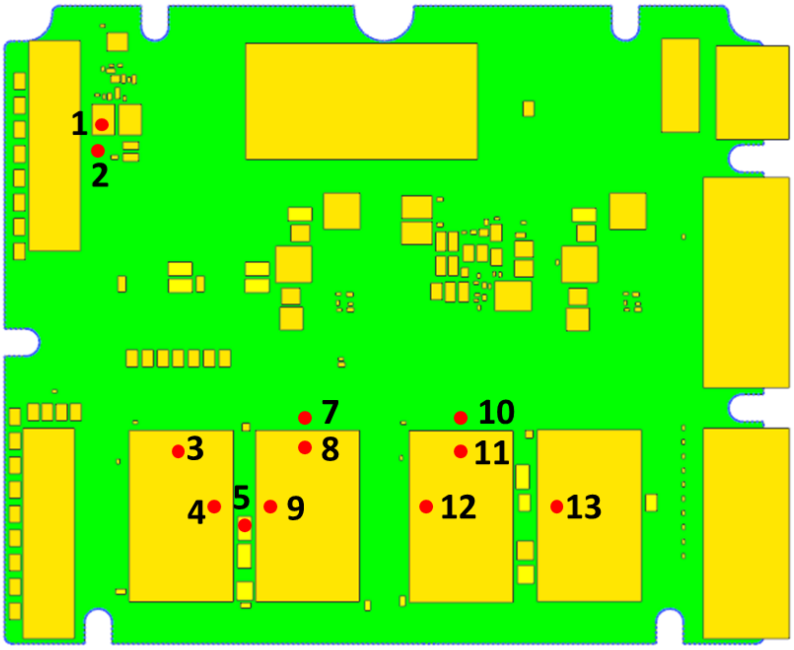

Figure 3.14 : Thermocouple layout on front side of PCB.

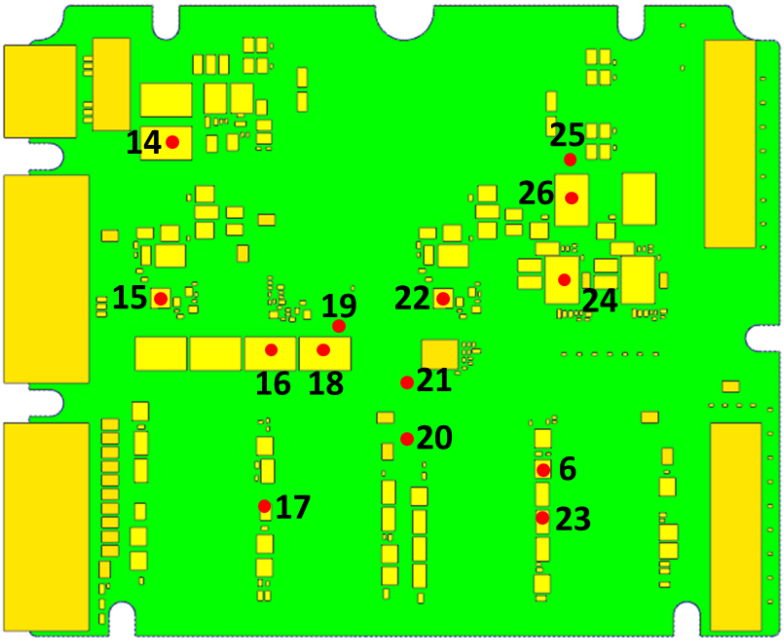

Figure 3.15 : Thermocouple layout on rear side of PCB.

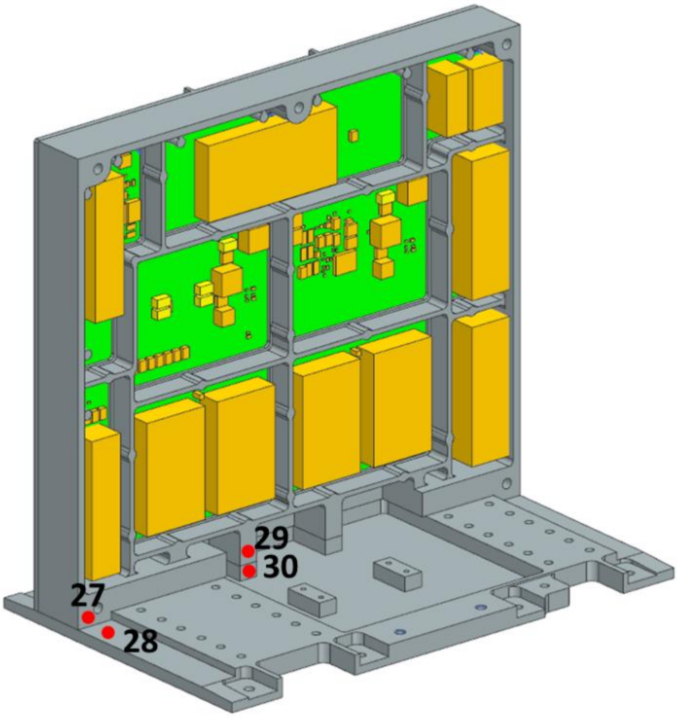

Figure 3.16 : Thermocouple layout on front side of aluminum parts.

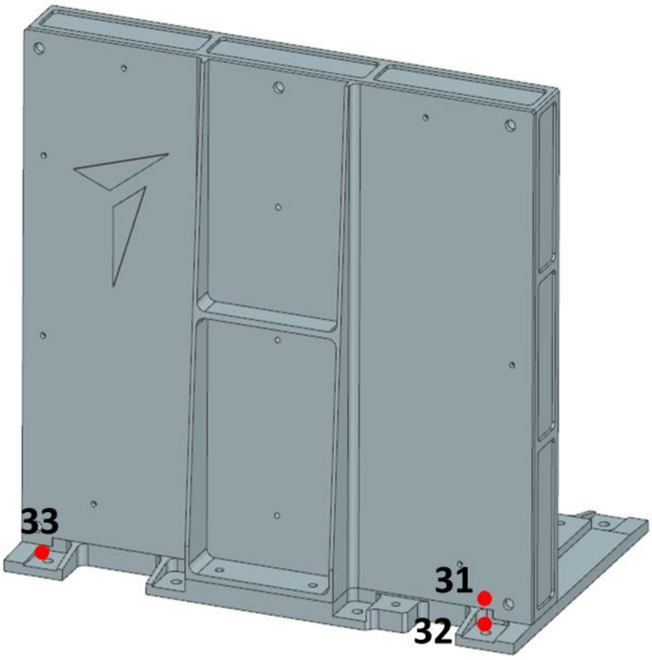

Figure 3.17 : Thermocouple layout on rear side of aluminum parts.

PT100 sensors were used to measure temperatures. Working principle of PT100 is which change in temperature results in a change in the electrical resistance of the sensor. During the TBT, temperature measurement uncertainties occur due to the measurement accuracy of PT100 sensors which is ±1°C [49]. Installation of thermocouples 31, 32, and 33 is shown closely in (Figure 3.18).

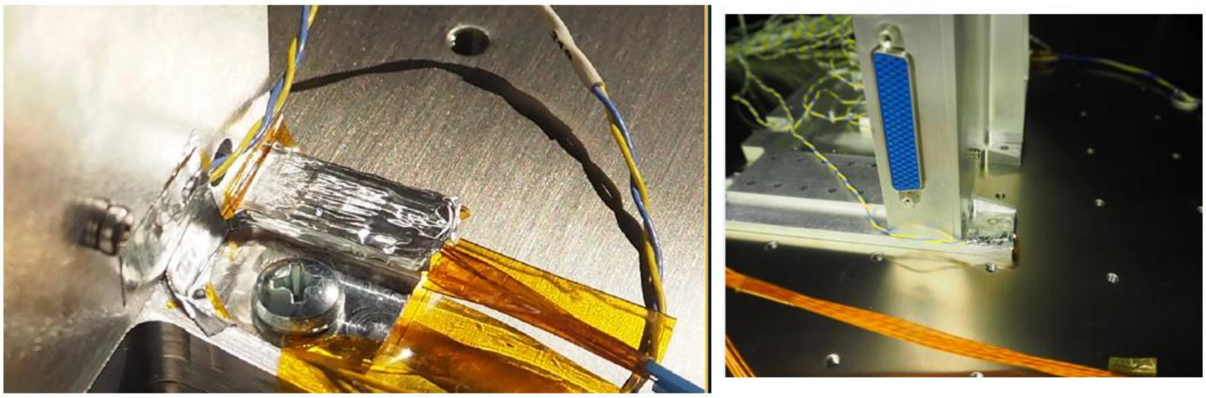

Figure 3.18 : a) Installation of thermocouple 31 and 32. b) Installation of thermocouple 33.

3.4.5 Application of test

Thermal balance test was performed for 60°C which is qualification temperature. Thermal plate and walls in thermal vacuum chamber were set to 60°C. In order not to damage the components, 20°C was chosen to start point. The temperature was gradually increased to 40°C and 60°C. Power configuration for 60°C test condition is given below in (Table 3.3).

Table 3.3 : Power configuration for IPS.

Test Case	Temperature	+5V Output Current	+15V Output Current
1	60	4	0,2

Test has been perfomed with one cycle. Time of cycle has been applied as,

- In case of no change of temperature, at least 2 hours on test steps,
- In case of changing of temperature, it has been performed as at least 0,5°C/hour for 60°C environment temperature.

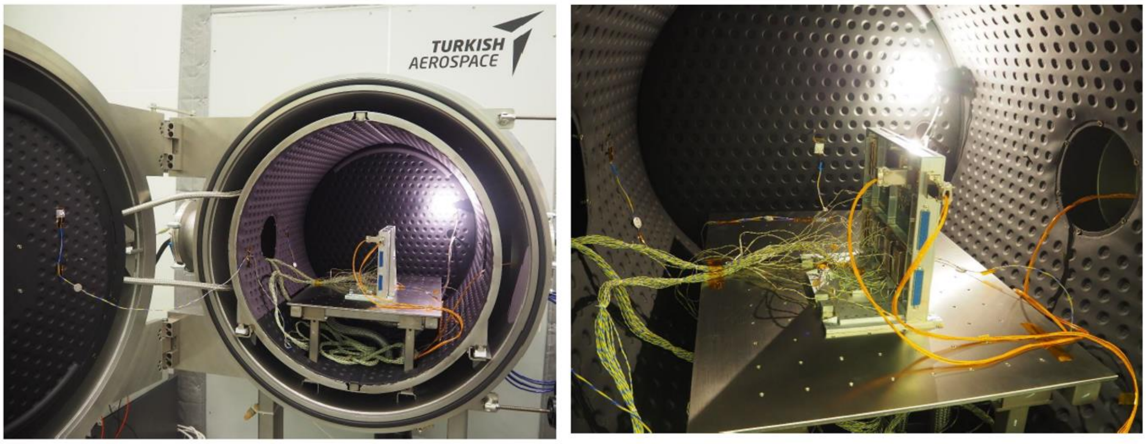

Figure 3.19 : IPS module in thermal vacuum chamber.

Before the test: Before starting the test, the thermocouple placements were made to the previously determined points with the help of aluminum kapton tape. The equipment was mounted on the thermal plate in TVAC. The picture of IPS module in TVAC is seen in (Figure 3.19). Before closing the door, it was checked whether the thermocouples were working. The test system has been made ready. The door is closed.

During the test: Firstly, vacuuming was carried out until the pressure dropped to 10^-5 mbar. Avoiding from the damage of components, firstly, the temperature of the walls and thermal plate was brought to 20°C. After the temperatures read from the thermocouples came to a steady state (1°C /hour), power was given according to the determined power configuration and the temperatures read from the thermocouples were expected to reach equilibrium. As the component temperatures were not in a dangerous state, the test continued with 40°C.

Since the test chamber was vacuumed, the test started by bringing the thermal walls and thermal plate to 40°C. The steps made for 20°C were also done for 40°C. The test continued until the equilibrium state (1°C/hr). Component temperatures did not reach a dangerous point in the case of 40°C. With the qualification temperature of 60°C, the actual testing will begin.

The test was started by bringing the temperature of the thermal walls and thermal plate to 60°C. After the temperatures read from thermocouples were brought to 0.5°C/hour, power was given according to the values in the determined power configuration. The test continued until the temperatures stabilized. The test took 14 hours.

In the return phase, the temperature of the thermal walls was increased to 25°C and the pressure was brought to 1000 mbar. The door has been opened.

4. MATHEMATICAL MODELLING

Electronic components generate heat via flowing electric current through them. This heat generation is related with the current and electrical resistance of the component. As the current passes through the components, the temperature of the components gradually rises. Unless this heat distributes and reject from the components, this leads to break-down of the components. There are three mechanisms for heat dissipation; namely, conduction, convection and radiation.

Within the scope of this thesis, electronic equipment for space applications has been investigated. Due to vacuum conditions, convective heat transfer will be ignored. The main focus is on conduction and radiation. The physical system under consideration consists of PCB, components and metal frame around them on a rectangular plate which are placed inside a cylindrical vessel which is kept under vacuum. Therefore, mathematical modeling of the tested system requires the solution of energy equation regardless of convection.

In this chapter, the energy equation with the mathematical model for the tested system is explained, followed by the numerical solution method.

4.1 Basic Equations of Heat Transfer

The first law of thermodynamics, conversation of energy principle, states that energy can neither be created nor destroyed during a process; it can only change forms [44]. The net change in the total energy of the system must be equal to the difference between the inlet energy to system and the outlet energy from the system. In the heat transfer analysis, due to conservation of energy, the following energy balance should be satisfied.

$$E_{in} + E_{generated} = E_{out} + \Delta U \tag{4.1}$$

where E_{in} is the energy entering the volume, $E_{generated}$ is energy generated inside, E_{out} is the energy leaving from the system, and ΔU is the change in stored energy. For 1-D systems, energy balance equation terms are defined below [51],

$$E_{in} = q''_x A dt$$

$$E_{out} = q''_{x+dx} A dt$$

$$E_{generated} = QAdxdt$$

$$Q = \Delta U = mc\Delta T = c(\rho A dx)dT$$

where Q is the net amount of heat transferred, c is specific heat, and $(\rho A dx)$ is mass. When the heat is transferred at a constant rate, heat transfer rate can be determined as,

$$q = \frac{Q}{\Delta T} \tag{4.2}$$

Equation 4.1 is replaced with the equations given above,

$$q''_x A dt + QAdxdt = c(\rho A dx)dT + q''_{x+dx} A dt \tag{4.3}$$

Using Fourier’s and Taylor expansion theorem,

$$q''_{x+dx} = -\left[k_{xx}\frac{dT}{dx} + \frac{d}{dx}\left(k_{xx}\frac{dT}{dx}\right)dx\right] \tag{4.4}$$

$$-k_x A\frac{dT}{dx}dt + QAdxdt = c(\rho A dx)dT - \left[k_{xx}\frac{dT}{dx} + \frac{d}{dx}\left(k_{xx}\frac{dT}{dx}\right)dx\right]Adt \tag{4.5}$$

If the material properties are function of temperature, the analysis becomes non-linear heat transfer analysis. Convection and radiation terms are added to equation (4.5).

$$q''_x A dt + QAdxdt = \Delta U + q''_{x+dx} A dt + q''_h P dxdt + q''_{rad} P dxdt \tag{4.6}$$

where $q''_h Pdxdt$ is convection term and $q''_{rad} Pdxdt$ is radiation term. Convection term will be ignored due to vacuum environment, equation 4.6 transforms into,

$$q''_x A dt + QAdxdt = \Delta U + q''_{x+dx} A dt + q''_{rad} P dxdt \tag{4.7}$$

$$k_{xx}\frac{\partial^2 T}{\partial x^2} + Q - \frac{\sigma\varepsilon FP}{A}(T^4 - T_\infty^4) = \rho c\frac{\partial T}{\partial t} \tag{4.8}$$

where P is perimeter around area A, F is view factor.

Energy balance equation can be derived for 3-D systems as in equation (4.9). Conduction and radiation have been included.

$$Q = \rho c\frac{\partial T}{\partial t} + \nabla^T . q''_{cond} + \nabla^T . q''_{rad} \tag{4.9}$$

where $\nabla^T = \left(\frac{\partial}{\partial x}, \frac{\partial}{\partial y}, \frac{\partial}{\partial z}\right)^T$, which is a gradient operator [50].

4.1.1 Conduction

Conduction is defined as the heat transfer from the more energetic particles of a body to the adjacent less energetic particles in consequence of interaction between the particles. Conduction occurs in the solid, liquid or gases environment. Geometry of the medium, thickness, and material of the medium, and temperature difference affect the rate of heat conduction.

$$q_{cond} = -kA\frac{\partial T}{\partial x} \qquad\qquad q''_{cond} = -k\frac{\partial T}{\partial x} \tag{4.10}$$

where q_{cond} is the rate of conduction heat transfer (heat flow), k is the thermal conductivity of the material, which is a measure of the ability of a material to conduct heat, ΔT is the temperature difference, and q''_{cond} is heat flux. A is the area normal to the heat flow and Δx is the thickness. The negative sign in equation 4.10 assures that heat is conducted in the direction of decreasing temperature, and temperature decreases with increasing x.

Thermal conductivity is important parameter especially in vacuum environment. For this reason, it should be explained more in detail. Thermal conductivity of a material can be defined as the rate of heat transfer through a unit thickness of a material per unit area per unit temperature difference. It is the measure of the capability of heat conduction. Good heat conductor material have the higher value of thermal conductivity, whereas low value of thermal conductivity specifies that the material is a poor heat conductor or insulator.

4.1.2 Radiation

Radiation can be defined as the energy which is emitted by matter in the electromagnetic waves or photons as a result of the alteration in the electronic configurations of atoms or molecules. In this thesis, thermal radiation, which is the type of radiation emitted by objects due to their temperature, is examined.

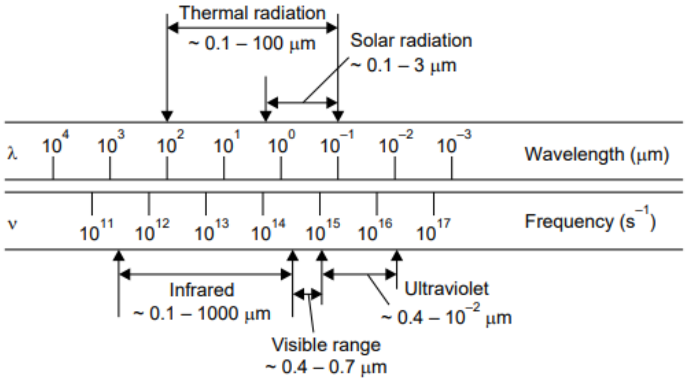

Figure 4.1 : Spectrum of electromagnetic radiation due to temperature of a body.

In contrast to conduction, radiation does not require medium to transfer heat. Since radiation occurs via electromagnetic waves, it is the fastest heat transfer mechanism and does not expose to an attenuation. When the surface is exposed to thermal radiation,

1. The surface of a body will absorb the radiation, and its temperature changes.

2. The surface of a body will reflect the radiation, and there will be no temperature change.

3. The radiation will pass through the surface of the object, and there will be no temperature change.

All objects which have temperature above absolute zero emit thermal radiation. Radiation is a volumetric phenomenon, whereas it is considered to be a surface phenomenon for solids. Stefan-Boltzmann law defines the rate of radiation that can be emitted from a surface at a temperature T_s,

$$q''_{rad} = \sigma \varepsilon F_{ij}(T_i^4 - T_j^4) \tag{4.11}$$

where $\sigma = \frac{5{,}670x10^{-8}W}{m^2}.K^4$ is the Stefan-Boltzmann constant, ε is the emissivity of the surface. Emissivity (ε) is a measure of how much thermal radiation a surface emits to its environment. Emissivity value ranges between $0 \leq \varepsilon \leq 1$. As the emissivity gets closer to 1, the surface feature gets closer to the blackbody.

Secondly, absorptivity (α) is another important radiation property. It can be defined as the fraction of the radiation energy incident on a surface which is absorbed by the surface. Its value is in the range $0 \leq \alpha \leq 1$. As in the emissivity, blackbody is a perfect absorber and its absorptivity value equals to 1. The rate at which a surface absorbs radiation is determined as,

$$q_{absorbed} = \alpha q_{incident} \tag{4.12}$$

where $q_{incident}$ is the rate at which radiation is incident on the surface and α is the absorptivity of the surface.

The third fundamental property of thermal radiation is reflectivity (φ). Reflectivity (φ) is a measure of how much of the radiation is reflected. Lastly, transmissivity (τ) is another important parameter of the radiation. Transmissivity (τ) is a measure of how much of radiation passes through the object. Each of these parameters ranges between 0 and 1. As all radiation must be either reflected, absorbed or transmitted, as a result, the following can be concluded,

$$\alpha + \varphi + \tau = 1 \tag{4.13}$$

Surface properties might have different values of these radiation parameters at different wavelength. Also, incident angle which hits the surface has an effect on these parameters. A blackbody is an ideal object which has perfect absorption, regardless of incident angle and wavelength. It has value of 0 reflectivity and transmissivity, and 1 absorptivity and emissivity at all wavelengths.

In this review, all surfaces are selected as opaque or gray body, further simplifying equation 4.13 as,

$$\alpha + \varphi = 1 \tag{4.14}$$

A gray body is ideal body which has the same emissivity value at all wavelength. It is more realistic than a blackbody because the value of its absorptivity may be less than 1 and the values of reflectivity and transmissivity is greater than 0.

The net radiation heat transfer is the difference between the rates of radiation emitted by the surface and the radiation absorbed by the surface. Generally, the determination of the net radiation heat transfer between two surfaces is complicated and depends on the property of the surfaces, their orientations (relative to each other), and interaction between the medium. When the thermodynamic temperature is surrounded by much bigger surface (or black), the net rate of radiation heat transfer between these two surfaces is given below,

$$q_{rad} = \varepsilon\sigma A(T_s^4 - T_{surr}^4) \tag{4.15}$$

Radiation heat exchange between two surfaces i and j are written as,

$$q_{rad} = \sigma\left(\varepsilon_i A_i F_{ij} T_i^4 - \varepsilon_j A_j F_{ji} T_j^4\right) \quad (4.16)$$

where F_{ij} the view factor which is a function of surface geometry and configuration between is surfaces i and j.

4.1.2.1 View factor calculations

In radiation heat transfer, heat exchange occurs between surfaces that are not directly connected. The view factor (F_{ij}) is the fraction of energy leaving from surface i to directly strike into the surface j. F_{ij} is the expression which defines function of geometrical system to calculate the radiation link. This function depends on geometry and position of surfaces relative to each other.

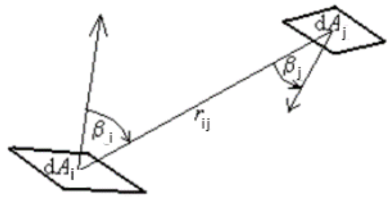

Figure 4.2 : View factor between two different surfaces.

There will be no heat transfer between two different surfaces if these two surfaces are at the same temperature. In this case, heat transfer by radiation can be expressed as [53],

$$q_{rad} = \sigma\varepsilon_i A_i F_{ij}\left(T_i^4 - T_j^4\right) - \sigma\varepsilon_j A_j F_{ji}\left(T_i^4 - T_j^4\right) \quad (4.17)$$

The view factor reciprocity relationship can be written as follows,

$$A_i F_{ij} = A_j F_{ji} \quad (4.18)$$

The general equation for calculation of view factor is given equation (4.19),

$$F_{ij} = \frac{1}{A_i}\int_{A_i}\left(\int_{Aj}\frac{\cos\beta_i\cos\beta_j}{\pi r_{ij}^2}dA_2\right)dA_1 \quad (4.19)$$

where two surfaces dA_i and dA_j as shown in Figure 4.2, distance between surfaces r_{ij}, tilting angle relative to centers β_i and β_j, with $0 \le \beta_i \le \pi/2$ and $0 \le \beta_j \le \pi/2$ [54].

View factors are limited with $0 \le F_{ij} \le 1$. When two target surfaces (j and k) are handled simultaneously, $F_{i,j+k} = F_{ij} + F_{ik}$, which is the distribution property of the view factor. Based on the property of reciprocity and distribution, composition property is defined as $F_{i,j+k} = \frac{A_i F_{ik} + A_j F_{jk}}{A_i + A_j}$.

4.2 Thermal Network Method

It is said that two systems are analogous when both have similar equations and boundary conditions. Equations which describes the behavior of one system can be turned into equations for another by simply changing the symbols of the variables. Thermal and electrical systems are two such analogous systems. The relationship between two systems is given in (Table 4.1) [55].

Table 4.1 : Thermal and electrical analogy.

Thermal System	Unit	Electrical System	Unit
Temperature Difference (ΔT)	°C	Voltage (V)	Volt (V)
Heat (Q)	J	Charge (q)	Coulomb (C)
Heat Flow (q)	J/s	Current (I)	Amper (A)
Thermal Resistance (R)	°C/W	Resistance (R)	Ohm (Ω)
Thermal Conductance (G)	W/°C	Conductance (1/R)	Siemens (S)
Thermal Capacitance (C)	J/°C	Capacitance (C)	Farad (F)
q=GT	J/s	I=E/R	Amper (A)

The analogy between electrical and thermal systems provides utilization of basic electrical laws such as Ohm’s law and Kirchhoff’s laws. Thermal networks are constituted by establishing a thermal-electrical analogy for studying heat transfer processes, in spite of discrepancies between heat and electricity exist. It is aimed to get simple and quick results by using thermal network method. Furthermore, thermal network method is used to create reduced thermal mathematical model (RTMM). RTMM of IPS module is given in Appendix A. The simplest modeling of equipment by using thermal network method provides ease to make system level thermal analysis. The partial differential equations which describe those systems are solved by numerical techniques. These numerical techniques are adapted to computer solutions of thermal networks, which enables the solving of complex models [44]. The numerical solution of thermal problems using the finite element method (FEM) has been developed and Simcenter 3D is widely used to solve heat transfer including conduction and radiation.

4.2.1 Elements of thermal networks

Appropriate models for thermal networks are prepared with the expressions for thermal resistances or thermal capacitance. Thermal resistance and thermal capacitance are main physical elements which establish the thermal network method. Thermal resistance defines resistance of a material to heat energy. For example, copper has low thermal resistance, so it conducts heat energy well. On the other hand, thermal capacitance defines how much heat can be stored by an object. If an object has thermal capacitance, its temperature rises as heat flows into the object and decreases as heat flows out. Examples of thermal resistance and capacitance is given in Figure 4.3 and Figure 4.4 for describing thermal-electrical analogy.

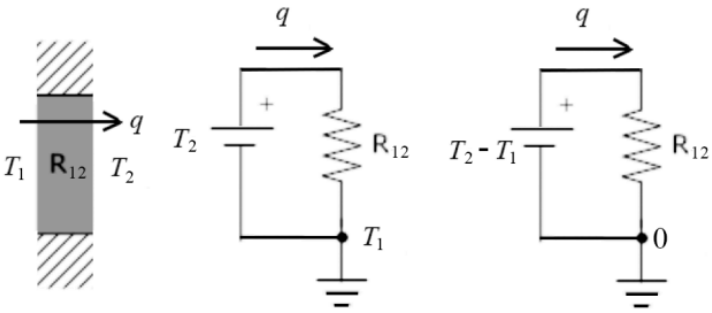

Figure 4.3 : Thermal-electrical analogy for resistance.

Figure 4.3 shows that one side of the wall is T_1 and the other side is T_2, q is heat flow, also the wall acts as thermal resistance, at the left figure. $T_2 - T_1$ identifies the voltage, R_{12} is electrical resistance, and q is current, at the right figure.

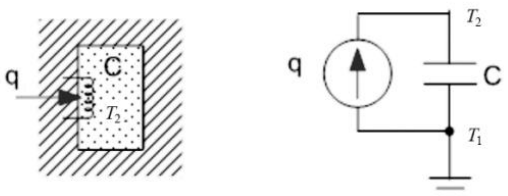

Figure 4.4 : Thermal-electrical analogy for capacitance.

Figure 4.4 shows that, at the left figure, coil represents power source and the dotted object is the thermal capacitance. In the thermal system, one terminal of the capacitor is always connected to the constant ambient temperature. Similarly, in the electrical system one terminal of capacitance is connected to the reference (or ground). The equation of capacitance is given in equation (4.20).

$$C\frac{d(T_2 - T_1)}{dt} = q \tag{4.20}$$

where C is thermal capacitance and it is comprised of mass and specific heat ($C = mc_p$). To be more explanatory, specific heat (J/kg.ºC) can be defined as the heat energy required to raise the temperature of a unit mass by 1ºC. Additionally, equation 4.20 can be written as in equation 4.21, since T_1 is constant.

$$C\frac{dT_2}{dt} = q \tag{4.21}$$

Thermal resistance and capacitance enable to simplify complicated thermal systems. Thermal capacitance property is used in transient thermal analysis. The main focus is on steady-state analysis in this thesis. As a consequence, thermal network method is constituted by using thermal resistances.

Series and parallel thermal networks are defined by analogy with circuit theory rules for equivalent resistance. The circuit theory defines the techniques which are used to describe the flow of energy. This theory includes Ohm's and Kirchhoff's laws, which specify the relationship between current, voltage and resistance. From circuit theory, resistance is defined as the ratio of electric potential difference to electric current. According to Ohm's law, electrical resistance equation is represented in equation (4.22).

$$R_{elec} = \frac{V}{I} \tag{4.22}$$

where V is voltage and I is current.
Since electrical and thermal systems are analogy, as shown in Table 4.1, voltage is similar to temperature difference and current can be represented with heat flow in thermal system. Equation of resistance in thermal system is given in equation (4.23).

$$R = \frac{\Delta T}{q} \tag{4.23}$$

where ΔT is the temperature difference, and q is heat flow.

In series networks, resistors produce equivalent resistance between input and output terminals. Recalling from circuit theory, each resistor has the same current flowing through it. Its equation can be written as follows,

$$R_{series\ eq} = \sum_i R_i \tag{4.24}$$

Similarly, the transfer of energy of many systems over a single heat path is modeled in series.

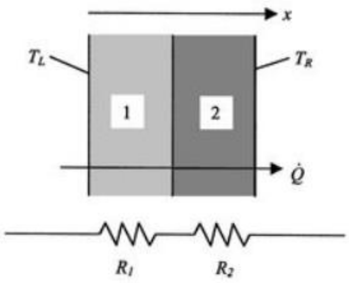

Figure 4.5 : Heat transfer in series thermal networks.

Figure 4.5 illustrates the heat transfer in series thermal networks. In this example, the equivalent thermal resistance would be the sum of each resistance. The resistances are in series and sum of them are shown in equation (4.25).

$$R = R_1 + R_2 \tag{4.25}$$

In parallel networks, as in electrical resistor, resistors for heat transfer produce equivalent resistance. In the case, multiple heat path exist between two modes, parallel network model is applicable. Equation of parallel network is written in equation (4.26).

$$R_{parallel\ eq}^{-1} = \sum_i R_i^{-1} \tag{4.26}$$

An example of parallel network for heat transfer is given in (Figure 4.6). In this case, bolt is covered with two different materials (different thermal conductivity) on both sides, for this reason, heat transfer is modeled by the parallel network method.

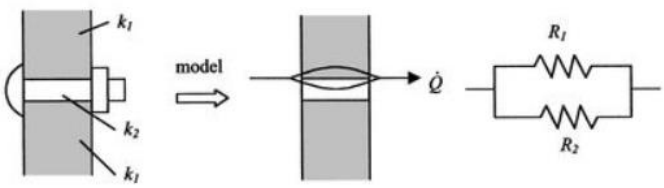

Figure 4.6 : Heat transfer in parallel thermal networks.

Total resistances in Figure 4.6 can be written as in equation (4.27).

$$\frac{1}{R} = \frac{1}{R_1} + \frac{1}{R_2} \tag{4.27}$$

It is important to emphasize that thermal model includes heat (or power) source which generates predetermined amount of heat (or power) in a system. This power can either be constant or a function of time. The power source is depicted by a current source.

For example, power source is symbolized with q as seen in (Figure 4.4). In practice, a power source is usually an electrical heating element consisting of a coil of wire heated by a current flowing through it. Furthermore, a diagram of a coil of wire is used to represent the power source.

4.3 Thermal Contact Resistance

The analogy between the flow of electric current and the heat flow provides the satisfactory definition of the heat transfer at the interface of two conducting media. Two solid surfaces will not constitute of a perfect contact when they are pressed together. Because of their roughness, tiny air gaps always prevail between the two contacting surfaces. Two conditions of heat transfer exist through the interface between the two contacting faces. The first one is solid-to-solid conduction which is very effective. Second of all, conduction through the gas filled gaps leads to poor thermal conductivity. An interfacial conductance or thermal contact conductance coefficient (h_c) which is a property indicating the thermal conductivity is placed between the conducting media on both sides, in serial network model.

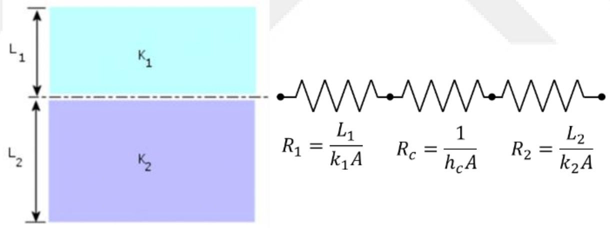

Figure 4.7 : Thermal contact resistance.

The conductance h_c is similar to the convection heat transfer coefficient. The equation of heat was given as $Q = Ah_c\Delta T$. Considering the electrical-thermal analogy, thermal contact resistance can be written as $R_c = \frac{1}{h_c A}$.

Thermal contact conductance (h_c) are based on the following factors,

- The surface finish of the contacting surfaces,
- The material of each surface,
- The pressure with which the surfaces are forced together,
- The substance in the gaps between the two contacting surfaces.

Under vacuum conditions, gaps are not filled with anything. The following table lists the thermal contact resistance for metallic interfaces under vacuum conditions [56].

Table 4.2 : Thermal resistance, $R_{thermal}x10^{-4}(m^2.K/W)$

Contact Pressure	100 kN/m^2	10,000 kN/m^2
Stainless Steel	6-25	0,7-40
Copper	1-10	0,1-0,5
Magnesium	1,5-3,5	0,2-0,4
Aluminum	1,5-5	0,2-0,4

4.4 Numerical Solution of Thermal Network Model by Using Finite Element Method

Analytical solutions are useful for only relatively simple cases. In spite of that, this simple solutions like thermal network method plays an important role to provide insight into complex engineering problems. Various problems which involve complex geometries, complex boundary conditions and thermal properties cannot be solved analytically. Several methods are evolved to solve these complex models, finite-difference, finite-element, and boundary element method. Another advantage of these methods, they allow the thermal model change more easily.

There are advantages and disadvantages of each method. In this thesis, the finite element method (FEM) will be examined. Finite element method provides the numerical solution for problems which are defined by partial differential equations and formulated as functional minimization. Finite element models based on meshes. Each finite-element model has hundreds of elements. In finite elements, approximate functions are determined in terms of the node values of a searched physical field. Discretized finite element problem is obtained by transforming continuous physical problem with the help of unknown nodal values. There are several approaches which are utilized to transform the physical formulation of the problem to its finite element discrete model. Galerkin method is the most popular method which are used if the physical formulation of the problem is known as a differential equation. Galerkin finite element method is effective method to transform partial differential equation of heat equation into finite element model [57]. A basic equation of heat transfer is written as,

$$-\left(\frac{\partial q_x''}{\partial x}+\frac{\partial q_y''}{\partial y}+\frac{\partial q_z''}{\partial z}\right)+Q=\rho c\frac{\partial T}{\partial t} \qquad (4.28)$$

where q''_x, q''_y, and q''_z are heat flux, $Q = Q(x, y, z, t)$ is the heat generation per unit volume, ρ is the density, c is the heat capacity, T is the temperature and t is time. According to Fourier's law, components of heat flow can be expressed as,

$$q''_x = -k\frac{\partial T}{\partial x}, \qquad q''_y = -k\frac{\partial T}{\partial y}, \quad q''_z = -k\frac{\partial T}{\partial z} \tag{4.29}$$

where k is thermal conductivity as mentioned before. Substitution equations (4.29) into equation (4.28),

$$\frac{\partial}{\partial x}\left(k\frac{\partial T}{\partial x}\right) + \frac{\partial}{\partial y}\left(k\frac{\partial T}{\partial y}\right) + \frac{\partial}{\partial z}\left(k\frac{\partial T}{\partial z}\right) + Q = \rho c\frac{\partial T}{\partial t} \tag{4.30}$$

Boundary conditions are defined below,

1. Temperature

$$T_s = T_1(x, y, z, t) \; on \; S_1 \tag{4.31}$$

2. Heat flow

$$q''_x n_x + q''_y n_y + q''_z n_z = -q''_s \quad on \; S_2 \tag{4.32}$$

3. Radiation

$$q''_x n_x + q''_y n_y + q''_z n_z = \varepsilon\sigma T_s^4 - \alpha q''_r \tag{4.33}$$

where q''_r is incoming heat flux.

In view of finite element method, body is divided into finite elements in a domain V. These finite element connection points are called as node. In finite element method, shape functions (N_i) are utilized for interpolation of temperature and temperature gradients. Temperature and temperature gradient relationship with respect to shape function are described below,

$$\begin{gathered} T = [N]\{T\} \\ [N] = [N_1 \;\; N_2 \;\; \dots] \\ \{T\} = \{T_1 \;\; T_2 \;\; \dots\} \\ \begin{Bmatrix} \dfrac{\partial T}{\partial x} \\ \dfrac{\partial T}{\partial y} \\ \dfrac{\partial T}{\partial z} \end{Bmatrix} = \begin{bmatrix} \dfrac{\partial N_1}{\partial x} & \dfrac{\partial N_2}{\partial x} & \dots \\ \dfrac{\partial N_1}{\partial y} & \dfrac{\partial N_2}{\partial y} & \dots \\ \dfrac{\partial N_1}{\partial z} & \dfrac{\partial N_2}{\partial z} & \dots \end{bmatrix} \{T\} = [B]\{T\} \end{gathered} \tag{4.34}$$

where {T} is temperatures at nodes, [N] is a matrix of shape functions and [B] is a matrix for temperature gradients interpolation.

Rewriting equation 4.28 by using Galerkin method,

$$\int_V \left(\frac{\partial q_x''}{\partial x} + \frac{\partial q_y''}{\partial y} + \frac{\partial q_z''}{\partial z} - Q + \rho c \frac{\partial T}{\partial t} \right) N_i dV = 0 \qquad (4.35)$$

Divergence theorem is applied to the first three terms in equation 4.34,

$$\int_V \rho c \frac{\partial T}{\partial t} N_i dV - \int_V \left[\frac{\partial N_i}{\partial x} \quad \frac{\partial N_i}{\partial y} \quad \frac{\partial N_i}{\partial z} \right] \{q''\} dV = \int_V Q N_i dV - \int_S \{q''\}^T \{n\} N_i dS \qquad (4.36)$$

$$\{q''\}^T = [q_x'' \;\; q_y'' \;\; q_z''], \qquad \{n\}^T = [n_x \; n_y \; n_z]$$

where {n} is an outer normal the surface of the body.

Boundary conditions which are specified in equation 4.31-4.33 are inserted into equation 4.36 as follows,

$$\int_V \rho c \frac{\partial T}{\partial t} N_i dV - \int_V \left[\frac{\partial N_i}{\partial x} \quad \frac{\partial N_i}{\partial y} \quad \frac{\partial N_i}{\partial z} \right] \{q\} dV = \int_V Q N_i dV - \int_{S_1} \{q''\}^T \{n\} N_i dS$$
$$+ \int_{S_2} q_s'' N_i dS - \int_{S_3} (\varepsilon \sigma T^4 - \alpha q_r'') N_i dS \qquad (4.37)$$

It should be noted that,

$$\{q''\} = -k[B]\{T\} \qquad (4.38)$$

The finite element equations for heat transfer problems can be written as,

$$[C]\{\dot{T}\} + ([K_c] + [K_h] + [K_r])\{T\} = \{R_T\} + \{R_Q\} + \{R_q\} + \{R_h\} + \{R_r\} \qquad (4.39)$$

$$[C] = \int_V \rho c [N]^T [N] \, dV \qquad (4.40)$$

$$[K_c] = \int_V k [B]^T [B] \, dV \qquad (4.41)$$

$$[K_r]\{T\} = \int_{S_3} \varepsilon \sigma T^4 [N] \, dS \qquad (4.42)$$

$$[R_T] = -\int_{S_1} \{q''\}^T \{n\} [N]^T \, dS \qquad (4.43)$$

$$[R_Q] = \int_V Q [N]^T \, dV \qquad (4.44)$$

$$[R_q] = \int_{S_2} q_s'' [N]^T \, dS \qquad (4.45)$$

$$[R_r] = \int_{S_3} \alpha q_r'' [N]^T \, dS \tag{4.46}$$

General equations for stationary linear and nonlinear problem are derived from equation 4.39, respectively.

$$([K_c] + [K_h])\{T\} = \{R_Q\} + \{R_q\} + \{R_h\} \tag{4.47}$$

$$([K_c(T)] + [K_h(T)] + [K_r(T)])\{T\} = \{R_Q(T)\} + \{R_q(T)\} + \{R_h(T)\} + \{R_r(T)\} \tag{4.48}$$

The simulations are carried out by a FEM model in Simcenter 3D. Thermal network model having a couple nodes has poor accuracy compared to numerical solution. Nevertheless, it can predict temperature variations properly. On the other hand, The FEM model, offers higher accuracy while it requires more time to get results because of the large number of nodes. The main purpose of all thermal-analysis studies is solving the energy balance equation. Applying the balance equation to the equipment including all components and PCB layers can be challenging and time consuming with the analytical approaches. Consequently, thermal analysis software tools have been developed based on numerical solution of the equipment to simulate complex physical thermal networks.

4.5 Simcenter 3D

Simcenter 3D is an independent computer aided engineering (CAE) application for analysis and discipline professionals working with data from any computer aided design (CAD) source. Simcenter 3D helps simulation engineers guide design in industries such as automotive, aerospace and industrial machinery. Simcenter 3D is a handy environment for 3D CAE with links to design, simulation, testing and data management. Simcenter 3D provides a quick simulation with geometry editing and relational simulation modeling. Thanks to its fast and accurate solvers, Simcenter 3D can perform many analyses such as structural, acoustic, and thermal. Its integration with NX provides a fairly fast update of geometries [58].

Simcenter 3D Pre/Post (also called Simcenter 3D Engineering Desktop) is a comprehensive finite element modeling and result visualization product. Pre/Post includes a complete suite of pre and post processing tools and supports a wide range of product performance evaluation solutions. Pre/Post provides support for a number of industry-standard solvers, such as Simcenter Nastran, ANSYS and Abaqus. For instance, the solver and type of analysis can be specified when either or both of a mesh and a solution is created. The software presents all meshing, boundary conditions and solution options using terminology of that solver and analysis type. In addition, solution of the model can be displayed directly in Pre/Post.

The Simcenter 3D Thermal/Flow solver environment is a comprehensive heat transfer and flow simulation pacakage. Like Simcenter Nastran, it is fully integrated into the Pre/Post environment. In the Simcenter 3D Thermal/Flow solver environment, there are many analysis types such as; thermal, flow, coupled thermal-flow, and mapping. Thermal analysis type utilizes thermal solver to solve steady state and transient heat transfer problems. The solver is depending on finite element formulation.

Simcenter 3D Electronic System Cooling (ESC) and Simcenter 3D Space System Thermal (SST) are comprehensive solver environments for the simulation of heat transfer. Both of them are fully integrated into the Pre/Post environment as in Thermal/Flow solver environment and includes all capabilities of Thermal/Flow solver. ESC and SST supports concentrated mass, beam, shell and solid meshes. Physical properties such as concentrated mass, beam, thin shell and PCB Stack can be used. Interface resistance, PCB and PCB components, radiation, thermal coupling, and thermal coupling-radiation properties are found in simulation object section. Simple radiation to environment and temperature can be assigned as a constraint. Thermal loads in ESC and SST can be grouped into three groups as of heat load, heat flux and heat generation. The heat load describes the flow or power of heat to the selected geometry or elements. The heat flux defines the heat flux (heat load per unit area) to the selected surface. The heat generation specifies the heat generation (heat load per unit volume) for the selected body. Thermal loads are applied directly to elements, to geometry or to non-geometric elements. Thermal solver uses the heat load per element. Within the scope of this thesis, components and PCB are modelled as 2D elements which refers actual surface area while mechanical structures are modelled with 3D elements for defining actual volume. Heat flux is imported to 2D meshes, whereas heat generation is assigned to 3D meshes (actual volume). Thermal load magnitude is defined as a constant value and a function independent variable in Simcenter 3D.

Electronic System Cooling is practical for the solution of heat transfer in electronic systems and components. The most important feature of ESC is NX PCB Exchange and ECAD/NX associative data exchange. Components are modeled as null shell as a feature of ESC. This null shell structure provides surface area and lenght of component. PCB stack property provides printed circuit board's complex in-plane conductivity in each layer. PCB Stack property includes PCB Layer and PCB Via modelling objects. Detailed traces and vias information from ECAD models can be imported. Capability of selecting trace and dielectric materials leads to simplified PCB model. Trace and dielectric material, thickness of PCB layer and percentage of the conductive material coverage on the PCB layer can be specified. Thermal conductivity of PCB can be calculated from the material and trace coverage. PCB Via modelling object specifies a linear thermal coupling between two or more layers of a PCB. PCB via material, coverage of vias, and beginning and terminals from PCB layers can be defined. In each layer, temperature can be calculated and post-processed.

Space System Thermal offers comprehensive thermal and radiation simulation tools for space applications. The solver is mainly applicable for aerospace applications, radiation simulation and orbital heating simulation. The conjugate gradient algorithm that utilizes a biconjugate gradient stabilized technique is used by thermal solver. Likewise, it provides high performance for large systems by using the Newton-Raphson method for nonlinear terms. Complex enclosures and shadowing surfaces require view factors for radiation thermal analysis. The solver also provides calculation of view factor automatically. Basic features of SST solver are coupled conduction, convection and radiation analysis, multiple radiation view factor calculation method, temperature-dependent material properties, and thermal couplings.

The basic workflow for modeling heat transfer is identical in Simcenter 3D Thermal/Flow, Simcenter 3D Electronic System Cooling, or Simcenter 3D Space System Thermal model. It should be specified that all analysis workflows begin with a model as simple as possible. Less significant parts or features are removed from geometry. In the thermal analysis, bolts are given as an example to less significant parts. Bolts are omitted from the geometry and holes of mechanical structures and PCBs are deleted.

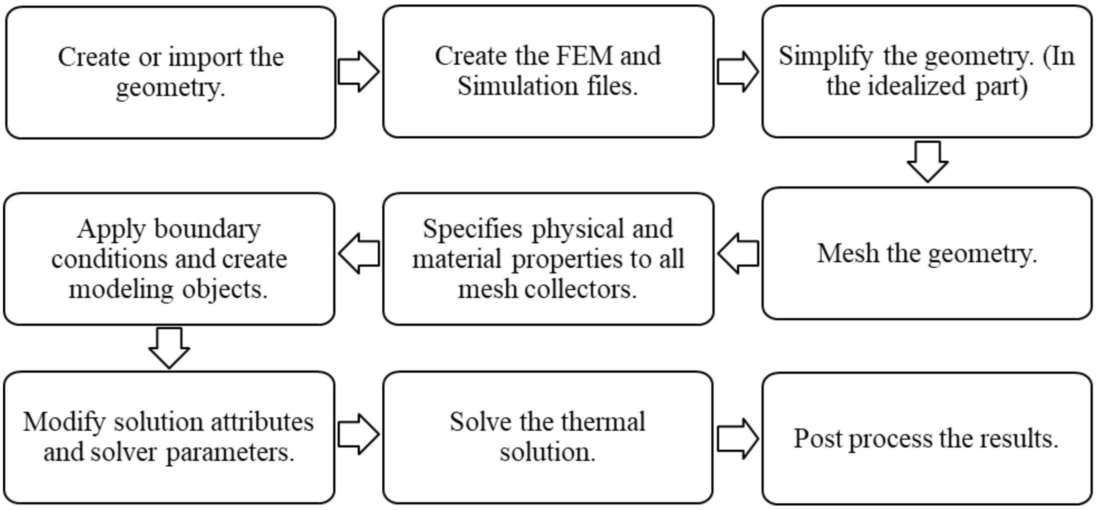

Figure 4.8 : Workflow for modeling heat transfer [59].

4.6 Two-Resistor Model for Thermal Simulation

Thermal models for thermal simulations can be categorized into two groups, such as compact thermal model (CTM) and detailed model. Two types of thermal models are standardized by JEDEC Solid State Technology Association for the CTM, which are called two-resistor model and DELPHI model. Two-resistor, DELPHI, and detailed models can be shown in (Figure 4.9).

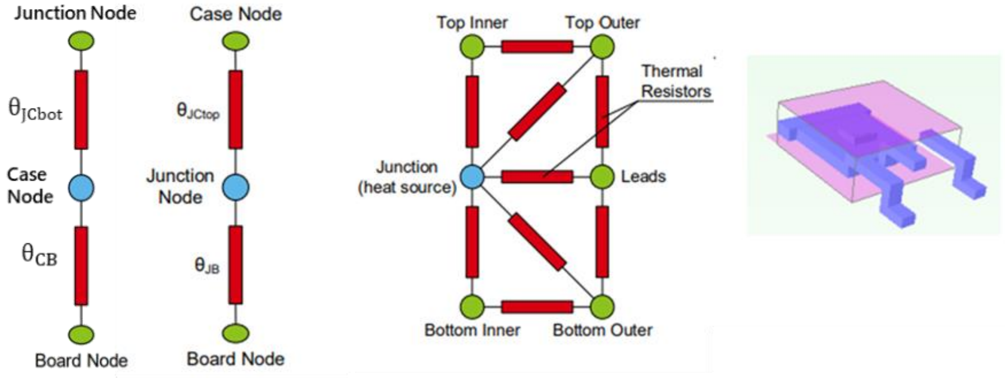

Figure 4.9 : (a) Two-resistor models. (b) DELPHI model. (c) Detailed model.

The DELPHI model represents a package with a multi-resistor network, therefore errors may be greatly reduced. It has more complicated structure to generate. For the detailed model, there is no standard, so companies have to create model variables themselves. Dimensions and physical properties should be defined precisely. Despite the best precision, simulation takes a long time for the detailed model. Since there is no standard, thermal-analysis tools are not suitable.

Two-resistor thermal model is the least complicated model. It simulates the thermal performance of a component via two major heat flow paths through a package. Typical data sheets generally contain standardized junction-to-ambient and junction-to-case thermal resistances (θja and θjc, respectively). It was clear that θja and θjc are not sufficient to represent environmentally-independent thermal properties of an IC packages. For thermal characterization and modeling, the more accurate junction temperatures prediction and better thermal representations of an IC packages have been developed over the years. The required information about the package internal structure and materials like die size, substrate material layer thickness and coverage, and lead tip are generally confidential information for manufacturers. These are not available for the end-users.

The two-resistor model was chosen because of its simplicity and ease of access to standards in the thesis. Currently, two-resistor CTMs are the most widely used among all CTMs. It is the simplest model among thermal models. Thanks to its simplicity, the model offers quick solutions with great precision compared to other models. Two-resistor model can be used in the initial design phase, furthermore for the development of analysis model. Two-resistor model is practical for discrete and large-scale integration (LSI) circuits. Discrete circuits can be defined as separately manufactured components like resistor, capacitor or transistor mounted on PCB. Large-scale integration is defined as integrated circuits having number of components between 500-300000 [60].

There are two different paths to apply two-resistor model in Simcenter 3D, such as Theta JC-CB (junction to case – case to board) and Theta JC-JB (junction to case – junction to board). These models are established only by vertically dividing a package at the junction. These models include three nodes, called case node, junction node, and board node as shown in (Figure 4.9). The package consists of a single integrated circuit. Single temperature node is used for representing the temperature. Thermal resistance network model is utilized to demonstrate the thermal flow path. In Figure 4.10, first picture shows that case node, junction node, and board node demonstrate the upper surface of the package, thermal source of the package, and the circuit board temperature at a position of 1 mm from the edge of the package, respectively. On the other hand, the picture on the right side in Figure 4.10, junction node, case node, and board node specify thermal source of the package, bottom surface of the package, and

PCB temperature. Due to the lack of convection, air temperature (ambient temperature) is ignored in space applications. Therefore, upper surface of package is replaced with the bottom surface of package. They are assumed to be identical in thermal simulation [58].

Figure 4.10 : Physical arrangement of two-resistor thermal model.

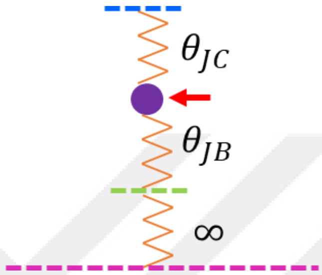

Figure 4.11 : Theta JC-JB

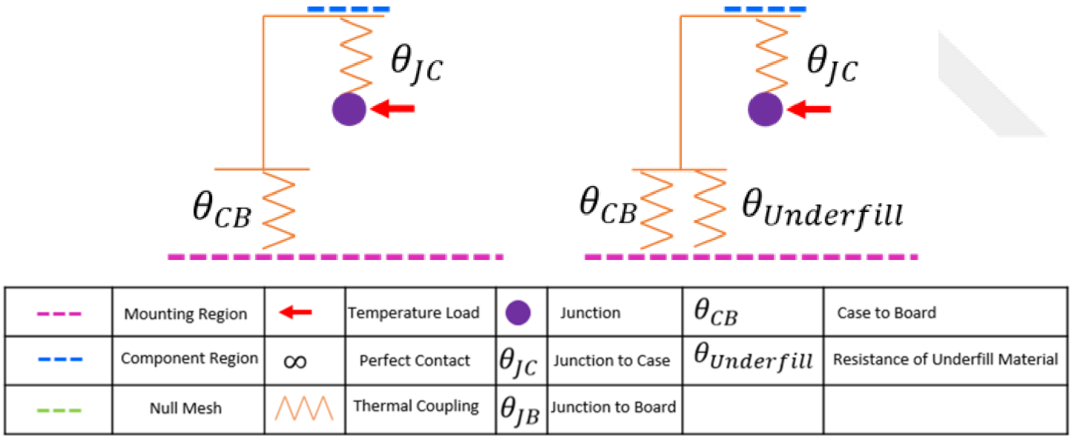

Figure 4.12 : (a) Theta JC-CB without underfill. (b) Theta JC-CB with underfill.

Two-resistor thermal models are composed of between junction-case nodes, case-board nodes and between junction-board nodes, which are called junction-to-case resistance (θ_{jc}), case-to-board resistance (θ_{cb}), and junction-to-board resistance (θ_{jb}). Thermal resistance values are obtained from component manufacturer's data sheets and JEDEC Standards. Typically, junction-to-case resistance (θ_{jc}) and junction-to-ambient resistance (θ_{ja}) can be found in data sheets. According to JESD15-3, junction-to-case resistance (θ_{jc}) can be defined as [62],

$$\theta_{jc} = \frac{T_J - T_C}{P_H} \tag{4.49}$$

where θ_{jc} represents the thermal resistance between the device junction and case, T_J is junction temperature when the device has achieved steady-state after application of P_H, T_C is case temperature, and P_H is heating power in the junction. In addition, junction-to-ambient resistance (θ_{ja}) can be given as,

$$\theta_{ja} = \frac{T_J - T_A}{P_H} \tag{4.50}$$

where θ_{ja} denotes the thermal resistance between the device junction and ambient with air. T_A is ambient temperature, and P_H is heating power in the junction.

θ_{ja} is determined from equation below,

$$\theta_{ja} = \theta_{jc} + \theta_{ca} \tag{4.51}$$

where θ_{ca} is the thermal resistance between the device case and the ambient with air. From equation 4.49 and 4.50, θ_{ca} can be calculated as,

$$\theta_{ca} = \frac{T_C - T_A}{P_H} \tag{4.52}$$

There are different approaches for the use of junction-to-ambient resistance. The ambient temperature represents the air near the heat source of an electronic device. Nevertheless, there is no air in the space environment. Initial approach is that ambient temperature refers to the temperature of the PCB board at the location where the electronic devices are mounted. θ_{ja} can be converted to the θ_{jb}, the thermal resistance between the junction and the board, equation 4.50 transforms into equation (4.53) [63]. Within the scope of this thesis, junction-to-board resistance (θ_{jb}) will be used indirectly. For the purpose of providing information, junction-to-board resistance (θ_{jb}) can be calculated as follows,

$$\theta_{jb} = \frac{T_J - T_B}{P_H} \tag{4.53}$$

where T_B is PCB board temperature.

Secondly, in absence of junction-to-case resistance, junction-to-ambient resistance can be used to calculate junction-to-case resistance using formula specified in equation (4.54).

$$\theta_{jc} = \theta_{ja} - \theta_{ca} \tag{4.54}$$

$$\theta_{jc} = \theta_{ja} - \frac{1}{hA} \tag{4.55}$$

where h is convective heat transfer coefficient and it can be obtained from Table 4.3, A is surface area.

Table 4.3 : Heat transfer coefficient.

Cooling Regime	Approximate Heat Transfer Coefficient Range (W/m^2.°C)
Natural Convection, Air	2-30
Forced Convection, Air	15-300
Forced Convection, Water	200-10,000
Pool Boiling, Water	3000-50,000

Case-to-board resistance (θ_{cb}) can be indicated considering thermal network method,

$$\theta_{cb} = \theta_{jb} - \theta_{jc} = \frac{T_C - T_B}{P_H} \tag{4.56}$$

Generally, the value of θ_{cb} ranges between 0,1 and 0,01 (ºC/W). Another approach for θ_{cb} can be given within the scope of this thesis as follows,

$$\frac{Solder\ thermal\ conductivity\ (W/m.°C)\ x\ Total\ solder\ cross\ sectional\ area\ (m^2)}{Solder\ length\ (m)} \tag{4.57}$$

Equation 4.57 specifies thermal conductance. Reciprocal of formulation in Equation 4.58 provides case-to-board resistance (θ_{cb}).

$$\frac{Solder\ length\ (m)}{Solder\ thermal\ conductivity\ (W/m.°C)\ x\ Total\ solder\ cross\ sectional\ area\ (m^2)} \tag{4.58}$$

For the last resistance which is used for two-resistor model, underfill material was symbolized in (Figure 4.12). Underfill material is used under some components based on requirements. Underfill material resistance value depends on specified material, thickness, and void fraction.

$$\theta_{underfill} = \frac{K_{underfill}}{t_{underfill} x(1 - void\ fraction)} \tag{4.59}$$

where $K_{underfill}$ is the thermal conductivity of the underfill material, $t_{underfill}$ is the thickness of the underfill, and void fraction is the void fraction of underfill, which specifies from 0 to 1.

With the help of different approaches as mentioned above, thermal analysis results are tried to converge to test results with iteration, where experiments are not applicable.

4.7 Application of Numerical Analysis

Thermal analysis is performed using Simcenter 3D software. Space System Thermal solver and PCB Exchange module was utilized to realize the analysis.

Simcenter PCB Exchange module is used to import PCB with required properties. These properties are geometry, layer, dielectric and copper layout, thermal conductivity, and traces and vias. PCB and components can be directly imported to Simcenter 3D with .idx format from ECAD software.

Firstly, by using PCB Exchange module, components and PCB were imported to Simcenter 3D. Holes were removed from the model, traces and vias have become active. Only critical components are left in the model. Board properties were defined from the file in .idx format. Layers and vias can be seen separately in PCB Exchange module.

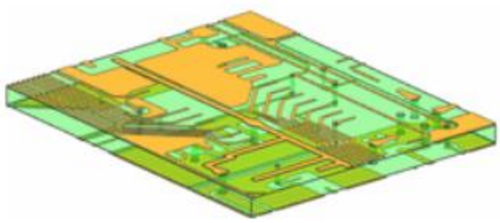

Figure 4.13 : PCB stack with top and bottom layers.

Space System Thermal solver is preferred especially for demonstration of space environment. Meshes of PCB can be automatically generated as 2D mesh thanks to PCB Exchange. As a Simcenter property, mesh collectors are created for common mesh types. 2D mesh collector has been rearranged for board materials as VT-901 for dielectric material and copper for traces. QUAD8 Thin Shell was assigned to PCB. 5810 elements and 17737 nodes were created for PCB finite element modelling. Thickness and thermal conductivity of each layer can be seen in PCB Stack module. Moreover, thermal-optical properties can be established like emissivity.

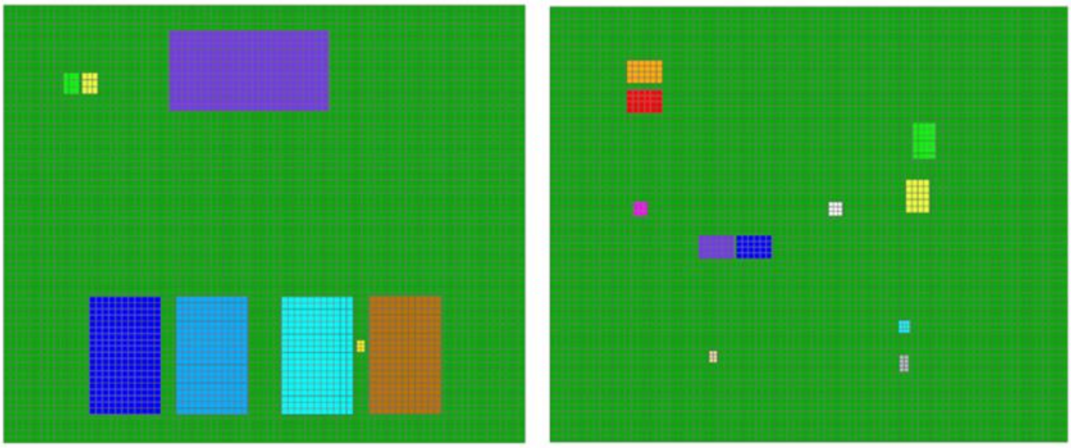

Figure 4.14 : Meshes of PCB and components.

Emissivity values have been assigned to mesh collector. Emissivity values which can be required in the equipment level thermal analysis are shown in (Table 4.4) [64].

Table 4.4 : Emissivity values for electronic equipment.

Surface	ε
Mirror Shiny	0,05
Oxidised Aluminum	0,2
Anodised Aluminum	0,8
Aluminum	0,05
PCB	0,8
Special Coatings	0,95
Paint	0,8
Plastic Mold Compound	0,8-0,9
Ceramic Mold Compound	0,8
Metal Mold Compound	0,75-0,85
Copper	0,03

Emissivities of aluminum and PCB were taken directly from Table 4.4 and assigned to related meshes. Emissivity of 0,8 was chosen for components.

Meshes for components are generated in different from PCB mesh collector which can be named as "Component". QUAD8 Thin Shell mesh was assigned to top surface of each component. 1157 elements and 4643 nodes were created for components. Element sizes were defined as 3 for relatively large components and 2 for small components. Thermo-optical properties were defined for the components such that their emissivity values were set to 0,8. Meshes of components can be seen in (Figure 4.14).

Mechanical parts must be imported to the analysis model. Therefore, carrier, cover and baseplate aluminum parts were added to the model in modeling section of Simcenter 3D. These parts were assigned 3D meshes in FEM section. Al-7075 is selected as material. Carrier, cover and baseplate are gathered under "Mechanics" mesh collector. Each one of them were assigned TET10 mesh type. 274677 elements and 507643 nodes were generated for 3D parts. The emissivity value, which has aluminum thermo-optical property, is set to 0,05. Meshes of mechanical parts can be seen in (Figure 4.15). In this way, FEM part has been completed. Other entities have been defined in simulation section.

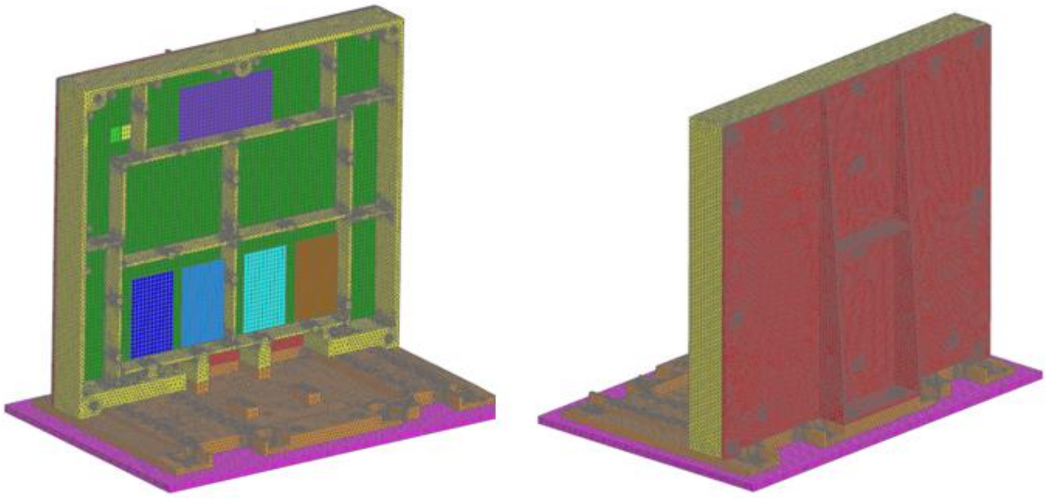

Figure 4.15 : Meshes of mechanical parts.

Each component has been defined under simulation object container. Model parameters are specified according to Theta JC-CB two-resistor model and input parameters are given in below. The two-resistance model requires 5 different pieces of information to be entered into the analysis, which are Theta JC, Theta CB, T_{max} case, T_{max} junction, and dissipation. For the thermal analysis, 14 types of components and a total of 16 components were simulated. Heat dissipation value for each component are given in (Table 4.5).

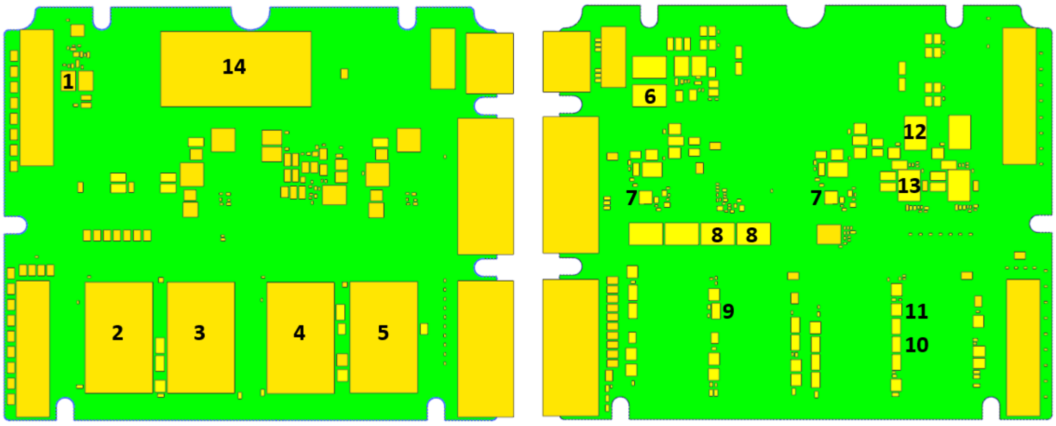

Figure 4.16 : Number of components.

Table 4.5 : Heat dissipation values for IPS module.

Component	IC Package Type	Heat Dissipation (W)	Thermal Conductivity (W/m.K)	Theta JC (ºC/W)	Theta CB (ºC/W)	Tmax Case (ºC)	Tmax Junction (ºC)
1	Ceramic Small-Outline Package (CSOP)	0,15	/	1.7	0,01	145	150
2	Solder Sealed Flangeless PCB Stud Mount	1	8	0,4	0,1	150	151
3	Solder Sealed Flangeless PCB Stud Mount	5,7	8	0,4	0,1	150	151
4	Solder Sealed Flangeless PCB Stud Mount	2,5	8	0,4	0,2 (K/W)	150	151
5	Solder Sealed Flangeless PCB Stud Mount	2	8	0,4	0,2 (K/W)	150	151
6	Ceramic Small-Outline Package (CSOP)	0,95	/	1,1	0,01	145	150
7	Ceramic Flat Pack (CFP)	1,25	/	20,4	0,1	135	150
8	Ceramic Small-Outline Package (CSOP)	0,15	/	1,1	0,01	145	150
9	Leadless Chip Carrier (LCC)	0	/	6,5	0,01	175	175
10	/	0	/	/	/	/	125
11	/	0	/	/	/	/	125
12	Ceramic Small-Outline Package (CSOP)	1,65	/	1,1	0,01	145	150
13	Ceramic Flat Pack (CFP)	0,65	/	0,6	0,1	124	125
14	Metal Hermetic Side-Leaded Packages	0,15	/	1,15	0,01	124	125

Component 10 and 11 are resistor, so that resistor models have been simulated as dissipation only. These values given above are obtained from data sheets and component manufacturers [65-70]. Thermal pad was applied under component 2 and 3. Thermal pad properties are given below.

Table 4.6 : Thermal pad properties [71].

Thermal Pad Properties		Unit
Density	3	g/cm^3
Thermal Conductivity	3	W/(m.K)
Specific Heat	1000	J/(kg.K)
Thickness	0,5	mm
Void Fraction	0,2	

It was stated that Theta CB generally ranges between 0,1 and 0,01. Despite of that, components 4 and 5 have special case. There is an aluminum bulk structure is placed under component 4 and 5. Also, between component-aluminum and aluminum-PCB, underfill material has been implemented. Calculation of resistance between components 4 and 5 is explained in Appendix A.

Maximum case and junction temperatures are maximum allowable temperature at case and maximum allowable temperature at junction, respectively. Thermal coupling has been established as seen in (Figure 4.17).

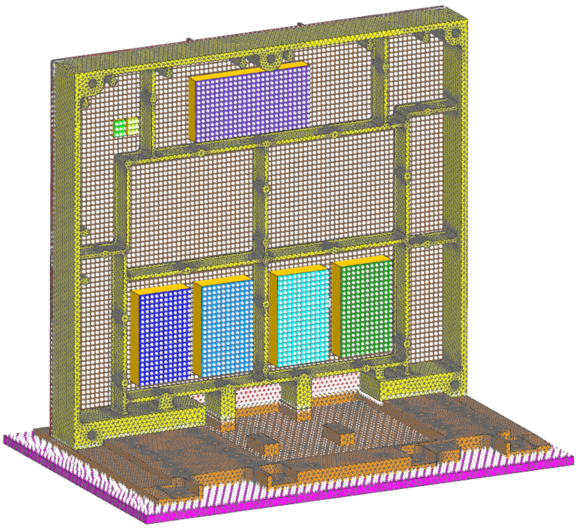

Figure 4.17 : Thermal couplings.

Thermal coupling has been created for carrier-cover, thermal plate-baseplate, baseplate-cover interface by dividing into 3 parts, baseplate-carrier interface by dividing into 6 parts, PCB-cover and PCB-carrier interface. Carrier was placed above the copper surface of PCB. Therefore, copper-aluminum interface was assumed for PCB-carrier interface.

Table 4.7 : Heat transfer coefficients of the interfaces.

Thermal Coupling	Heat Transfer Coefficient (W/m^2.K)
Carrier-Cover	2000
Thermal plate-Baseplate	80
Cover-Baseplate	500
PCB-Cover	100000
PCB-Carrier	100000

In Table 4.7, heat transfer coefficient values have been obtained from the experimental correlations which has been performed in Turkish Aerospace Space Systems. In the end of several iterations, these values have been found as the best inputs.

Table 4.8 : Thermal coupling of carrier to baseplate.

Thermal Coupling of Carrier to Baseplate	Total Resistance (K/W)
1	0,0599
2	0,0176
3	0,1575
4	0,1575
5	0,0292
6	0,0761

Interfaces between carrier and baseplate was divided into 6 pieces. Thermal pad was applied to these interfaces. Thermal resistance calculations are explained in Appendix A.

Subsequently, radiation has been constituted in the thermal analysis. Both simple radiation to environment and object to object radiation were applied. Simple radiation to environment has been calculated by using “Enclosure Radiation” which is the Simcenter property. View factors have been calculated as 1 for the cover and exterior surfaces of the carrier. Also, view factor was assigned to the baseplate and open-sided of the carrier and PCB as 0,7. Object to object radiation was used for closed-side of the equipment, and view factor was assigned as 1. Rear components, rear side of the PCB and inner side of the cover was performed via object to object radiation. These were calculated by using the formula in (Table 4.9).

Table 4.9 : View factor calculation [72].

Case	View Factor	Plot
Between two unequal parallel strips of width W_1 and W_2, and separation H, with w_1=W_1/H and w_2=W_2/H. 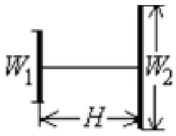	$F_{12} = \frac{\sqrt{(w_1 + w_2)^2 + 4}}{2w_1} - \frac{\sqrt{(w_2 - w_1)^2 + 4}}{2w_1}$	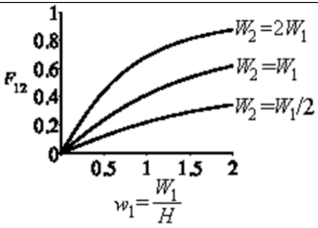

Cover length is equal to 216 mm and the lengths of component ranges between 5-17 mm. The distance between components and cover is about 3 mm.

$$W_1 = 5mm, \ \ H = 3mm, \ \ W_2 = 216mm$$

$$w_1 = \frac{5}{3} = 5{,}66, \qquad w_2 = \frac{216}{3} = 72$$

$$F_{12} = \frac{\sqrt{(1{,}66 + 72)^2 + 4}}{2 * 1{,}66} - \frac{\sqrt{(72 - 1{,}66)^2 + 4}}{2 * 1{,}66} = 0{,}999$$

$$W_1 = 17mm, \ \ H = 3mm, \ \ W_2 = 216mm$$

$$w_1 = \frac{17}{3} = 5{,}66, \qquad w_2 = \frac{216}{3} = 72$$

$$F_{12} = \frac{\sqrt{(5{,}66 + 72)^2 + 4}}{2 * 5{,}66} - \frac{\sqrt{(72 - 5{,}66)^2 + 4}}{2 * 5{,}66} = 0{,}999$$

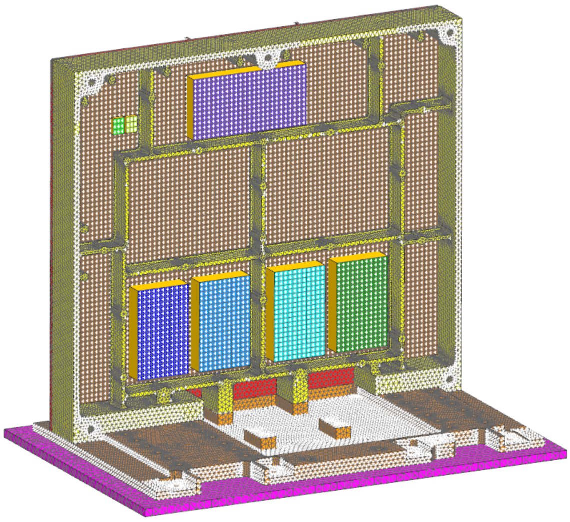

Figure 4.18 : Radiation application on the analysis model.

Finally, boundary condition was determined as 60°C which is qualification temperature on thermal plate. It was expected that TRP was 60°C, unfortunately, thermal pad could not be applied between baseplate and thermal plate, large temperature gradient arised between baseplate and thermal plate because of surface roughness. To simulate this condition, thermocouple measurement results have been utilized. The heat transfer coefficient was determined as 80 W/m^2K between thermal plate and baseplate by iterations. Boundary condition is applied to the thermal plate as 60°C which can be seen in (Figure 4.19).

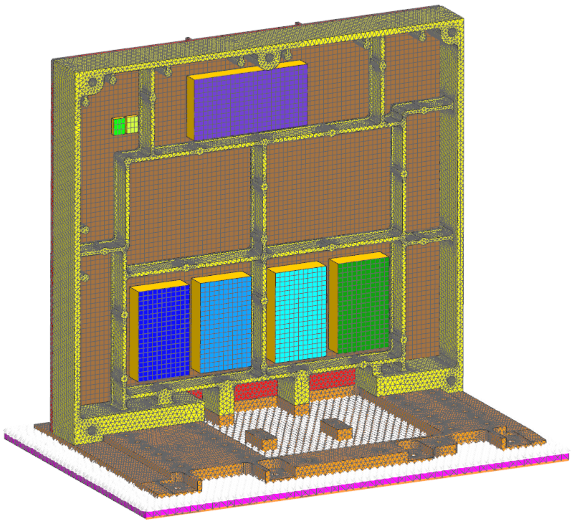

Figure 4.19 : Boundary condition application on the analysis model.

5. CONCLUSIONS AND RECOMMENDATIONS

The main purpose of this thesis is to verify the numerical solution using two resistor model. The inputs and assumptions used for the analysis made after the experimental study are explained. In this section, the test and analysis results will be given, and finally, suggestions for future studies will be made.

5.1 Test Results

Test conditions, tested device and requirements was mentioned in Chapter 3. In this section, test results will be given.

Test results are obtained from the thermocouples on IPS module. Total number of 33 thermocouples was replaced on the IPS module. The first 26 demonstrates the thermocouples on PCB and components, the last 7 ones defines the thermocouples on mechanical structures.

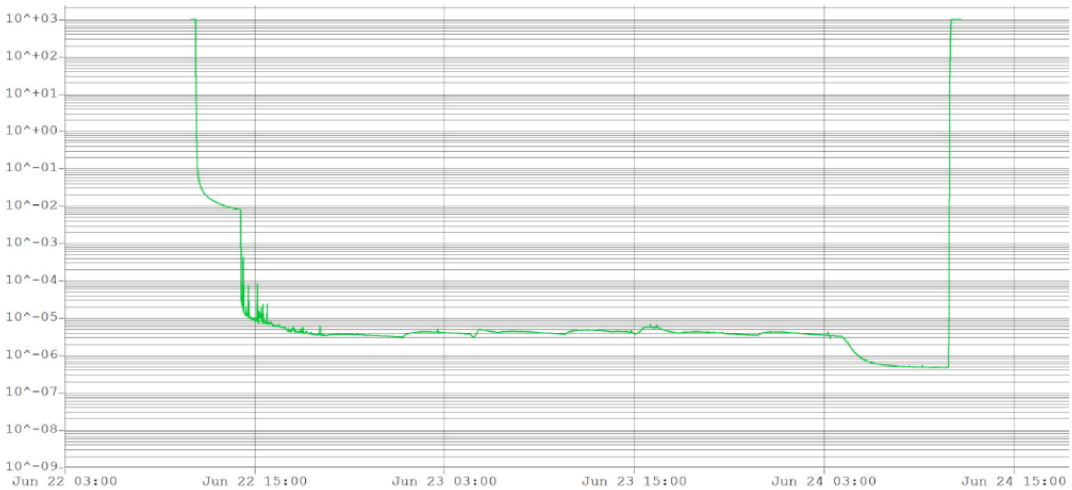

Figure 5.1 : Pressure-Time graph of TVTS.

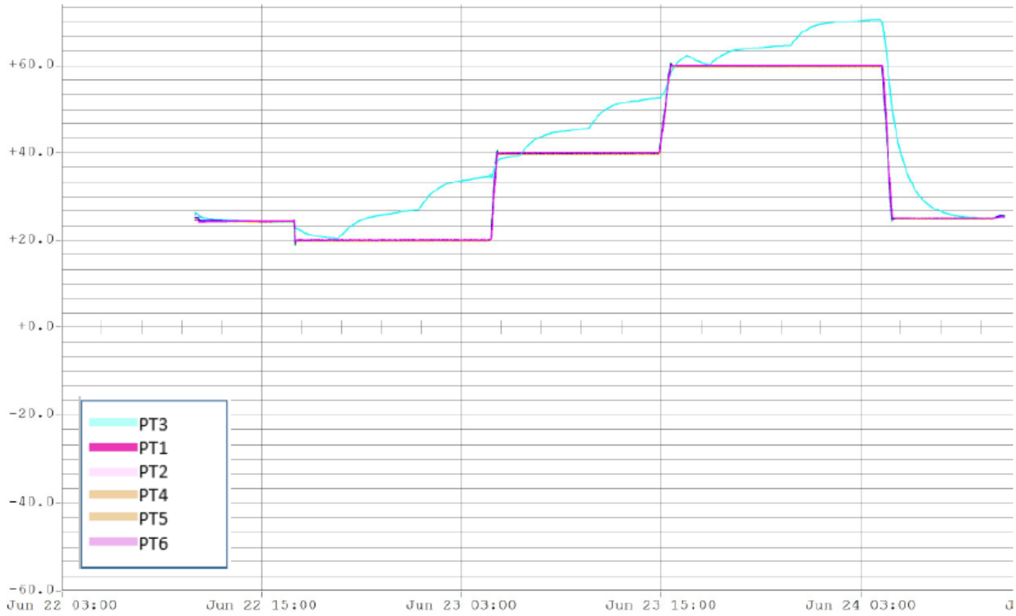

Figure 5.2 : Temperature-Time graph of TVTS.

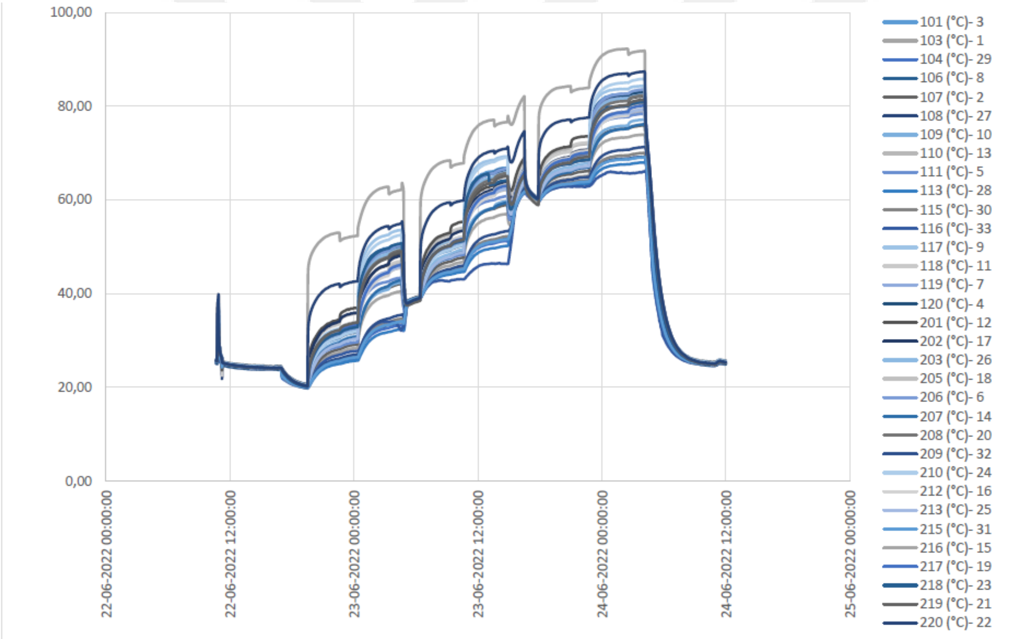

Figure 5.3 : Test results of IPS module.

To be more clear, test results for 60°C test case is given in (Table 5.1).

Table 5.1 : Test results for 60°C test case.

Thermocouple Number	Test Results (°C)	Thermocouple Number	Test Results (°C)
1	73,9	17	80,3
2	75,9	18	80,3
3	83,2	19	80,1
4	82,9	20	82,3
5	78,4	21	81,4

Table 5.1 (continued) : Test results for 60°C test case.

Thermocouple Number	Test Results (°C)	Thermocouple Number	Test Results (°C)
6	83,6	22	87,4
7	82,8	23	80,9
8	82,9	24	85,8
9	84,3	25	79,3
10	77,1	26	82,4
11	80,5	27	69,2
12	82,1	28	68
13	78,9	29	69,1
14	76,2	30	70
15	91,8	31	69,1
16	79,5	32	71,3
		33	66

5.2 Numerical Analysis Results

The analysis method was explained in Chapter 4. In this section, only the analysis results will be given.

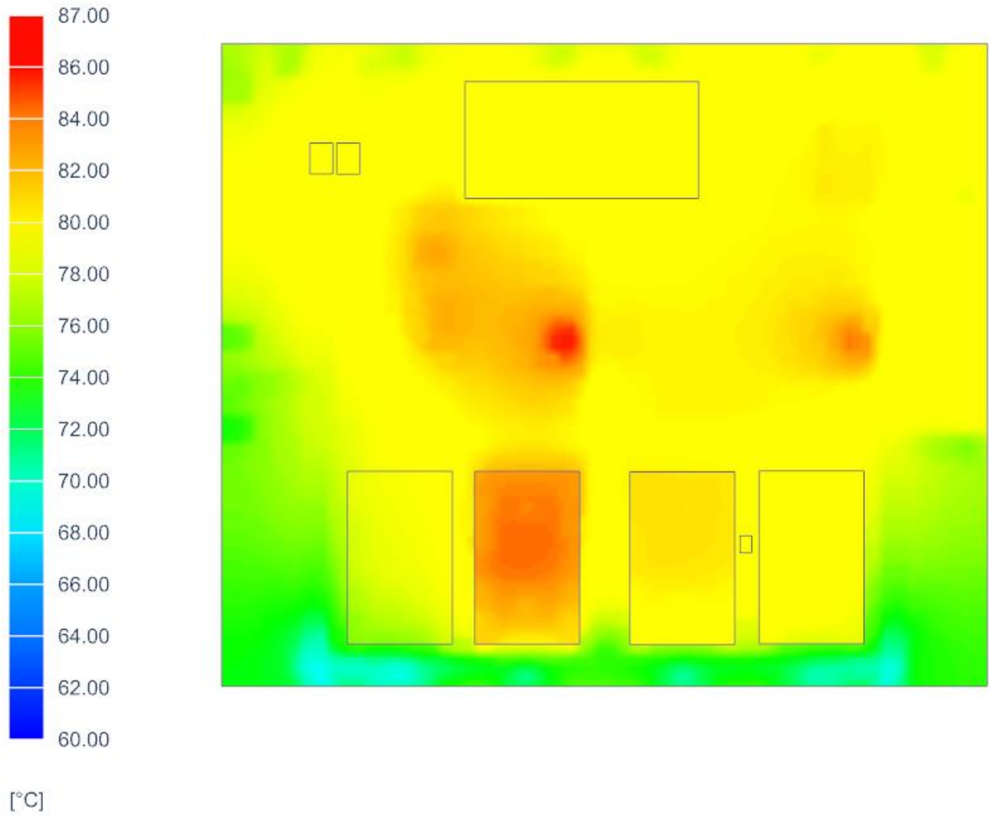

Figure 5.4 : Analysis results of front side of PCB.

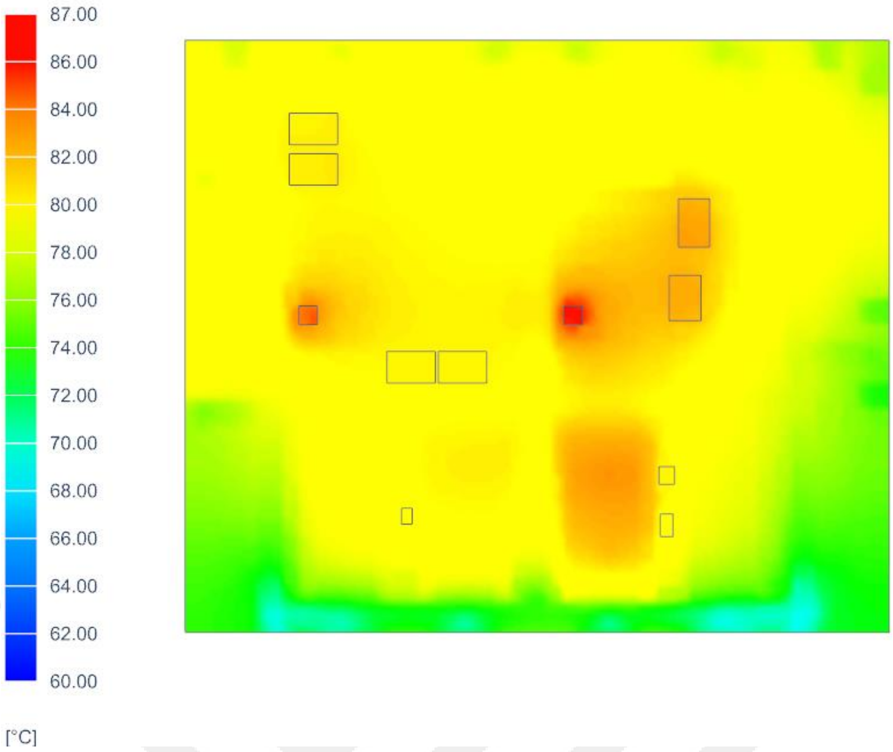

Figure 5.5 : Analysis results of rear side of PCB.

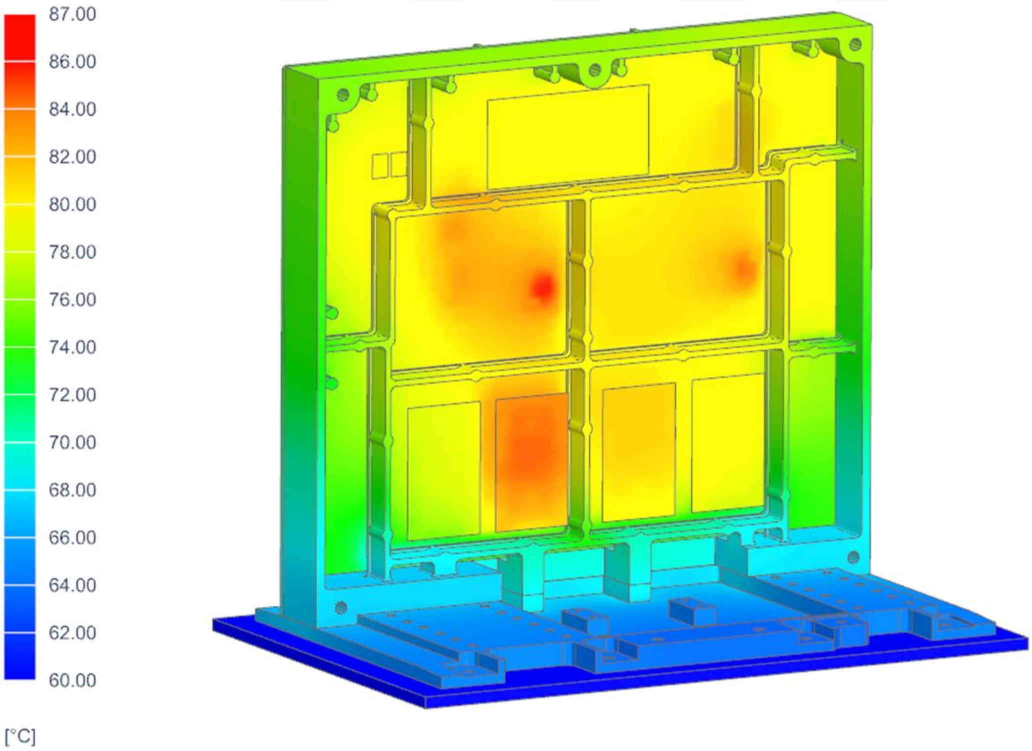

Figure 5.6 : Analysis results of front side of aluminum parts.

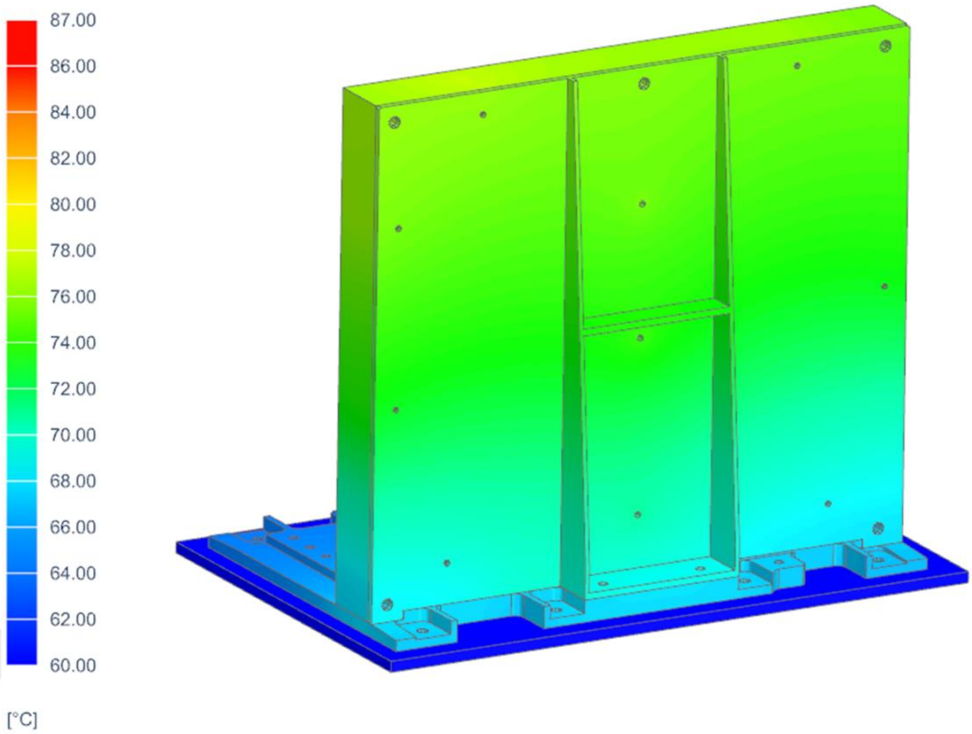

Figure 5.7 : Analysis results of rear side of aluminum parts.

Table 5.2 : Analysis results for 60°C test case.

Thermocouple Number	Analysis Results (°C)	Thermocouple Number	Analysis Results (°C)
1	79,4	17	79,6
2	79,5	18	80,8
3	78	19	80,7
4	77,5	20	81,5
5	78,5	21	80,1
6	80,7	22	85,8
7	81,3	23	80,1
8	84	24	83
9	84,3	25	80,5
10	80,1	26	83
11	81,2	27	67,2
12	81,2	28	66,6
13	79,3	29	69,1
14	80,9	30	68,4
15	84,8	31	68,1
16	80,8	32	67,1
		33	67,4

5.3 Comparison of Analysis Results with Test Results

Several iterations of thermal analysis were performed to validate the test results. Considering the ECSS, the difference between test and analysis results shall be ±3°C. Within the scope of this thesis, it is aimed that the difference is maximum 10%. The reasons of that can be listed as,

- All of the components on PCB cannot be modeled since it is quite time-consuming.
- Heat dissipation cannot be calculated with 100% accuracy.
- Thermocouples may measure temperature with an error range ±1°C.
- θ_{jc} and θ_{cb} values cannot be found in some data sheets, so assumptions has been made.
- Contact resistance has not been measured experimentally, therefore assumptions has been made.
- Thermal pad cannot be applied under baseplate, it causes large temperature gradients.

In Table 5.3, the difference between the test and analysis is given for 60°C test conditions.

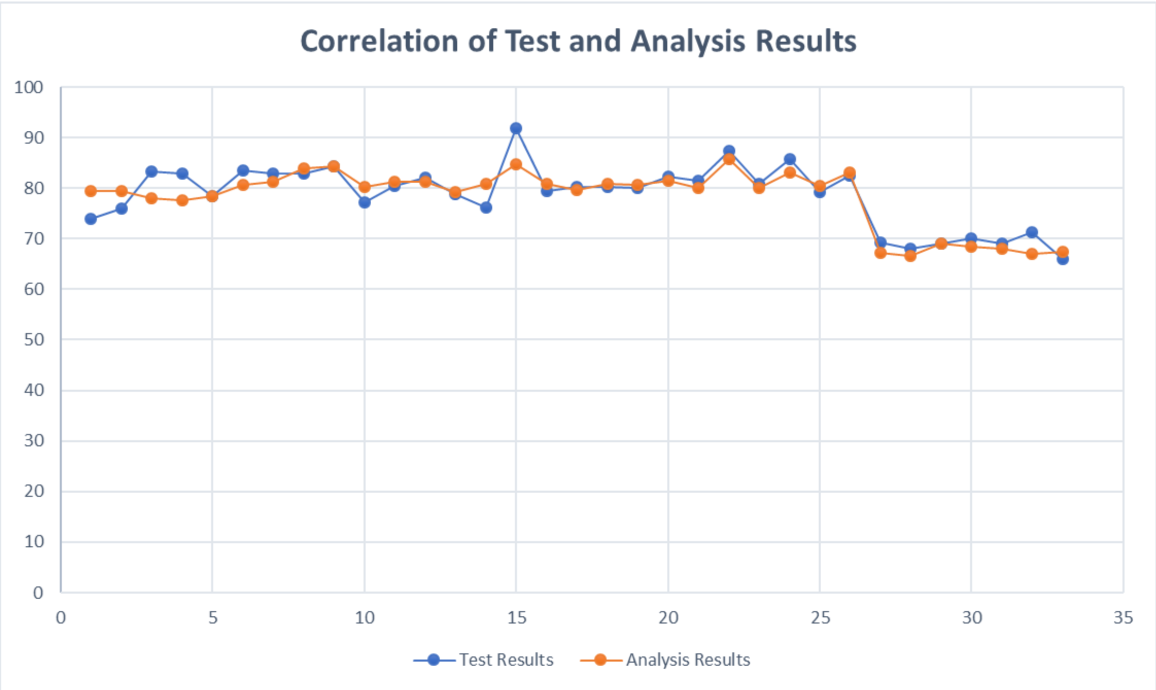

Figure 5.8 : Correlation of test and analysis results.

Table 5.3 : The difference between the test and analysis results for 60°C test conditions.

Thermocouple Number	Difference of the Results (°C)	Thermocouple Number	Difference of the Results (°C)
1	-5,5	17	0,7
2	-3,6	18	-0,5
3	5,2	19	-0,6
4	5,4	20	0,8
5	-0,1	21	1,3
6	2,9	22	1,6
7	1,5	23	0,8
8	-1,1	24	2,8
9	0	25	-1,2
10	-3	26	-0,6
11	-0,7	27	2
12	0,9	28	1,4
13	-0,4	29	0
14	-4,7	30	0,7
15	7	31	1
16	-1,3	32	4,2
		33	-1,4

As can be seen in Table 5.3, the differences are generally under ±3°C, except 7 cases. The thermocouple number 1 was placed on component 1. Information about component 1 was given in (Table 4.5). The reason that analysis gives warmer results may be that heat dissipation was not calculated correctly. Another reason may be that mounting of fastener at that region may not be done properly before the test.

The thermocouple number 2 was placed nearby component 1. It can be seen that thermocouple number 2 is warmer than thermocouple number 1 in (Table 5.1). Actually, this is an unexpected results. It was expected that component got warmer and PCB region nearby component 1 and carrier was colder. The main reason may be that heat dissipation through frame leads to increase temperature more in that region than expected.

The thermocouple number 3 and 4 was placed top surface of the DC-DC converter. Test results are warmer than the analysis results. As can be seen from the results, temperatures of the component 2 and 3 (DC-DC converters) is higher at the test results. This may be because the manufacturer gave the thermal conductivity value and the resistances of the joints were calculated by hand. Additionally, heat dissipation may varies from the real value.

The thermocouple number 14 was placed on component 6. It can be seen that analysis offers warmer results for thermocouple number 14. The reason that analysis gives warmer results may be that heat dissipation was not calculated correctly. Subsequently, θ_{jc} is given for a maximum value in data sheets, for this reason θ_{jc} may be smaller than from 1.1°C/W . Also, component 6 was placed behind the carrier. In the analysis, the contact resistance between the PCB and the carrier is defined the same for each element. Under test conditions, there are fasteners above and near the component 6. Torque value may not be same for each fastener, also roughness of PCB and carrier may lead to gap. These subjects may give rise to that dissipation of heat cannot be as expected. Since the component 6 behind the carrier, conductivity of PCB itself may be different from real case.

On the contrary, test result is warmer than analysis result for thermocouple number 15. The reason may be that small components which were not modeled in the analysis may lead to arise heat. Thermocouple number 15 was placed on one of the number 7 components. It can be seen that θ_{jc} of component 7 is quite larger than other components in (Table 4.5). This causes to excess heat of this small component. For a better correlation, θ_{cb} was imported as 0,1 for this component.

Lastly, thermocouple number 32 was placed on the baseplate nearby mounting region and the cover. According to test results, thermocouple number 32 is quite warmer than than the analysis result. Mechanics were modeled uniform, and surface roughness and geometrical irregularity were not included in the analysis. In real life, there was no thermal pad between the cover and the baseplate and there may be gap between them. Furthermore, the measurement was done right next to the fastener, may be this caused to misread of the value.

In Table 5.4, the difference between the test and analysis results in terms of percentage is given for 60°C test conditions. As can be seen in Table 5.4, all of the results are below 10% as expected.

Table 5.4 : The difference between the test and analysis results in terms of percentage for 60°C test conditions.

Thermocouple Number	Difference of the Results (%)	Thermocouple Number	Difference of the Results (%)
1	7,4	17	0,9
2	4,7	18	0,6
3	6,3	19	0,7
4	6,5	20	1,0
5	0,1	21	1,6
6	3,5	22	1,8
7	1,8	23	1,0
8	1,3	24	3,3
9	0,0	25	1,5
10	3,9	26	0,7
11	0,9	27	2,9
12	1,1	28	2,1
13	0,5	29	0
14	6,2	30	1,0
15	7,6	31	1,4
16	1,6	32	5,9
		33	2,1

5.4 Recommendations

The analysis of electronic components is quite complicated. Since the data of the components are kept confidential by the manufacturers, it is difficult to collect the necessary data. Gathering correct data may be the most difficult part of the thermal analysis of electronic equipment.

This study revealed that two resistor model is simple and easy to use for thermal analysis. Although it has some deficiencies, it gives quite good results. It necessitates less information than other modeling techniques.

To improve analysis results in future researches, experimental study should be considered for each step. Such that, each component and PCB have different properties, so heat dissipation and resistances shall be measured for more accurate results. In addition, heat dissipations of components can be measured during TVAC. In this way, heat dissipation inputs to the analysis will be error-free. Finally, to avoid from radiation environment simulation of open-sided equipment, MLI shall be utilized to cover open-sided of the equipment. This makes easier to correlate conduction in the analysis model.

REFERENCES

[1] **Wang, Z. & *et al.*** (2015). Thermal Modeling and Optimization for Electronic Packages. *IEEE: 16th International Conference on Electronic Packaging Technology*, Changsha, China, August 11-14. doi: 10.1109/ICEPT.2015.7236769

[2] **Zhang, Y. W., Liang L., and Xia Y.** (2007). Highly Efficient Modeling Automation for Electronic Package Thermal Analysis. *Electronic Components and Technology Conference: IEEE*, China.

[3] **Tal, Y.** (2002). An Improved Two-Resistors Compact Thermal Model by means of Modified Top-Surface-Area. *Eighteenth Annual IEEE Semiconductor Thermal Measurement and Management Symposium. Proceedings 2002 (Cat.No.02CH37311)*, San Jose, CA, USA, March 12-14.doi:10.1109/STHERM.2002.991347

[4] **Tal, Y. & Nabi A.** (2001). A Simple Analytic Method for Converting Standardized IC-Package Thermal Resistances (θ_{ja}, θ_{jc}) into a Two-Resistor Model (θ_{jb}, θ_{jt}). *Semiconductor Thermal Measurement and Management: Seventeenth Annual IEEE Symposium.* doi: 10.1109/STHERM.2001.915162

[5] **Kim, J. H., Koo J.C.** (2004). Efficient Thermal Modeling in Development of a spaceborne Electronic Equipment. *Proceedings of International Conference on Astronomy and Space Science: Celebrating 20th Anniversary of Korea Space Science Society*, Jeju, Korea, October 1.

[6] **Seo, H. S., Rhee, J., Han E. S., Kim I. S**. (2013). Thermal failure of the LM117 regulator under harsh space thermal environments. *Aerospace Science and Technology* (Vol. 27, pp.49-56). Retrieved from https://www.sciencedirect.com/science/article/abs/pii/S1270963812001046

[7] **Yovanovich, M. M**., **et al.** (1981). Thermal Contact Correlations. *Technical papers from the AIAA 16th Thermophysics Conference*, 164, Palo Alto, CA, June 23-25.

[8] **Peterson, G. P. & Fletcher L. S.** (1990). Measurement of the Thermal Contact Conductance and Thermal Conductivity of Anodized Aluminum Coatings. *Jounal of Heat Transfer, 112*, 579-585.

[9] **Toh. K. C. & Ng K. K.,** (1997). Thermal Contact Conductance of Typical Interfaces in Electronic Packages Under Low Contact Pressures. *IEEE/CPMT Electronic Packaging Technology Conference.* Singapore: October 10. doi: 10.1109/EPTC.1997.723899

[10]**Url-1** <*http://www.kampuskod.com/wp-content/uploads/2018/10/uydu-aglari-ve-sistemleri-uzaydaki-uydular-1.jpg*>, date retrieved 09.11.2022

[11]**Url-2** **<***https://www.esa.int/Enabling_Support/Space_Transportation/Types_of_orbits#GEO>*, date retrieved 09.11.2022

[12]**Url-3** <*https://www.esa.int/Enabling_Support/Space_Transportation*/Types_of_orbits#GEO>, date retrieved 09.11.2022

[13]**Url-4** <*https://earth.esa.int/web/eoportal/satellite-missions/t/tet-1>*, date retrieved 09.11.2022

[14]**Earth observation satellite.** (2020). *Wikipedia.* Retrieved October 13, 2022, from https://en.wikipedia.org/wiki/Earth_observation_satellite

[15]**GÖKTÜRK-2.** (n.d.). Retrieved November 7, 2022, from https://www.tusas.com/urun/Gokturk-2

[16]**Lehnert, J. S.** (2022). *Telecommunication*. Retrieved November 8, 2022 from https://www.britannica.com/technology/telecommunication

[17]***TÜRKSAT 6A.*** (n.d.). Retrieved September 20, 2022, from https://www.tusas.com/urun/turksat-6a

[18]***Weather satellite***. (2021). Retrieved September 21, 2022, from https://en.wikipedia.org/wiki/Weather_satellite

[19]***Spacecraft thermal radiators.*** (n.d.). Retrieved September 21, 2022, from https://www.aascworld.com/portfolio/thermal

[20] **Henry, C.** (2015). *Airbus Defence and Space Receives 3-D Printed Satellite Parts - Via Satellite*. Retrieved September 21, 2022, from https://www.satellitetoday.com/innovation/2015/03/20/airbus-defence-and-space-receives-3-d-printed-satellite-parts/

[21]***Satellite Central Cylinder Structures.*** (n.d.). Retrieved September 21, 2022, from https://www.ruag.com/en/products-services/space/spacecraft/satellite-structures/satellite-central-cylinder-structures-radiator/

[22]***NASA to Launch Sea Level Satellite Used to Monitor Ocean Levels at California Spaceport.*** (2020). Retrieved September 22, 2022 from https://orbitaltoday.com/2020/10/05/nasa-to-launch-sea-level-satellite-used-to-monitor-ocean-levels-at-california-spaceport/

[23] **Engines, U., Borogove, R., & Adler, M.** (2022). *Usages of electric propulsion versus chemical engines*. Retrieved October 5, 2022, from https://space.stackexchange.com/questions/12283/usages-of-electric-propulsion-versus-chemical-engines

[24]**Airbus.** (2017). *Space qualification testing of next-generation Fibre-Optic Inertial Reference Unit nears completion.* Retrieved September 21, 2022,from https://www.airbus.com/newsroom/press-releases/en/2014/05/space-qualification-testing-of-next-generation-fibre-optic-inertial-reference-unit-nears-completion.html

[25]**Url-5** <https://www.esa.int/Enabling_Support/Space_Engineering_Technology/Power_Systems>, date retrieved 20.10.2022

[26]**Guest, A. N.** (2013). Telemetry, Tracking, and Command (TT&C). In: Pelton J.N., Madry S., Camacho-Lara S. (Eds.), *Handbook of Satellite Applications* (pp. 1067-1078). Springer, New York, NY. doi: https://doi.org/10.1007/978-1-4419-7671-0_69

[27]***Command & Data-handling Systems***. (2022). Retrieved September 28, 2022, from https://mars.nasa.gov/mro/mission/spacecraft/parts/command/

[28]**Electronic Packaging.** (2022). *Wikipedia*. Retrieved November 20, 2022 from https://en.wikipedia.org/wiki/Electronic_packaging

[29]**Bhunia, S., & Tehranipoor, M.** (2019). Printed Circuit Board (PCB): Design and Test. *Hardware Security*, 81–105. doi:10.1016/b978-0-12-812477-2.00009-5

[30]***Here's a Quick Way to Know about Major Electronic Components.*** (n.d). *Retrieved October 19, 2022, from* https://www.elprocus.com/major-electronic-components/

[31]**Resistor (n.d)** *Wikipedia***.** Retrieved October 13, 2022, from https://en.wikipedia.org/wiki/Resistor

[32]**İndüktör** (t.y.) *Vikipedi*. Erişim: 13 Ekim 2022, https://tr.wikipedia.org/wiki/%C4%B0nd%C3%BCkt%C3%B6r

[33]**Köseni H., ve Yıldız A. B.,** (2019). Geri Dönüşlü DC-DC Dönüştürücünün Genelleştirilmiş Düğüm Denklemleri ile Analizi. Politeknik Dergisi, 22 (1), 179-184.

[34]**Url-6** < https://www.aydinlatma.org/transistor-nedir-ne-ise-yarar.html>, date retrieved 13.10.2022.

[35]**Diode** (n.d.) *Wikipedia***.** Retrieved October 13, 2022, from https://en.wikipedia.org/wiki/Diode

[36]**Electrical connector** (n.d.) *Wikipedia*. Retrieved October 163, 2022, from https://en.wikipedia.org/wiki/Electrical_connector

[37]**Url-7** <https://www.omnicalculator.com/physics/efficiency,> date retrieved 12.04.2022.

[38]**Jin, J. M.** (2020). "*Light, Thin, Short and Small", The Development of Semiconductor Packages*. Retrieved: November 6, 2022 from https://news.skhynix.com/light-thin-short-and-small-the-development-of-semiconductor-packages/

[39]**Agnihotri, N**. (n.d.). *What are the different types of IC packages?* Retrieved: November 6, 2022 from https://www.engineersgarage.com/ic-packages-types/

[40]**Moreau D.** (n.d.) *Test Requirements for Space Equipment* Retrieved August 13, 2022, from http://dma.ing.uniroma1.it/users/lsa_ds/MATERIALE/Test%20Requirements%20for%20Space%20Equipment.pdf

[41]**ECSS.** (2012). *Space engineering/Testing* (ECSS-E-ST-10-03C). Retrieved from http://everyspec.com/ESA/download.php?spec=ECSS-E-ST-10-03C.048162.pdf

[42]***Temperature Cycle Test (TCT).*** (2001) Retrieved August 13, 2022, from https://www.eesemi.com/TCT.htm

[43]***Thermal Vacuum Testing*.** (n.d.). Retrieved August 14, 2022, from https://www.element.com/product-qualification-testing-services/thermal-vacuum-testing

[44]**Gilmore, D. G**. (2002). *Spacecraft Thermal Control Handbook: Volume 1: Fundamental Technologies.* E1 Segundo, California.

[45]**MIL-STD.** (1982) *Military Standard: Test requirements for space vehicles* (MIL-STD-1540B). Retrieved from http://everyspec.com/MIL-STD/MIL-STD-1500-1599/MIL-STD-1540B_17789/

[46]**ECSS.** (2002). *Space engineering/Testing* (ECSS-E-ST-10-03A). Retrieved from http://everyspec.com/ESA/ECSS-E-10-03A_14019/

[47]**ACS.** (2018). *Environmental Test Chambers Range od Production.* Retrieved from,https://www.american-aviation.co.il/sites/american/UserContent/files/Range_of_Production.pdf

[48]**THP Systems.** (2018). *ACS Thermal Vacuum Chambers (TVC).* Retrieved from, https://www.thp-systems.com/test-systems/acs-thermal-vacuum-chambers-tvc/#info-tabs

[49]**Ozdisan.** (n.d.). *PT100.* Retrieved from, https://www.ozdisan.com/optolar-ve-sensorler/sensorler/sicaklik-sensorleri/PT100?gclid=CjwKCAiAkfucBhBBEiwAFjbkr_OrHDNbIwu0OyrJLmytQiFDoDoJ1QOH4YODZx3-MHBR96h-h-gDHxoCD3MQAvD_BwE

[50]**Ömür C., and Uygur A. B**. (2010). *Numerical and Experimental Investigation of the Thermal Behaviour of a Newly Developed Attitude Determination Control Unit in a Vacuum Environment* (Master’s thesis). Middle East Technical University, Mechanical Engineering, ANKARA.

[51] **University of Central Florida.** (n.d.). Energy Transfer by Heat. Retrieved from https://pressbooks.online.ucf.edu/thermorit/chapter/energy-transfer-by-heat/

[52] **Url-8 <** https://slideplayer.com/slide/7755556/>, date retrieved 19.11.2022

[53] **Arı, B. B.** (2021). *Spacecraft thermal modelling and analysis using the thermal network model* (Master's thesis). Istanbul Technical University, ISTANBUL.

[54]**Martinez I.** (2022). *Radiative View Factors.* Retrieved October 5, 2022, from http://webserver.dmt.upm.es/~isidoro/tc3/Radiation%20View%20factors.pdf

[55]***Thermal-Electrical Analogy: Thermal Network*** (n.d.). Retrieved: October 9, 2022, http://www.ingaero.uniroma1.it/attachments/2176_Cap_3%20Thermal-electrical%20analogy.pdf

[56]**Thermal Contact Resistance**. (2011). *Solidworks Help.* Retrieved November 1, 2022 from https://help.solidworks.com/2011/english/solidworks/cworks/legacyhelp/simulation/analysisbackground/thermalanalysis/thermal_contact_resistance.htm.

[57] **Nikishkov N. P.** (2001). *Introduction to the Finite Element Method.* Lecture Notes, UCLA.

[58]**Url-9** <https://simofis.com.tr/urun/simcenter-3d>, date retrieved 19.10.2022.

[59]**Siemens.** (n.d.) *Siemens Help.* Retrieved November 13, 2022, from https://docs.plm.automation.siemens.com/tdoc/nx/1872/nx_help#uid:id1384854

[60]***Integrated Circuits -IC** (n.d.) Retrieved October 20, 2022, from* https://www.daenotes.com/electronics/devices-circuits/integrated-circuits-ic

[61]**Two-Resistor Thermal Model** (n.d.) *Siemens Help.* Retrieved November 13, 2022, from https://docs.plm.automation.siemens.com/tdoc/nx/1872/nx_help#uid:id1384854

[62]**JEDEC** (2008). *Two-Resistor Compact Thermal Model Guideline* (JESD15-3). Retrieved from https://www.jedec.org/system/files/docs/JESD15-3.pdf

[63]**Seo, H. S., Rhee, J., Han E. S., Kim I. S**. (2013). Thermal failure of the LM117 regulator under harsh space thermal environments. *Aerospace Science and Technology* (Vol. 27, pp.49-56). Retrieved from https://www.sciencedirect.com/science/article/abs/pii/S1270963812001046

[64]**Url-10** <https://resources.ema-eda.com/blog/msa2021-the-emissivity-and-temperature-relationship-in-radiation-heat-loss-in-ics>, date retrieved 12.04.2022.

[65]**Url-11** <https://www.st.com/resource/en/datasheet/st1843.pdf>, date retrieved 12.10.2022.

[66]**Url-12** <https://www.craneae.com/sites/default/files/documents/SFME28_Space_EMI_Input_Filters.pdf>, date retrieved 12.10.2022.

[67]**Url-13** <https://www.irf.com/product-info/datasheets/data/irhnj597130.pdf>, date retrieved 12.10.2022.

[68]**Url-14** <https://html.alldatasheet.com/html-pdf/1114854/TI1/TPS7H2201-SP/67/1/TPS7H2201-SP.html>, date retrieved 12.10.2022.

[69]**Url-15** <https://www.st.com/en/space-products/1n5811u.html>, date retrieved 12.10.2022.

[70]**Url-16** <https://mdipower.com/mdi/pdf/5680-Series.pdf>,date retrieved 12.10.2022.

[71]**Url-17** < https://www.farnell.com/datasheets/2615235.pdf>,date retrieved 18.12.2022.

[72]**Url-18**

<http://webserver.dmt.upm.es/~isidoro/tc3/Radiation%20View%20factors.pdf>, date retrieved 12.11.2022.

APPENDICES

APPENDIX A:

1. Reduced Thermal Mathematical Model of IPS Module:

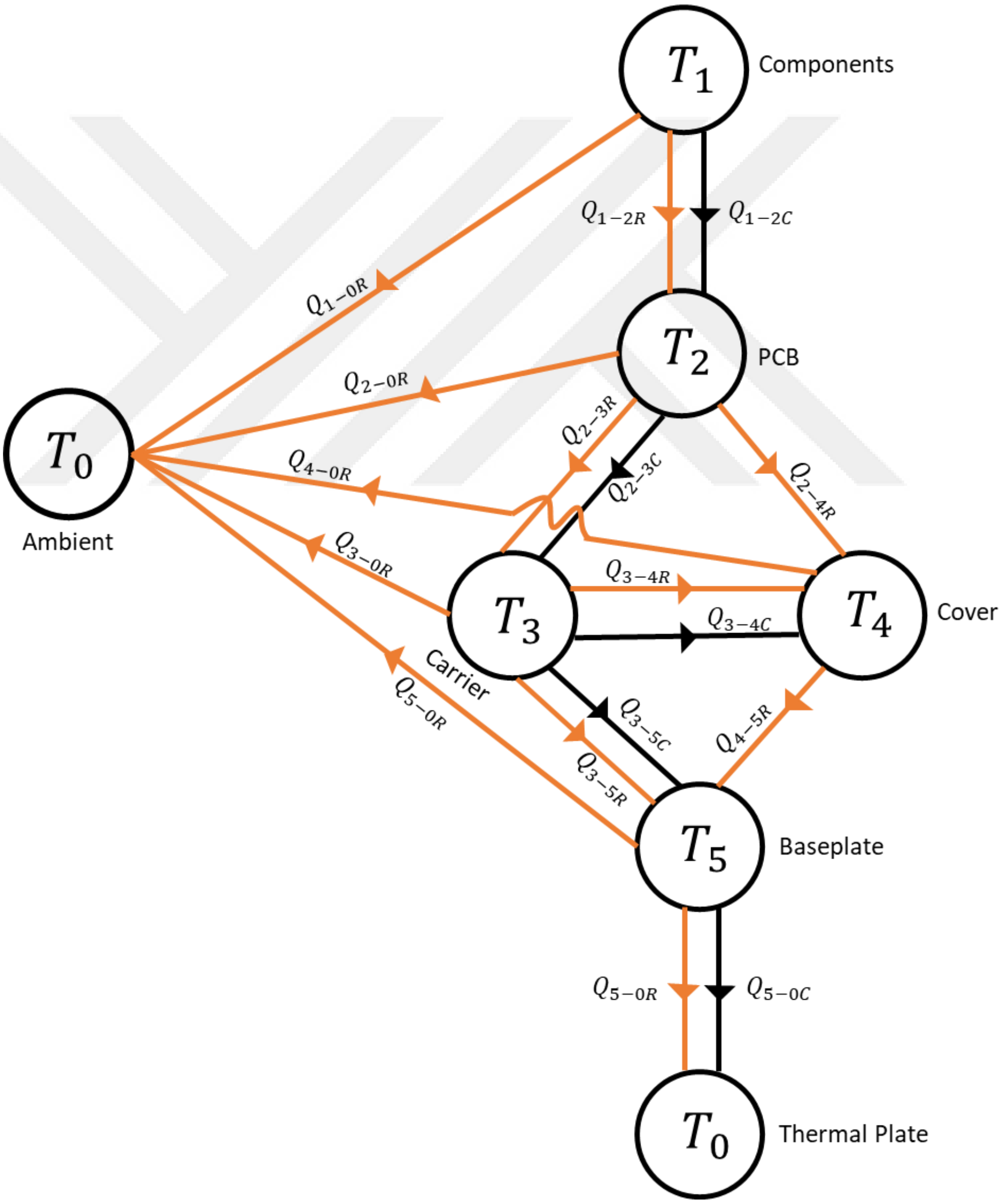

Figure A.1 : Reduced thermal mathematical model for IPS module.

1. Calculation of θ_{cb} for Components 4 and 5:

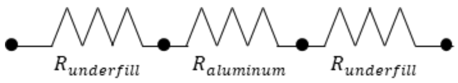

Figure A.2 : Diagram of resistance for components 4 and 5.

Resistance has been calculated from the diagram defined in (Figure A.2).

$$\theta_{cb} = R_{underfill} + R_{aluminum} + R_{underfill}$$

$$R = \frac{L}{A.k}$$

$$\theta_{cb} = \left(2x\frac{5x10^{-4}}{2x10^{-3}x3}\right) + \frac{1,2x10^{-2}}{2x10^{-3}x160} = \frac{1}{6} + 0,0378 \cong 0,2\frac{K}{W}$$

2. Calculation of thermal resistances between carrier and baseplate, in which thermal pad was applied:

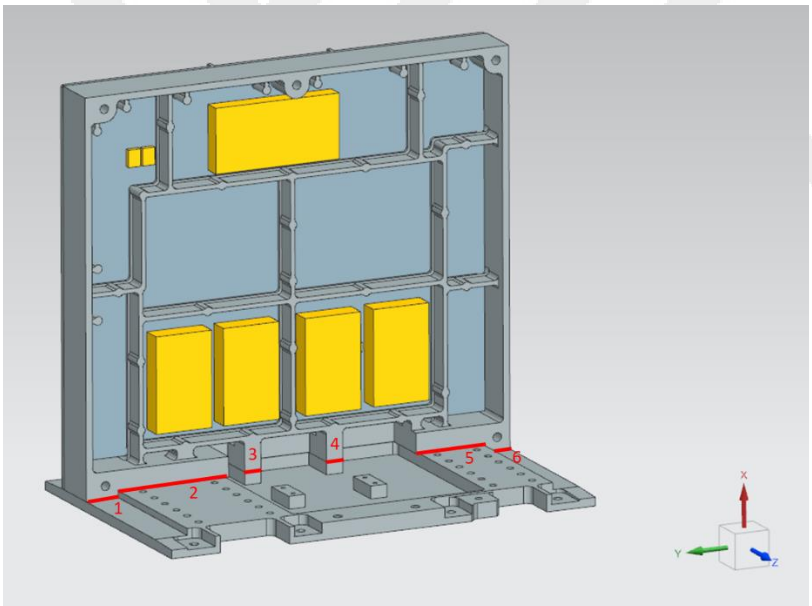

Figure A.3 : Interfaces between carrier and baseplate, in which thermal pad was applied.

Thermal resistance is a heat property and a measurement of a temperature difference by which an object or material resists a heat flow. The thermal resistance for conduction formula is given in equation (A.1).

$$R = \frac{L}{kA} \tag{A.1}$$

where L is thickness, k is material conductivity, and A is area. Thermal resistances between carrier and baseplate.

Table A.1: Thermal resistances between carrier and baseplate.

Interface Number	Area (mm^2)	Area (m^2)	Thermal Conductivity (W/m.K)	Thickness (mm)	Thickness (m)	Thermal Conductance (W/K)	Thermal Resistance (K/W)
1	556,8	0,0006	3	0,1	0,0001	16,7040	0,0599
2	1892,45	0,0019	3	0,1	0,0001	56,7735	0,0176
3	211,6	0,0002	3	0,1	0,0001	6,3480	0,1575
4	211,6	0,0002	3	0,1	0,0001	6,3480	0,1575
5	1141	0,0011	3	0,1	0,0001	34,2300	0,0292
6	437,9	0,0004	3	0,1	0,0001	13,1370	0,0761

CURRICULUM VITAE

Name Surname **:** Sima Aslım Yakut

Place and Date of Birth **:**

E-Mail **:**

EDUCATION **:**

- **B.Sc.** **:** 2019, Istanbul Technical University, Faculty of Aeronautics and Astronautics, Astronautical Engineering

PROFESSIONAL EXPERIENCE AND REWARDS:

- 2019-…System Installation Responsible Engineer for TURKSAT 6A Project and Mechanical Design and Analysis Responsible Engineer of electronic equipment developed in Turkish Aerospace.